THE EFFECTS OF AUXIN TRANSPORT ON ROOT SYSTEM ARCHITECTURE'S RESPONSE TO PHOSPHATE DEPRIVATION IN *ARABIDOPSIS*

MALIHA HASAN
Bachelor of Science in Botany, University of Dhaka (Bangladesh), 2020

A Thesis submitted
in partial fulfilment of the requirements for the degree of

MASTER OF SCIENCE

in

BIOLOGICAL SCIENCES

Department of Biological Sciences
University of Lethbridge
LETHBRIDGE, ALBERTA, CANADA

THE EFFECTS OF AUXIN TRANSPORT ON ROOT SYSTEM ARCHITECTURE'S RESPONSE TO PHOSPHATE DEPRIVATION IN *ARABIDOPSIS*

MALIHA HASAN

Date of Defense: August 15, 2024

Dr. Elizabeth Schultz Supervisor	Professor	Ph.D.
Dr. Larry Flanagan Thesis Examination Committee Member	Professor	Ph.D.
Dr. Jenny McCune Thesis Examination Committee Member	Associate Professor	Ph.D.
Dr. Theresa Burg Chair, Thesis Examination Committee	Professor	Ph.D.

Abstract

Root system architecture (RSA) involves the spatial and temporal distribution of primary roots, lateral roots, and root hairs. The RSA provides the plants' anchorage and facilitates the uptake of water and nutrients. Lateral roots and root hairs provide the root system a high degree of developmental plasticity and are crucial to respond to any environmental stressor like drought, salinity, and nutrient deficiency. Plants, for their optimum growth and development, require some macronutrients, among which phosphorus is of great importance. Reduced availability of phosphorus causes defects in plant growth and development. RSA is highly plastic to phosphate deficiency and compensates for deficiency by modulating the length and density of lateral roots, altering the length of primary roots and root hairs. Auxin signaling and biosynthesis have been found to be involved in the phosphate starvation signaling pathways but very little is known about the involvement of auxin transport in these pathways. My research aims at understanding if *Arabidopsis* mutants that cause defects in auxin transport could also affect the RSA's response to phosphate deprivation. My findings suggest that the auxin transport mutants demonstrate significantly different primary root length, tip to the first lateral root distance, and root hair length compared to the Wt. Unexpectedly, the mutant *fkd1/fl1-2/fl2/fl3* produced significantly longer root hairs compared to the Wt and the remaining mutants (*cvp2cvl1* and *sfc40*). This finding also suggests the defective PIN2 localization at the epidermal region of the *fkd1/fl1-2/fl2/fl3* mutant leading to longer root hairs. It was also evident that the defective PIN localization of the mutants

affected their ability to respond to the phosphate starvation. The mutants *fkd1/fl1-2/fl2/fl3* and *sfc40* was unable to respond to the phosphate deprivation. My findings provide more information regarding the involvement of auxin transport in modulating the RSA under low phosphate concentration along with the importance of *FKD1*, *CVP2*, *CVL1*, and *SFC40* genes in this process. Understanding the mechanism through which these genes alter plant's ability to modulate RSA under phosphate deficiency could lead to improved phosphate uptake efficiency and improved crop production in the future.

Acknowledgements

I would like to express my sincere gratitude to The University of Lethbridge for letting me be a part of this incredible team and excellent teaching environment. Further and most importantly I would like to thank my supervisor Dr. Elizabeth Schultz for her thoughtful recommendations and insights that steered me through this research. I would also like to thank her dedicated support and excellent guidance. Dr. Schultz continuously was always willing and enthusiastic to assist in any way she could throughout this project. I would like to express my sincere gratitude to her for being so kind and patient with an international student like myself. A special thanks and gratitude to my committee members- Dr. Larry Flanagan and Dr. Jenny McCune. Their valuable feedback and suggestions were instrumental in shaping my work. I am also grateful to Dr. Dmytro Yevtushenko for providing me the camera and other equipment for my research. I would like to thank Dr. Tegan Barry for helping me out with my data analysis and statistics. This journey would have been more difficult without the suggestions and words of encouragement from my lab mate- Jaxon Reiter, so thank you, Jaxon. A very special thanks to my parents, brother, husband and in-laws for their constant love and support. I couldn't have done it without their unwavering encouragement. Thank you maa and baba, for believing in me.

Table of Contents

Chapter Two: Materials and Methods

Chapter Three: Results

List of Tables

List of Figures and Illustrations

List of Abbreviations

ABCB/ MDR/ PGP = ATP- BINDING CASETTE subfamily/ MULTIDRUG RESISTANCE/ P-GLYCOPROTEIN

ACD = Asymmetric Cell Division

AFB = Auxin-F Box

ARF = Auxin Response Factors

ARF-GAP = ADP RYBOSLATION FACTOR GUANOSINE TRYPHOSPHATE HYDROLASE (GTPase) ACTIVATING PROTEINS

AtDAO = ARABIDOPSIS DIOXYGENASE FOR AUXIN OXIDATION

AUX1 = AUXIN1

AUX1 = AUXIN-RESISTANCE1

AUXREs = Auxin Response Elements

CVL1= CVP2-LIKE

CVP2 = COTYLEDON VASCULAR PATTERN2

CWI = Cell Wall Integrity

CYCB;1 = Cell cycle associated B-type cycline

DR5 = DIRECT REPEAT 5

DSC = Distal Stem Cells

DZ = Differentiation Zone

ECA = Endodermal Cell Ablation

EDZ = Elongation Differentiation Zone

ein2 = ethylene-insensitive 2

EIN3 = ETHYLENE INSENSITIVE 3

ER = Endoplasmic Reticulum

err = enhancers of response regulators

EXPAs = EXPANSINs

EZ = Elongation Zone

FER = FERONIA

FKD1 = FORKED1

FUS3 = FUSKA3

GH3 = GRETCHEN HAGEN (3)

GL2 = GLABLA2

GUS = β- Glucuronidase

HAE = Leucine-rich repeat receptor-like kinase HAESA

IAA = Indole Acetic Acid

IAA/TAR = TRYPTOPHAN AMINOTRANSFERASE OF ARABIDOPSIS/ TRYTOPHAN AMINOTRANSFERASE RELATED

IAO_X = Indole-3-Acetaldoxime

IBA = Indole-3-Butyric-Acid

IDA = INFLORESCENCE DEFICIENT ABCISSION

IP6 = Polyphosphorylated Inositol hexaphosphatase

IP_YA = Indole-3-Pyruvic Acid

LBD16 = LATERAL ORGAN BOUNDARIES DOMAIN 16

LEC2 = LEAFY COTYLEDON 2

LR = Lateral Root

LRC = Lateral Root Cap

LRE = Lateral Root Emergence

LRFC = Lateral Root Founder Cells

LRP = Lateral Root Primordium

LUC = Luciferase

MARK4 = MEMBRANE-ASSOCIATED KINASE REGULATOR

NOX = NICOTINAMIDE ADENINE DINUCLEOTIDE PHOSPHATASE-OXIDASE

OXIAA = 2-oxo-indole-3-acetic acid

OZ = Oscillation Zone

P1BS = PHR1-binding cite

PH = Pleckstrin Homology

PHR = PHOSPHATE STARVATION RESPONSE FACTOR

PHT1 = PHOSPHATE TRANSPORTER 1

PI = Phosphoinositides

PI4Kβ1/PI4Kβ2 = PHOSPHATYDYLINOSITOL 4-OH KINASE BETA 1 and 2

PILS = PIN-LIKES

PIN = PIN-FORMED

PIP = PLASMAMEMBRANE INTRINSIC PROTEIN

PIP5K3 = PHOSPHATIDYLINOSITOL-4 PHOSPHATASE 5- KINASE3

PL = Pleckstrin Homology-Like

PLT = *PLETHORA*

PM = Plasma Membrane

PM = Proximal Meristem

PPP = Phloem Pole Pericycle Cells

PR = Primary Root

PSI = Phosphate Starvation Induced genes

PUCHI = Ethylene Response Factor

QC = Quiescent Center

RHD6 = ROOT HAIR DEFECTIVE 6

ROP2 = RHO-RELATED PROTEIN FROM PLANTS

ROS = Reactive Oxygen Species

RSA = Root System Architecture

RSL19 = ROOT HAIR SPECIFIC 19

RSL4 = RHD6-LIKE 4

SFC/*VAN3 = SCARFACE/VASCULAR NETWORK DEFECTIVE 6*

SHY= *SHORT HYPOCOTYL*

SLR2 = SOLITARY ROOT 2

SYPL23 = SYNTAXIN OF PLANTS 23

TAA/YUCCA = Tryptophan aminotransferase of *Arabidopsis*

TGN = TRANS GOLGI NETWORK

TIR = Transport Inhibitor Response

TZ = Transition Zone

VAB = VAN3 BINDING PROTEIN

WOX5 = WUSCHEL RELATED HOMEOBOX 5

XPP = Xylem Pole Pericycle Cells

Introduction

The root system architecture (RSA) is often regulated by auxin transport, biosynthesis, and signaling pathways. The modulation of RSA is a crucial mechanism adopted by plants in response to different environmental signals such as phosphate deficiency. Primary root, lateral root, and root hairs are key components of RSA. At low phosphate conditions, plants exhibit shorter primary root length, more lateral roots and longer root hairs.

Previous studies have looked at the involvement of auxin biosynthesis and signaling pathways modulating the RSA but there is not much information available on the effects of auxin transport in the modulation of RSA. In this study, I worked with *Arabidopsis* auxin transport mutants *fkd1/fl1-2/fl2/fl3*, *cvp2cvl1*, and *sfc40*. I hypothesized that the mutants that alter the auxin transport, could also affect their RSA and RSA response to phosphate deficiency.

The gene products encoded by *FKD1*, *FL1-3*, *SFC/VAN3*, *CVP2*, and *CVL1* are proposed to act within the secretory pathways and help regulate the localization of auxin efflux transporter PIN1 (Mariyamma et al., 2018; Carland and Nelson, 2009; Naramoto et al., 2010). Previous studies have suggested that the mutation in these genes results in discontinuous vein pattern formation in *Arabidopsis*. Disrupted PIN1 localization has been observed in the provascular cells of *fkd1/fl1-2/fl2/fl3* leaves (Mariyamma et al., 2018) and the mutant *sfc40* is unable to maintain PIN1 polarity in the leaf procambial

cells (Scarpella et al., 2006). These studies focused on the involvement of these genes to maintain the leaf vein pattern formation. Mariyamma et al., 2018 observed decreased gravitropic response and root elongation in *fkd1/fl1-2/fl2/fl3* quadruple mutants and *fkd1/fl1-2* double mutants which suggests a role for these gene products within the roots. In my study, I observed these auxin transport mutants (*fkd1/fl-1/fl2/fl3*, *cvp2cvl1*, and *sfc40*) to determine if the disruptive PIN1 localization could alter their RSA and affect their ability to respond to phosphate deficiency.

Chapter One: Literature Review

1.1 The Plant Hormone Auxin

The plant hormone auxin controls almost all aspects of growth and development in plants. Auxin is a master regulator involved in variety of processes, including vascular tissue development, apical dominance, and lateral root development (Woodward and Bartel, 2005; Enders and Strader, 2015). There are three main regulatory processes involved in auxin regulation: auxin biosynthesis and inactivation, directional auxin transport, and signaling (Chapman and Estelle,2009; Zazimalova et al., 2010; Ludwig-Muller,2011; Hayashi, 2012; Kasahara, 2016). Auxin action regulation is mostly dependent on the intercellular auxin concentration gradient. Together with auxin metabolism, which involves auxin biosynthesis, inactivation, and degradation, auxin polar transport coordinately produces the auxin gradient (Korasick et al., 2013; Naramoto, 2017).

1.1.1 Auxin Biosynthesis

Auxin biosynthesis is crucial for various plant developmental processes including root development. In the *Arabidopsis* Indole 3-pyruvic acid (IPyA) pathway (Kasahara, 2016), tryptophan undergoes two consecutive enzymatic steps to convert to Indole-3-Acetic Acid (IAA) (Mashiguchi et al. 2011; Won et al. 2011). First, tryptophan in *Arabidopsis* is converted to IPyA by three aminotransferases encoded by the *TRYPTOPHAN AMINOTRANSFERASE OF ARABIDOPSIS1/TRYPTOPHAN AMINOTRANSFERASE RELATED*

(*TAA1*/*TAR*) gene family. Subsequently, IPyA is oxidatively decarboxylated to IAA by the YUCCA (YUC) flavin monooxygenase family (Figure 1.1). Furthermore, in a supplemental IAA biosynthetic process of the Brassicaceae family, tryptophan is converted into indole-3-acetaldoxime (IAOx) by the CytP450 monooxygenases (Sugawara et al., 2009). IAOx is subsequently transformed into IAA. It has been suggested that tryptamine, indole 3-acetamide, and indole 3-acetaldehyde are also IAA precursors; however, it is uncertain what contributions these precursors play in IAA biosynthesis (Kasahara, 2016).

1.1.2 Conjugation and Oxidation of IAA

IAA homeostasis depends on the reversible and irreversible catabolism of IAA, which also co-ordinates the local auxin gradient and hence can affect developmental processes (Ludwig-Muller, 2011; Korasick et al., 2013). Two main mechanisms lead to the inactivation of IAA: conjugation of amino acids and oxidation. One of the most well-studied early auxin-responsive genes encoding the IAA-amino acid conjugate synthase is *GRETCHEN HAGEN3* (*GH3*). At least seven of the 19 members of the *Arabidopsis GH3* gene family can catalyze the synthesis of IAA amide conjugates (Staswick et al., 2005).

The 2-oxo-indole-3-acetic acid (oxIAA) route is another important avenue for inactivation. The 2-oxoglutarate/iron-dependent dioxygenase family is encoded by *Arabidopsis DIOXYGENASE FOR AUXIN OXIDATION 1 (AtDAO1)*, which catalyzes the oxidation of IAA to produce 2-oxo-indole 3-acetic acid (oxIAA) (Zhang and Peer, 2017) (Figure 1.1). It is possible that *AtDAO1* and group II GH3 cooperate to control the

catabolism of IAA, because the loss-of-function dao1-1 mutant exhibits a buildup of IAA-Asp and IAA-Glu that compensates for the loss of the oxIAA pathway (Porco et al., 2016) (Figure 1.1). It has been observed that DAO acts as an oxidase of IAA-amino acid conjugates to form oxIAA-amino acid conjugates downstream of *GH3*, and also inactivates IAA (Hayashi et al., 2021).

1.1.3 Polar Auxin Transport

After biosynthesis, IAA is sent to different locations of the plant via the auxin polar transport system, which generates an asymmetric auxin concentration gradient that controls tropic growth, embryo development, lateral root formation, and vascular and root development (Fukui and Hayashi, 2018).

Auxin influx and efflux proteins regulate the auxin polar transport (Adamowski and Friml, 2015; Zazimalova et al., 2010). The directional movement of auxin is called polar transport of auxin. Like amino acid permeases, AUXIN-RESISTANT 1/LIKE AUX1 (AUX1/LAX) proton gradient-driven symporters serve as auxin influx transporters for auxin import (Figure 1.1). The *Arabidopsis aux1* loss-of-function mutant demonstrated a lack of response to gravity or exogenous auxin (Marchant et al., 1999). Two different groups of proteins, the ATP-BINDING CASSETTE subfamily and PIN-FORMED (PIN) efflux carriers work together to regulate the direction and rate of intercellular auxin flow in auxin efflux transport (Zazimalova et al., 2010). Eight PIN family proteins have been identified in *Arabidopsis*, of which PIN1, PIN4 and PIN7 are located at the plasma

membrane (PM) of particular cells and serve as carriers of auxin efflux (Adamowski and Friml, 2015; Naramoto, 2017). Secretory pathways target PIN to the plasma membrane, after which PIN proteins must be regulated to prevent lateral diffusion and maintain a polar distribution (Kleine-Vehn et al., 2011; Langowski et al., 2016). To allow shifts in the direction of auxin maxima, PIN proteins must be flexibly translocated and recycled to different positions on the PM (Habets and Offringa, 2014). PIN5, PIN6, PIN8, and PIN-LIKES (PILS) proteins are found in the endoplasmic reticulum (ER) (Figure 1.1) (Barbez et al., 2012), where they transport auxin between the cytosol and ER to control auxin homeostasis (Adamowski and Friml, 2015) (Figure 1.1). The ABCB proteins of *Arabidopsis* have also been identified as auxin transporters. Single and multiple loss-of-function mutants for *PIN* and *ABCB* genes demonstrate significant abnormalities in lateral organ development, shoot and root tropism, and embryogenesis (Zazimalova et al., 2010). The auxin gradient controlling plant growth and development is eventually determined by the subcellular localization, expression, and cell type-specificity of the AUX/LAX, PIN, and ABCB proteins (Fukui and Hayashi, 2018).

1.1.4 Auxin Signaling

After auxin enters into the cells, it can regulate transcription of numerous genes via the activation of Auxin Response Factors (ARFs). This change in gene expression initiates the cellular auxin response. In *Arabidopsis*, there are 23 *ARF* genes (Ulmasov et al., 1995), whose products bind to the promoters of auxin-responsive genes through cis-regulatory auxin response elements (AuxREs) (Ulmasov et al., 1995). ARF proteins can function as

transcriptional activators or repressors, depending on the type of ARF (Santner and Estelle, 2009). In *Arabidopsis*, the 29 members of the *Aux/IAA* family encode short-lived nuclear proteins that function as repressors of auxin-responsive gene expression. The 3rd and 4th domains of *AUX/IAA* repressors heterodimerize with specific ARF transcription factors (Hayashi et al., 2012) and the binding inhibits the transcriptional activity of ARFs (Chapman and Estelle,2009; Hayashi, 2012). According to Delker et al. (2008), the *GH3* family has been identified as a subset of auxin-inducible genes, which also includes *Aux/IAA* genes, that are up-regulated by ARF transcription factors following auxin treatment to produce more auxin amide conjugates (Santner and Estelle, 2009), thus attenuating the auxin response (Fukui and Hayashi, 2018).

Through encouraging the interaction between Aux/IAA and the F-box protein auxin receptor TIR1, auxin increases the ubiquitination of the repressor Aux/IAA and increases the transcription of ARF (Hayashi et al., 2012; Salehin et al., 2015). TIR1, an F-box protein that serves as the auxin receptor, and five other TIR1 homolog proteins AFB1–5 (Auxin F-Box), are present in *Arabidopsis* (Hayashi, 2012; Salehin et al., 2015). The leucine-rich repeat (LRR) domain of TIR1 forms a surface pocket where auxin nestles. TIR1-bound auxin strengthens the interaction between TIR1 and the Aux/IAA (Tan et al., 2007). Tan et al., (2007) report that Aux/IAA functions as a co-receptor to build the tiny hydrophobic cavity in the auxin-binding region of TIR1, suggesting that auxin functions as a "molecular glue" to firmly link the two proteins together (Fukui and Hayashi, 2018).

Formation of the TIR1–auxin–Aux/IAA ternary complex subsequently catalyzes the ubiquitination of Aux/IAA repressors (Figure 1.1) (Salehin et al. 2015, Tan et al. 2007). The TIR1-auxin-AUX/IAA associates with Skp1, ASK1 and Cullin (CUL1) to form a Ring E3 ubiquitin ligase, SCF^{TIR1} which catalyzes addition of ubiquitin to the AUX/IAA protein (Figure 1.1). The 26S proteasome pathway recognizes ubiquitinated AUX/IAA repressors and degrades them, activating ARF transcriptional activity (Hayashi et al., 2012; Salehin et al., 2015) (Figure 1.1). Consequently, through the SCFTIR1/AFB-proteasome pathway, auxin induces breakdown of Aux/IAA and activates ARFs to enhance the expression of auxin-responsive genes (Chapman and Estelle,2009; Hayashi, 2012) resulting in auxin-related developmental responses (Chapman and Estelle 2009).

Auxin biology has advanced over the past few decades, revealing the basic elements and molecular mechanisms of auxin catabolism, biosynthesis, and auxin transport. These processes spatiotemporally regulate the auxin concentration gradient. The developmental output is then modified by transducing the auxin gradient to the auxin signaling machinery. Cooperation between these auxin-related regulatory systems also modifies the developmental response to environmental signals (Fukui and Hayashi, 2018).

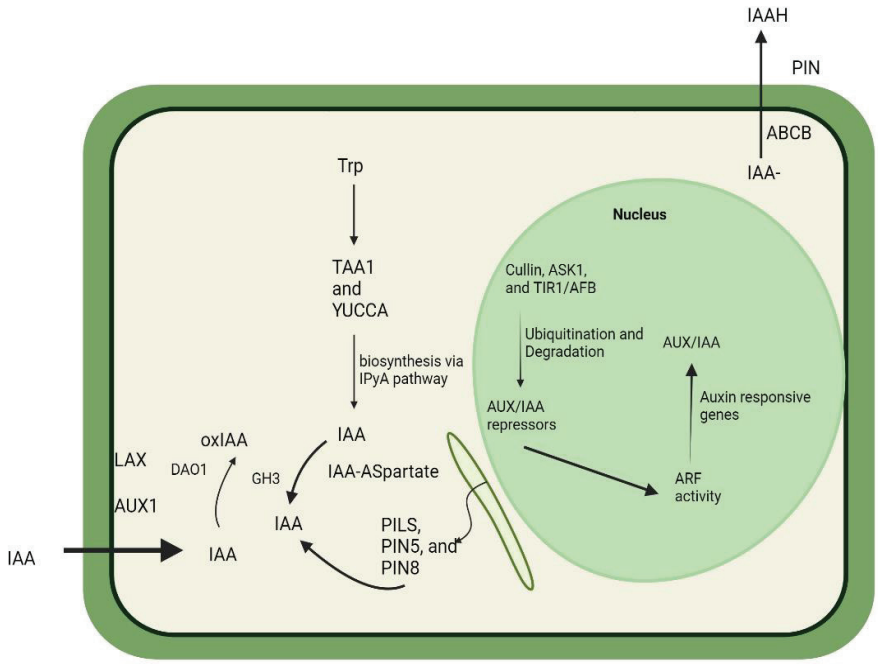

Figure 1.1: Cellular model of signaling, transport, and auxin production. The arrows indicate a pathway of influence with pointed heads indicating a positive influence. *Figure redrawn from- Manipulation and Sensing of Auxin Metabolism, Transport and Signaling, Plant and Cell Physiology, pages-1500-1510, Fukui and Hayashi, 2018. Image created with Biorender.*

1.2 Root System Architecture

Root System Architecture (RSA) comprises of primary root length, number and length of lateral roots and root hairs. Primary roots (PRs) grow downward and anchor the plant system into the soil and lateral/secondary roots (LRs) explore the soil layer for better nutrient acquisition (Figure 1.2) (Waidmann et al., 2020). The formation of lateral roots plays an important role in water, nutrient uptake, and anchorage by plants and hence holds great agronomic importance. A healthy root system is crucial for agriculture

because it directly regulates the plant's ability to grow, produce crops and withstand adverse environmental conditions. A well-developed root system helps improve the plant's water and nutrient uptake capacity as well as fertilizer usage which is essential for maximized crop production. Therefore, the number and location of lateral roots are major determinants of RSA (Dubrovsky and Laskowski, 2017). The molecular aspects of primary and lateral root initiation, organization of lateral root meristem, its growth and emergence and root hair initiation and elongation have been studied extensively in the model plant *Arabidopsis.*

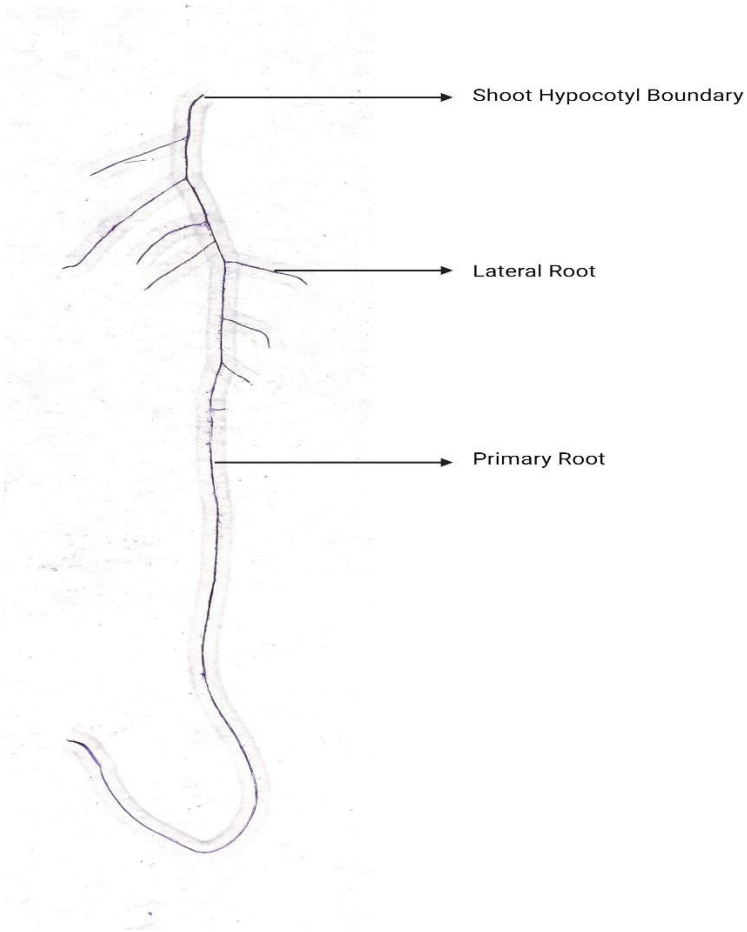

Figure 1.2: Scanned image of *Arabidopsis* root grown for 8 days on standard ATS medium. Different root types are indicated by arrows.

1.2.1 Primary Root Development

The two primary developmental axes of roots are the radial axis, which extends transversally from the vascular bundles to the epidermis, and the proximodistal axis, which extends longitudinally from the root-shoot junction (proximal) to the root apex (distal) (Scheres et al., 2002). At the root tip, the root organizing center consists of the quiescent center (QC), and the surrounding long-term stem cells that make up the stem

cell niche (García-Gómez et al. 2021). The root cap is distal to the QC and the stem cell niche and protects the meristematic cells. The central part of the root cap, known as the columella root cap, is formed from distal stem cells (DSC) (Sabatini et al., 2003; Drisch and Stahl, 2015) and is situated below the quiescent center (Dolan et al., 1993). The lateral root cap (LRC) derives from epidermis/LRC initials, which are positioned laterally to the columella stem cells (Kumar and Iyer-Pascuzzi, 2020). The LRC is a crucial structure for auxin transport and homeostasis in the root meristem (Verbelen et al., 2006, Roychoudhury and Kepinski, 2021).

To create a pattern of auxin distribution in the root tip, distinct PIN transporters are targeted to certain cell membranes in the root apex. Several PINs, but mostly PIN1, are localized to rootward cell membranes in the stele, resulting in a high auxin flux tip ward. Auxin is distributed laterally via PIN3, PIN4, and PIN7 in the root cap's columella cells toward the lateral root cap, from where it is shot through the epidermis by PIN2 and the AUX/LAX proteins (Hu et al., 2021) (Figure 1.3). Auxin is also refluxed back into the rootward stream in the stele at the transition zone through lateral, inward transport by PIN2, PIN3, and PIN7 (Blilou et al., 2005). The topology of PIN proteins in the root apex creates the maximum auxin that positions the stem cell niche (García-Gómez et al. 2021) (Figure 1.3).

Divisions within the stem cell niche produce daughter cells which progress into two different zones of the root. The long-term stem cells divide asymmetrically to form short-term stem cells, which undergo many cell divisions with little expansion. Daughter cells, which are tiny and cytoplasmically dense, accumulate longitudinally in the proximal meristem (PM) (Verbelen et al., 2006). Subsequent cell divisions push the daughter cells further away from the stem cell niche up until the cells reach the transition zone (TZ), where they start elongating instead of dividing. The length and width of cells in the TZ grow slowly (Verbelen et al., 2006), but once the cells move into the elongation zone (EZ), they experience substantial lengthening (up to 300% in 3 hours) with no cell division. Shortly after the EZ comes the differentiation zone (DZ), where the cells cease elongation and acquire their cell-type-specific characteristics and functions (Verbelen et al., 2006; Markakis et al., 2012). While the cells are still in the process of elongation, several signaling mechanisms that induce differentiation start functioning (Datta et al., 2015). Due to this, the region where the process of cell elongation and differentiation overlap is often described as a single zone called "elongation differentiation zone" (EDZ) (Takasuda and Umeda, 2014).

An auxin maximum, localized at the root apex, positions and maintains the stem cell niche and QC (Sabatini et al., 1999; Grieneisen et al., 2007). The auxin maximum is specified during embryogenesis and creates the population of root stem cells in the hypophyseal cell at the base of the embryo. Maintenance of the auxin maximum is critical to controlling the balance between cell division and differentiation in growing

roots, with increased cell divisions contributing to increased root length and differentiation stopping root growth. Auxin concentrations are reduced close to the meristem where daughter cells divide frequently before differentiating. It is important to note that auxin concentrations increase once more within the DZ, as auxin is required for proper cell differentiation (Verbelen et al., 2006). The expression and subcellular localization of auxin efflux transporters of the PIN family are crucial for the development of the auxin maxima in both the embryo and post-embryonic roots (Blilou et al., 2005; Michniewicz et al., 2007; Zourelidou et al., 2014).

The primary root apex's transition from division to elongation is specified by a complicated network of auxin and cytokinin signaling pathways, that support sustainable root growth by establishing TZ and preserving a sufficiently large meristem. The transition from the meristem into the elongation/differentiation zone is facilitated by the activation of cytokinin response factors *ARR12* and, later, *ARR1* (Salvi et al., 2020). Activation of ARR1, a key transcription factor that responds to cytokinin, defines the TZ position (Dello Ioio et al., 2008, Di Mambro et al., 2017). *ARR1* activates the gene *SHY2/IAA3* (*SHY2*), which is a repressor of auxin signaling and negatively controls the PIN auxin transport genes. This leads to auxin redistribution, which in turn triggers cell differentiation. On the other hand, auxin promotes *SHY2* protein breakdown, which promotes PIN activity and auxin redistribution that leads to cell division. Therefore, through cytokinin and auxin both affecting the *SHY2* gene (Figure 1.3), the balance between cell differentiation and division required to control root meristem size and root

growth is achieved (Dello Ioio et al., 2008). *SHY2* gain- and loss-of-function mutant phenotypes are consistent with this model. Seedlings with the *shy2-2* gain-of-function mutant allele have a smaller root meristem and a shorter root (Tian and Reed, 1999; Knox et al., 2003). Conversely, seedlings with the *shy2-31* loss-of-function mutant allele (Knox et al., 2003) continue to accumulate cells in the meristem and display a higher number of meristematic cells, which results in a faster rate of root growth (Dello Ioio et al., 2008).

Recent investigations indicate that both auxin biosynthesis and conjugation are important in regulating auxin levels in the root tip. Establishment of the auxin maximum is cytokinin-independent and reduces auxin in lateral root cap (LRC) via conjugation by the GH family (Di Mambro et al., 2017). Through mathematical modeling, the scientists demonstrated that adjusting the GH expression level perturbed the auxin maximum, altered TZ placement and caused changes in root meristem size (Di Mambro et al., 2017). Recent research has also shown that root growth is affected by tissue-specific auxin production (Roychoudhury et al., 2023).

Auxin preserves stem cell activity by inhibiting the differentiation of distal stem cells (DSC) (Sabatini et al., 2003; Drisch and Stahl, 2015; Ding and Friml, 2010). Local auxin levels are strictly regulated in the root tip and act through the ARF10/16 signaling pathway, which then influences the transcription factors PLETHORA (PLTs) (Figure 1.3) and WUSCHEL RELATED HOMEOBOX5 (WOX5) (Sabatini et al., 2003; Drisch and Stahl,

2015; Ding and Friml, 2010). The *WOX5* expression is suppressed by ARF10 and ARF16 activities and is therefore limited to the QC, where WOX5 is necessary for PLETHORA action (Ding and Friml, 2010). By controlling local auxin levels through the ARF10/16-IAA17/AXR3 signaling pathway, which in turn regulates the production of key transcription factors, PLETHORA (PLTs) and WOX5, auxin sustains stem cell activity in the root tip.

By regulating the gradient distribution of PLTs, auxin in turn affects the positioning of the TZ (Figure 1.3) (Aida et al., 2004; Mähönen et al., 2014; Durgaprasad et al., 2019). PLT genes control root zonation in a dose-dependent manner. In QC, slow cell divisions are regulated by high PLT levels, rapid cell divisions are induced by intermediate PLT levels, and the beginning of cell expansion and differentiation are facilitated by low PLT levels at the TZ. Extended elevated auxin exposure results in a narrow PLT transcription domain close to the stem cell niche, which creates a gradient of PLT protein (Figure 1.3) (Galinha et al., 2007; Mähönen et al., 2014). As cells divide and travel away from the root tip, cell division dilutes the PLT protein enabling the most shootward localized meristematic cells to convert from a division to an elongation state (Mähönen et al., 2014, Salvi et al., 2020). By increasing the PLT expression near the stem cell niche and controlling cell division in the PM, auxin regulates PLT levels and dispersion and thus affects various aspects of root development (Galinha et al., 2007; Mähönen et al., 2014) and hence controls primary root growth.

The intricate connection between auxin-cytokinin-PLT signaling pathway in root growth was further uncovered by recent systems biological techniques. Pacifici et al., (2018) observed that cytokinin regulates both root growth and meristem size. Cytokinin directly inhibits cell division by activating the *KRP2* gene and promotes cell expansion by activating the α-EXPANSIN (EXPA) proteins (Salvi et al., 2020). This suggests that the process of going from division to differentiation involves both the active induction of differentiation and the repression of cell division, rather than only the cytokinin-induced repression of division promoting signals (auxin and PLTs). Auxin homeostasis is impacted by the activity of both *ARR12* and *ARR1*, which raise the expression of *SHY2* and GH3.17 and lower PLT levels (Dello Ioio et al., 2008, Di Mambro et al., 2017). Moreover, ARR1 inhibits cell proliferation through KRP2, which stops PLT2 protein expression. The final meristem size is determined by the combined effects of the ARR1-mediated auxin and cell division antagonist, which severely limit the extent of the PLT gradient (Salvi et al., 2020).

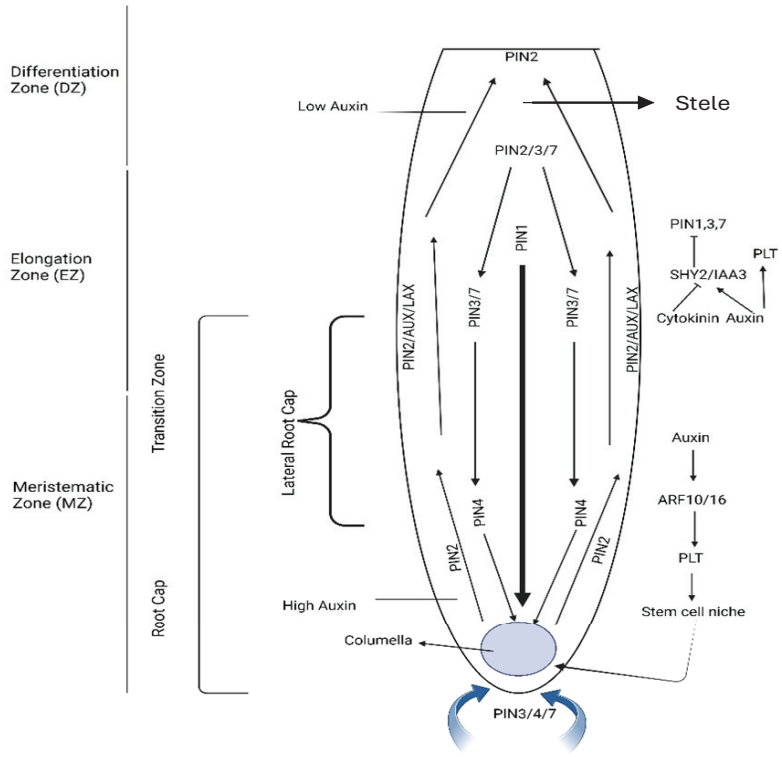

Figure 1.3: Gene expression and auxin transport routes that define *Arabidopsis* main root organization. High levels of *PLETHORA* expression are carefully controlled by coordinated hormone signaling pathways and determine the identity of the stem cell niche. PLT levels are intermediate in the transition zone and further decrease in the elongation-differentiation zone, where cells stop elongating. The meristematic and transition zones' identities are preserved by further antagonistic interactions between auxin and cytokinin, which are partly mediated by the control of *Aux/IAA*, *SHY2/IAA3* levels (Roychoudhury and Kepinski, 2021). The black arrow indicates the transport of auxin downward through the stele via PIN1, PIN3, PIN4 and PIN7. Blue arrows indicate the redistribution pattern of auxin shootward via PIN3 and PIN7. The black arrow with vertical head indicates inhibition and the arrows with pointed heads indicate pathway of influence. *Figure redrawn from- Auxin in Root Development, Cold Spring Harbor Perspectives in Biology, Roychoudhury and Kepinski, 2021. Image illustrated with Biorender.*

1.2.2 Lateral Root Development

In *Arabidopsis* roots, single-layered pericycle and central vasculature tissues are surrounded by layers of epidermal, cortical, and endodermal tissues. The pericycle is a mass of heterogeneous tissue composed of 2 cell types, xylem pole pericycle cell (XPP) and phloem pole pericycle cell (PPP), with different cytological features and cell fate (Beeckman et al., 2001; Himanen et al., 2004; Laplez et al., 2005; Mähönen et al., 2006; Parizot et al., 2008). Lateral roots arise through the division of pericycle cells (Dubrovsky et al., 2000). Based on the characterization of ultrastructure (small vacuoles, dense cytoplasm, and ribosome) and cell division ability (XPP cells last longer than PPP cells in the G2 phase of the cell cycle), XPP cells are considered to be semi-meristematic, whereas PPP cells are quiescent (Beeckman et al., 2001; Himanen et al., 2004; Parizot et al., 2008). As a result, XPP cells are proficient in LR formation (Parizot et al., 2008). Due to proficiency to form the lateral roots, XPP are crucial to maintain the complexity and efficiency of RSA.

1.2.2.1 Lateral Root Positioning

The arrangement of lateral roots (emerged LRs), called rhizotaxis (Laskowski et al., 2008; Hofhuis et al., 2013), is a collective outcome of lateral root primordium (LRP) formation. The oscillation of transcriptional regulators and LRFC specification processes are considered to be critical positioning mechanisms for the spatial distribution of LRP (Dubrovsky et al., 2006; Hofhuis et al., 2013).

1.2.2.2 Pre-patterning of LR initiation Sites Through Oscillation 0f LRFCs

According to the molecular evidence, early LR patterning events initially take place in the root tip and require the periodic transcriptional increase and decrease (oscillation) of auxin-responsive genes. The oscillation provides cellular information and is regarded as the priming step (De Smet et al., 2007). Oscillating expression of the synthetic auxin-responsive promoter *DR5* (*DIRECT REPEAT 5*) fused to the *β-glucuronidase* (*GUS*) reporter gene is observed in the two protoxylem cell files neighboring the XPP cells for a period of 15 hours (De Smet et al., 2007). The region where the dynamic *DR5:GUS* expression pattern takes place is called the oscillation zone (OZ) and it covers the basal meristem and the elongation zone (Moreno- Risueno et al., 2010; Van Norman et al., 2013). By labeling that part of the root tip where *DR5:GUS* expression is anticipated with black toner particles, it was found that *DR5: GUS* expression sites in the basal meristem correlate with subsequent sites of LRP (De Smet et al., 2007). The in-vivo activity of the *DR5* promoter fused to the Luciferase (LUC) *DR5:LUC*; (Moreno- RIsueno et al., 2010) confirms the timing and positioning exhibited by *DR5:GUS*. During oscillation, XPP cells are thought to receive signals from the neighboring *DR5:GUS* marked protoxylem cells (De Smet et al., 2007).

While *DR5:GUS* expression is regarded as a substitute for auxin distribution, it has been suggested that auxin itself is not sufficient for the oscillatory *DR5* behavior in the OZ and the subsequent formation of LR pre-branch sites (Moreno-Risueno et al., 2010; Van Norman et al., 2013). This conclusion was drawn based on the observations that not all

auxin-responsive genes demonstrate the same periodic expression as the *DR5:GUS* reporter in the OZ and that exogenously applied auxin in the OZ fails to trigger new LR pre-branch sites (Moreno-Risueno et al., 2010; Van Norman 2013). Gene expression analysis of the OZ led to the inference that thousands of genes exhibit an oscillation pattern either in phase/antiphase with *DR5:GUS* reporter, and this oscillation reflects a large-scale developmental response (Moreno-Risueno et al., 2010). The initiation of lateral roots is a complex process and involves the oscillatory pattern of multiple genes in the OZ. By determining which cells in the pericycle will become activated to form new lateral roots, the oscillations in gene expression help coordinate the growth of the entire root system.

Periodic gene activities in the OZ at least partially correlate with auxin signaling to position new LRP/LR (Dubrovsky et al., 2006; Hofhuis et al., 2013). Several transcriptional regulators including *ARF7,* and *LATERAL ORGAN BOUNDARIES DOMAIN 16* (*LBD16*) are confirmed to exhibit oscillating expression and function in LR development (Okushima et al., 2007; Moreno-Risueno et al., 2010). Furthermore, aberrant oscillations and irregular pre-branch sites marked by *DR5:LUC* are demonstrated by *arf7* mutants, suggesting that ARF7 plays a crucial role in the periodic gene expression in OZ (Moreno-Risueno et al., 2010).

1.2.2.3 Lateral Root Cap Derived Auxin Modulates Oscillation

The timing and positioning of LRP/LR initiation sites can be influenced by an auxin source residing in Lateral Root Cap (LRC) cells (Casimiro et al., 2001; Swarup et al., 2005; De Smet et al., 2007; Xuan et al., 2015, 2016). This influence was first detected in agravitropic auxin-resistant (*aux1*) mutant roots through a tissue-specific complementation experiment (Swarup et al., 2005; De Smet et al., 2007). Wild type roots demonstrate a wavy pattern, whereas roots of the *aux1* mutant form coils by bending constitutively in one direction (Swarup et al., 2005; De Smet et al., 2007). Additionally, *aux1* mutant roots had reduced oscillatory activity of *DR*5:*GUS* expression in the basal meristem and have fewer LRs that are, for the most part, distributed on the convex side of curve (Marchant et al., 2002; De Smet et al., 2007; Swarup et al., 2005). Both *aux1* agravitropic phenotype and the aberrant branching patterns could be fully rescued through the targeted expression of *AUX1* to LRC (Swarup et al., 2005; De Smet et al., 2007). We can conclude that *AUX1* activation in the lateral root cap is critical for initiation and positioning of lateral roots.

The oscillation amplitude, as determined by the *DR5:LUC* intensity in the OZ, is positively modulated by the lateral root cap IBA-to-IAA conversion efficiency (the conversion of auxin precursor Indole-3-Butyric acid (IBA) to the Indole-3-Acetic acid (IAA)) (De Rybel et al., 2012; Xuan et al., 2015). The importance of IBA to IAA conversion was revealed by a small molecular screen that identified Naxillin as a non-auxin molecule required for LR

initiation. Naxillin was found to stimulate the conversion of IBA to IAA (De Rybel et al., 2012). As revealed by the tissue-specific analysis, this pathway is particularly active in the outer LRC cells and produces IBA-derived auxin, which is predicted to be transported towards the OZ via *AUX1* (Xuan et al., 2015, 2016).

1.2.2.4 Lateral Root Founder Cell Specification

LRFCs are those XPP cells that will divide asymmetrically to generate a stage 1 LRP. LRFC specification and activation take place in the differentiation zone of the root, where other cells have stopped dividing and growing and have differentiated. It is unknown whether XPP cells remain undifferentiated or dedifferentiate before redifferentiating into LRFCs (Dubrovsky et al., 2000; Laskowski et al., 1995; Malamy and Benfey, 1997). The first sign that certain XPP cells have developed an LRFC identity is the activation of *DR5* expression (Dubrovsky et al.,2008). XPP cells at one side of the xylem pole express the *DR5:GFP* reporter before LR initiation. According to Moreno-Risueno et al. (2010), prebranch sites are static points of *DR5:LUC* expression that arise at the periodic oscillation peak of *DR5* in the protoxylem (Dubrovsky et al., 2008). Clonal sectors with high auxin were created randomly in the roots, including patches in XPP, using a heat-shock inducible system expressing the auxin biosynthetic enzyme indole acetic acid tryptophan monooxygenase (iaaM) (Dubrovsky, et al., 2008). Auxin-producing pericycle sectors gave rise to additional LRP, suggesting that LRFCs could be specified by a local auxin input regardless of the tissue context along the primary root (Dubrovsky, et al., 2008).

The spacing of LRFCs is proposed to be partially controlled by the wavy root growth described above. Laskowski et al., (2008), based on an in-silico root system, suggested that variable XPP cell geometry between the two sides of the curve where cells are slightly stretched on the convex side and compressed on the concave side might function as a trigger to ascertain the sidedness of LRFCs. Compared to other cells, the stretched XPP cells are proposed to be better suited to create a potent new auxin maximum (Laskowski et al., 2008). Laskowski further suggested that founder cells are inhibited from being specified in the distal rootward region by the existing LRFCs because the formation of a robust new auxin maximum in the selected XPP cell depletes auxin in the surrounding cells. This lateral inhibition seems to require proper expression of auxin influx and auxin efflux carriers (Laskowski, M. et al., 2008), since altered branching patterns, with closely grouped, or even sometimes fused LRP/LRs or fewer LRP/LRs have been observed in the mutants that alter auxin polar transport and signaling, such as *pin2*, *pin3*, *pin7*, weak alleles of *gnom*, *shy2* (*Short hypocotyl 2*/ *iaa3*; gain of function), *bdl* (*bodenlos*/ *iaa26*; gain of function) mutant roots (Geldner et al., 2004; Laskowski et al., 2008; De Smet et al., 2008; Goh et al., 2012b; Okumura et al., 2013).

Several factors downstream of auxin are potential candidates for LRFC specification. For example, the auxin regulatory *GATA23* transcription factor (De Rybel et al., 2010) is expressed in XPP cells that leave the basal meristem, and *GATA23* expression marks LRFC and LRP at early stages (De Rybel et al., 2010) (Figure 1.4). Altered number and

spacing of LRP and LRs are observed in *GATA23* loss and gain of function mutants, providing further evidence for a role in LRFC specification (De Rybel et al., 2010). *GATA23* expression is regulated by an auxin signaling cascade involving IAA28 and its interacting ARF binding factors (ARF 6,7,8 and 9) in the basal meristem (De Rybel et al., 2010) (Figure 1.4) . A downstream molecular component of the IBA-to-IAA pathway called MEMBRANE-ASSOCIATED KINASE REGULATOR-4 (MARK4) is another candidate regulator of LRFC specification (Xuan et al., 2015).

1.2.3 Lateral Root Initiation

The second phase of lateral root development is lateral root initiation, which is signaled by prior asymmetric cell division (ACD). Prior to ACD, pairs of founder cells expand radially, and nuclei travel toward the common cell wall, where radial expansion is the greatest (De Smet et al., 2006; Goh et al., 2012). During migration, the spindle-like nuclear shape is transformed to a nearly round shape. This nuclear shape transformation is regarded as the sign of LRFC activation and an indicator for the start of LR initiation. The first anticlinal cell division occurs in adjacent founder cells 4-7 hours after nuclear repositioning (Figure 1.4). Asymmetric division gives rise to two short daughter cells surrounded by two longer cells (Casimiro et al., 2001; Dubrovsky et al., 2001; De Smet et al., 2008; De Rybel et al., 2010; Lucas et al., 2013; Fernandez et al., 2015; Von Wangenheim et al., 2016). When the first formative divisions are accomplished and the proper daughter cell fates are established, LR initiation is completed (De Smet et al., 2006) (Figure 1.4).

1.2.3.1 Signaling Inputs Required for Cell Division

Auxin biosynthesis, transport, and signaling play an important role in the establishment of cellular patterning and promote cell division and meristem maintenance. Auxin biosynthesis activation and auxin influx carrier AUX1 create and maintain an auxin maximum in specified LRFCs (Laskowski et al., 2008; Tang et al., 2017) (Figure 1.4). The expression of the auxin biosynthetic gene *YUCCA4* in LRFCs is induced by the interaction between plant specific B3 transcription factor FUSKA3 (FUS3) and LEAFY COTYLEDON2 (LEC2) (Tang et al., 2017). SOLITARY-ROOT (SLR)/ IAA-14-ARF7/ARF19 module is an important auxin signaling component for LR initiation, in which ARF7 and ARF19 transcription factors are de-repressed by the auxin-induced degradation of labile SLR proteins and activate downstream gene expression (Fukaki et al., 2002, 2005; Okushima et al., 2005; Wilmoth et al., 2005) (Figure 1.4). Both dominant-negative *slr* and loss of function *arf7* and *arf19* mutant roots virtually lack LRP and LRs (Fukaki et al., 2002, 2005; Okushima et al., Wilmoth et al., 2005). In plants with slow-degraded SLR variants, resulting from different point mutated *SLR* alleles, LRP/LR density decreases, suggesting that LRP/LR density negatively correlates with the SLR degradation rate and that for LR initiation, SLR degradation acts as an auxin-initiated timer (Guseman et al., 2015).

Initiation of mitosis in the LRFCs is regulated by auxin. The cell cycle-associated B-type cyclin, CYCB1;1, which marks the G2-M transition, is strongly expressed in LRFCs undergoing the first division (Himanen et al., 2002; Vanneste et al., 2005). Entry into mitosis during LR initiation is driven by SLR and *ARF7/ARF19*, as indicated by the

absence of *CYCB1;1* expression in *slr, arf7* and *arf19* mutant roots (Vanneste et al., 2005; Okushima et al., 2007). The effects of SLR and ARF17/19 on the cell cycle may be through the members of the LBD protein family, which are direct downstream targets of *ARF7* and *ARF19* (Figure 1.4). LBD proteins play a crucial role in LR development and initiation (Okushima et al., 2005,2007; Bercmans et al., 2011; Goh et al., 2012a), and bind the promoter of the *E2Fa* gene, which encodes a transcriptional activator of cell cycle genes (Berckmans et al., 2011; Du and Scheres, 2017).

As well as the SLR-mediated auxin signaling in LRFCs, auxin-induced mechanical signaling in the endodermal cells adjacent to the pericycle plays a crucial role in LR initiation (Vermeer et al., 2014; Vermeer and Geldner, 2015). *SHOOT HYPOCOTYL 2* (*SHY2*) degradation results in endodermal cell volume loss and allows the subsequent cell division to initiate LRP, by accommodating the turgidity of underlying LRFCs (Vermeer et al., 2014) and triggering the swelling of XPP cells (Marhavy et al., 2016). Cell divisions induced by endodermal cell ablation (ECA) are frequently periclinal and do not result in the formation of LRP (Marhavy et al., 2016). Following ECA, auxin treatment of pericycle cells can reposition the cell division plane to the usual anticlinal pattern (Du and Scheres, 2017).The auxin-induced repositioning of the cell division plane involves PIN3 (Marhavy et al., 2013). When nuclear migration takes place, PIN3 is transiently induced in the endodermal cells overlying LRFCs (Marhavy et al., 2013), where PIN3 localizes toward the inner membrane adjacent to the LRFCs, resulting in auxin transport from the endoderm to pericycle founder cells (Figure 1.4). In *pin3* mutant roots, LRFC asymmetric

cell divisions are temporarily delayed suggesting that PIN3 stimulates LR initiation (Marhavy et al., 2013).

1.2.4 Lateral Root Outgrowth

Primordium patterning and growth are regulated by developmental signals within the primordium itself and these signals help to specify the LR and meristem tissues. At the final stage of LR outgrowth, a dome-shaped primordium emerges from the primary root as an LR through the cell growth and subsequent rounds of anticlinal, periclinal and tangential cell division (Lucas et al., 2013; von Wangenheim et al., 2016). The emerged LRs have a fully functional meristem that highly resembles the primary root meristem (Scheres, 2007; Bennett and Scheres, 2010).

Root segments containing LRP can give rise to LRs on growth medium without additional auxin supply (Laskowski et al., 1995), suggesting that an autonomous functional meristem has formed in the primordium with as few as 3-5 cell layers (Laskowski et al., 1995). QC marker expression is confined to the stem cell niche at this developmental stage (Goh et al., 2016). Re-localization of PIN proteins (mainly PIN1) is required for the proper establishment of an auxin maximum in the primordium, which leads to the formation of a *de novo* meristem (Benková et al., 2003; Péret et al., 2009a; Márhavy et al., 2011, 2014). Auxin distribution is often modulated by cytokinin, which can regulate the direction of auxin flow during LR outgrowth (Márhavy et al., 2011, 2014). Cytokinin modulation of PIN1 endocytic recycling causes PIN1 depletion at specific cellular

domains, leading to a rearrangement of PIN1 membrane localization and thus affecting the auxin distribution within plant tissues and organs (Márhavy et al., 2014).

During LR outgrowth, the auxin-regulated *PUCHI* gene, which encodes an APETALA2-like transcription factor and functions downstream of ARF7/ARF19, is also involved in the specification of primordium boundaries (Hirota et al., 2007; Kang et al., 2013). In the early developmental stages, *PUCHI* is expressed in all the primordium cells. After that, expression becomes gradually restricted to the peripheral margin of the primordium (Hirota et al., 2007). Additive phenotypes are observed in double and triple *puchi* and *lbd* mutants indicating that *PUCHI* co-acts with *LBD* genes, *LBD16* and *LBD18*, to specify primordium boundaries (Kang et al., 2013).

1.2.5 Lateral Root Emergence

Mutual interaction between the growing primordium and its overlying tissues, including the endodermis, cortex, and epidermis, is required for LR emergence (LRE). At the beginning of LR emergence, the LRP first encounters the endodermis. The changing shape of the overlying endodermal cells that began at LR initiation continues during the outgrowth of the primordium (Vermeer et al., 2014). Endodermal cell walls contain a ring-like supracellular hydrophobic thickening called the Casparian strip that sets up the apoplastic diffusion barrier between the endodermal cells (Naseer et al., 2012; Lee et al., 2013b; Vermeer et al., 2014). These cells undergo cell volume loss and become progressively flattened to such an extent that the plasma membranes from both sides

fuse, resulting in cell death (Vermeer et al., 2014). During this process, local degradation consolidates diffusion barriers between the LRP and the endodermis preserving the Casparian strip integrity and the isolation of the vascular bundle from the outside (Vermeer et al., 2014; Vermeer and Geldner, 2015). Penetration of the primordium through the endodermis is initiated by a localized opening in the endodermal cell layer (Kumpf et al., 2013; Vermeer et al., 2014). In the endodermal cells directly overlying the LRP, auxin inducible peptide IDA (INFLORESCENCE DEFICIENT IN ABSCISSION) signaling via HAE (leucine-rich repeat receptor-like kinase HAESA) causes expression of enzymes which break down cell walls and create an opening for the growing LR (Kumpf et al., 2013).

The emergence of LR from the cortex and epidermis is regulated by auxin transport and signaling (Marchant et al., 2002; Swarup et al., 2008; Péret et al., 2013; Porco et al., 2016). A fast “dome-shaped” transition is associated with emergence from the cortical and epidermal cells (Kumpf et al., 2013; Lucas et al., 2013; Von Wangenheim et al., 2016). This shape change is independent of increased cell proliferation and probably results from radial cell expansion due to the release from the physical constraints of the overlying tissues (Lucas et al., 2013; Von Wangenheim et al., 2016). Unlike endodermal cells that are tightly connected during LR emergence, cortical and epidermal cells are pushed away due to a loss of cell-to-cell adherence (Laskowski et al., 2006; Péret et al., 2009b; Kumpf et al., 2013; Vermeer and Geldner, 2015). Shoot derived auxin is crucial for LR emergence (Marchant et al., 2002; Swarup et al., 2008; Péret et al., 2013). The

auxin is diffused from the LRP tip during LR emergence and is governed by IAA14/SLR-ARF7,19 and IAA3/SHY2-ARF7 signaling pathways (Swarup et al., 2008) (Figure 1.4). To coordinate cell separation during LR emergence, sequential *LBD29* and *LAX3* induction are necessary (Porco et al., 2016). The auxin SLR-ARF7 signaling pathway (Swarup et al., 2008; Lavenus et al., 2015; Porco et al., 2016) is a direct positive *LAX3* regulator (Okushima et al., 2007; Porco et al., 2016) (Figure 1.4). To ensure that cell separation occurs exclusively from their shared walls, spatially precise *LAX3* expression is restricted to the adjacent cortical cell files (Péret et al., 2013). *LBD18* acts downstream of *LAX3* and it is expressed in the overlying cortical and epidermal cells where it upregulates a subset of *EXPANSIN* (*EXP*) genes, which encode non-hydrolytic cell-wall loosening biomolecules and allow LR emergence (Kim and Lee, 2013; Lee et al., 2013, 2015; Lee and Kim, 2013).

LR emergence is also regulated by water flow between LRP and the overlying tissues (Péret et al., 2012; Vilches-Barro and Maizel, 2015). A water reflux model whereby water transport from the overlying tissues to the primordium is encouraged, while water uptake in the overlying tissues is repressed, is crucial for LR emergence (Péret et al., 2012; Vilches-Barro and Maizel, 2015). By depleting water in the overlying tissues, this mechanism decreases the resistance of overlying tissues to the expansion of the growing LRP (Péret et al., 2012). Water influx into LRP requires plasma membrane channels called Aquaporins (Péret, et al., 2013). Aquaporins can be divided into several sub-families whose members typically respond negatively to auxin (Péret et al., 2012). In

tissues overlying LRP, aquaporin-dependent water transportation is negatively regulated by auxin (Péret et al., 2012). As the LRP forms, the highly expressed aquaporin PIP2;1 is retained at the LRP base and in the underlying vascular tissues of the primary root but is gradually excluded from the auxin response maximum within the LRP. According to modeling, lateral root emergence is slowed by the positive and negative perturbations of *PIP2;1* expression, which change the water flow into LRP (Péret et al., 2012). In later developmental stages, enhanced callose deposition in the plasmodesmata causes symplastic isolation of LRP from the vasculature (Benitez-Alfonso et al., 2013).

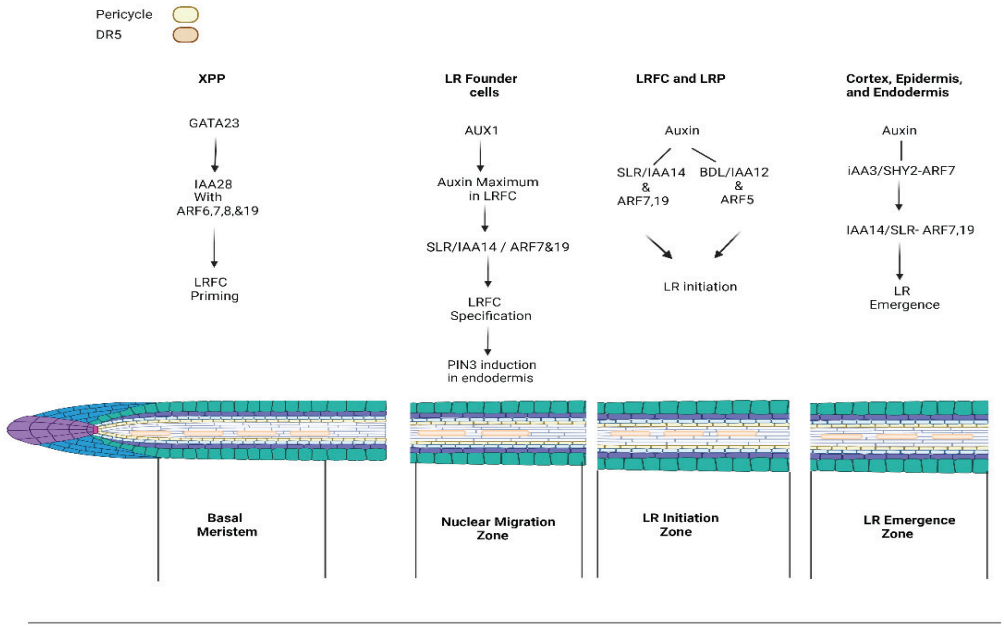

Figure 1.4: Through a variety of auxin-transport and signaling regulated modules, auxin regulates the development of lateral roots. The different root zones are shown in different colours. The arrows indicate a pathway of influence, with pointed heads indicating a positive influence. *Figure redrawn from- Lateral root development in Arabidopsis: fifty shades of auxin, Trends in Plant Science, Lavenus et al., 2013. Image illustrated with Biorender.*

1.3 Root Hair Development

Root hairs are outgrowths of epidermal cells that occur near the tip of a plant root. They are necessary for efficient nutrient uptake, microbe interaction and plant anchorage. The response of root hair initiation and elongation to environmental factors is a crucial

strategy that alters the number and length of root hairs and allows plants to cope with the surroundings (Shibata and Sugimoto, 2019). Epidermal cell fate and growth of root hairs can be influenced by the availability of nutrients such as P, Fe, N, Mg, and Zn, along with some phytohormones including auxin, ethylene, and abscisic acid (Grierson et al., 2014). For example, the elongation of root hairs is promoted in low phosphate environments and repressed in high phosphate environments (Shibata and Sugimoto, 2019).

1.3.1 Cell Fate Specification

Early root development leads to the differentiation of epidermal cells into either trichoblast (root hair forming cells), or atrichoblasts (non-hair forming cells). Generally, the root epidermis follows one of 3 strategies for epidermal cell specification (Datta et al., 2011). In plants that follow type-1 patterning, such as rice, root hairs develop randomly, and all the epidermal cells have the potential to differentiate into root hairs. In plants like *Brachypodium* that follow type-2 pattern, asymmetric cell division causes the smaller daughter cell to acquire root hair identity and the larger daughter cell to become a non-hair cell. For plants like *Arabidopsis* that adopt type 3 patterning, the position of cells determines root hair identity. In these plant species, epidermal cells with two underlying cortical cells become hair cells, whereas those with only one underlying cortical cell become non-hair cells (Datta et al., 2011). In *Arabidopsis*, the absence (trichoblasts) or presence (atrichoblasts) of the homeodomain-leucine zipper transcription factor GLABLA2 (GL2) determines the fate of the epidermal cell at an early

stage of development via a complex regulated pathway (Balcerowicz et al., 2015; Schiefelbein et al., 2014) (Figure 1.5).

Auxin distribution triggers the process 'root hair priming' where specific cells in the root epidermis are prepared to form root hairs. Auxin also establishes the planar polarity of trichoblasts and controls root hair outgrowth (Jones et al., 2009; Leyser, 2018). Severe root hair spacing, shape, and length abnormalities have been identified in major auxin signaling and transport mutants (Leyser,2018; Park and Nebenführ, 2013; Fischer et al., 2007; Pitts et al., 1998; Velasquez et al., 2016). Trichoblasts and atrichoblasts have different auxin levels due to unique intercellular trafficking of PIN2. Trichoblasts have quicker PIN2 internalization rates and lower protein levels at the PM (Löfke et al., 2015). As a result, atrichoblasts have higher auxin levels and are thought to act as auxin repositories for trichoblasts (Dolan and Davies, 2004).

1.3.2 Root Hair Positioning

According to Ikeda et al. (2009), auxin controls the outgrowth of the root hair from the basal (root-ward) end of the cell, which is known as planar polarity. The placement and length of root hairs are influenced by the ethylene-dependent regulation of auxin production in the root meristem (Ikeda et al., 2009). To establish the planar polarity of root hairs, intercellular auxin transport from its local biosynthetic maximum in the root meristem into the differentiation zone is necessary, involving AUX1/LAX and PIN2 carriers (Ikeda et al., 2009).

Consistent with the hypothesis that an auxin gradient plays a role in root hair positioning, adjusting the auxin gradient along the root can change the positioning of root hair along the trichoblast (Fischer et al., 2006; Ikeda et al., 2009). For example, the root hair location of mutants with defects in root tip auxin biosynthesis is shifted shootward (Ikeda et al., 2009). In contrast, root hairs appear at more rootward locations along the trichoblast cells when this gradient is flattened, as in *aux1,* ethylene-insensitive2 (*ein*2), and $gnom_{eb}$ (gn_{eb}) triple mutant. By applying auxin rootward of the differentiation zone, proper rootward placement of root hairs can be recovered in these *aux1*, *ein2*, and $gnom_{eb}$(gn_{eb}) triple mutants (Fischer et al., 2006). Interestingly, by applying auxin shootward of the differentiating hair, root hair location can be skewed to the shootward end (Ikeda et al., 2009).

1.3.3 Root Hair Elongation

Root hairs expand to attain their maximum size due to cytoskeletal rearrangement and exocytosis of vesicles at the root hair tip (Rounds and Bezanilla, 2013; Takatsuka and Ito, 2020; Žárský et al., 2009). Well-studied cellular elements necessary for root hair growth and elongation include: auxin gradients and signaling (dependent on PIN2 action), RHO-RELATED PROTEIN FROM PLANTS 2 (ROP2) positioning, cytoskeleton rearrangement induced by cell wall remodeling, the signaling molecules ROS and Ca2+, expansion of PM and cell wall via exocytosis, and vacuole expansion (Retzer and Weckwerth, 2021) (Figure 1.5).

When shootward auxin transport is disrupted due to the knockout mutation in PIN2 or AUX1, root hairs are shorter compared to the Wt (Leyser, 2018; Velasquez et al., 2016). Auxin activates signaling cascades and the transfer of structural proteins to the PM, which alter the composition of the cell wall and initiate loosening, an important process during cell elongation (Majda and Robert, 2018; Franck et al., 2018).

Just before the developing root hair bulge is apparent (Fu et al., 2002), ROPs migrate to the PM region of the trichoblast where they polarize subcellular structure and permit root hair elongation (Fu et al., 2002; Denninger et al., 2019) (Figure 1.5). Together with ROS, ROP proteins help regulate a positive feedback loop necessary for root hair tip growth (Vernoud et al., 2003; Vanneste and Friml, 2009; Xu et al., 2010) (Figure 1.5). Plants overexpressing ROP2 produce multiple root hair outgrowths per trichoblast (Yang et al., 2007) and longer root hairs, compared to the Wt plants (Jones et al., 2002) suggesting that all stages of root hair development require proper functioning of ROP2 (Retzer and Weckwerth, 2021).

Positioning of ROP accumulation is a complex process requiring numerous factors. ROP2 is positioned in the PM by the Kinase FERONIA (FER), which then stabilizes actin filaments there (Duan et al., 2010; Zhu et al., 2020) (Figure 1.5). The *fer* mutants demonstrate poor auxin-induced root hair growth, which can be restored by overexpressing ROP2 (Duan et al., 2010). Because of ROP2 expression and FER activity, PIN2 accumulates at the root tip and PM is stabilized through actin configuration (Lanza

et al., 2012; Singh et al., 2014) (Figure 1.5). Due to improper F-actin cytoskeleton assembly, which prevents the creation of an appropriate auxin gradient, the *fer*4 mutant exhibits abnormal PIN2 polarity in the root tips (Dong et al., 2018). YPT-INTERACTING PROTEIN 4a and YPT-INTERACTING PROTEIN 4b, which are located in the trans-Golgi network, are involved in the activation and accumulation of ROPs in the plasma membrane during hair initiation (Gendre et al., 2019). PHOSPHATIDYLINOSITOL-4-PHOSPHATE5-KINASE3 (PIP5K3) also establishes the accumulation site for ROP2 (Figure 1.5), and its overexpression causes multiple root hairs to emerge from a single trichoblast and shorter root hairs (Jones et al., 2002; Kusano et al., 2008).

ROP2 and FER activate ROS accumulation, which is required for root hair tip outgrowth because it modifies cell wall characteristics (Monshausen et al., 2007), cytoskeleton composition, PM rearrangement, and the quantity and distribution of secondary messenger, Ca2+ (Jain et al., 2018). ROP2 together with FER signaling (Zhou et al., 2020; Jones et al., 2007; Gu and Nielson, 2013) act via NICOTINAMIDE ADENINE DINUCLEOTIDE PHOSPHATE-OXIDASE (NOX) to produce ROS required for root hair elongation (Zhou et al., 2020; Chapman et al., 2019; Foreman et al., 2003) at the growing root hair tip (Jones et al., 2007; Duan et al., 2010). ROS is also activated by absence of GL2 in trichoblasts, which induces the transcription factor RHD6, that, by activating its homolog RHD6-LIKE1 (RSL4), induces the formation of ROS (Vijaykumar et al., 2016; Datta et al., 2015; Yi et al., 2010). ROS accumulation activates calcium channels in root hair cells, which in turn increases ROS production creating a positive

feedback loop (Grierson et al., 2014). The calcium gradient at the root hair tip (Grierson et al., 2014) helps deliver exocytic vesicles carrying cell wall components to the growing cell wall by enabling the vesicles to fuse with the apical plasma membrane (Pei et al., 2012), and determines the direction of root hair growth (Grierson et al., 2014). The positive feedback loop of ROS also causes differential bundling of microtubules and actin at the root hair tip (Baluška et al., 2000; Molendijk et al., 2001) facilitating changes in PM composition (Yalovsky et al., 2008) including PIN2 accumulation and stabilization at the root hair tip.

Exocytosis of vesicles that supply freshly produced PM and cell wall components to the developing root hair tip are critical for polar tip development (Grierson et al., 2014; Synek et al., 2006; Drdová et al., 2013; Ovečka et al., 2005). To keep the increasing root hair from bursting, cell wall integrity must be maintained during root hair tip expansion (Franck et al., 2018 ; Westermann et al., 2019). Phosphoinositides (PI) play a crucial role in membrane trafficking and subsequent root hair growth. As *Arabidopsis* root hair cells grow, a unique trans-Golgi network compartment with a developmentally controlled polar distribution is labeled by the RabA4b GTPase. Plant phosphatidylinositol 4-OH kinase, PI-4Kβ1, is selectively recruited by GTP-bound RabA4b; other PI-4K families are not recruited. PtdIns(4,5)P2 are localized to the elongating root hair apex by PIP5K3, which is also a major regulator of the machinery that starts and encourages root hair tip growth (Kusano et al., 2008; Stenzel et al., 2008) (Figure 1.5). Several kinases, including PHOSPHATIDYL INOSITOL 4-OH KINASE BETA 1 and 2 (PI4Kβ1, PI4Kβ2), which are crucial

for the control and transport of secretory cargo to the tip of developing root hair, interact to maintain the composition of the membrane (Preuss et al., 2004; Preuss et al., 2006; Thole et al., 2008). Additionally, through facilitating the recruitment of proteins with PI-4P or PI-4, 5P2 binding domains, which regulate tip elongation (Yoo et al., 2012; Bubb et al., 1998), 1-PHOSPHATIDYLINOSITOL-4-PHOSPHATE5-KINASE3 (PIP5K3) is necessary for proper tip growth control in root hairs (Kusano et al., 2008; Stenzel et al., 2008) (Figure 1.5).

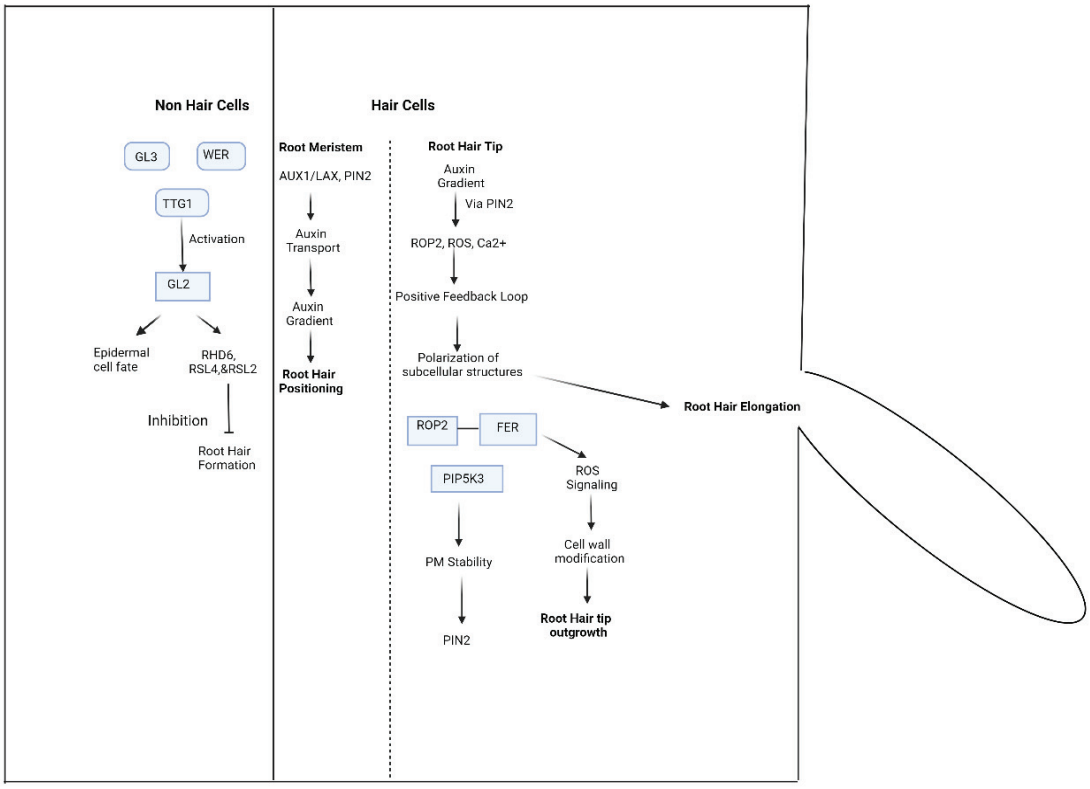

Figure 1.5: Genetic regulatory mechanism of root hair development. Auxin efflux transporter PIN2 and auxin signaling-mediated pathways regulate root hair initiation and elongation. Arrows indicate a pathway of influence with pointed heads indicating a positive influence and the vertical lines indicating inhibition. *Figure Inspired from- A gene regulatory network for root hair development, Journal of Plant Research, Shibata and Sugimoto, 2019. Image illustrated with Biorender*.

1.4 Effects of Phosphorus on Root System Architecture

Plants require specific macronutrients (N,P,K) and some micronutrients for optimum growth and development. Plant growth is significantly affected due to the absence of these nutrients. Inorganic phosphate (P_i) is an important constituent of various critical organic molecules and is necessary for optimum plant development. A very low

percentage of organic phosphate is available to plants due to its low mobility and poor distribution in the soil. Additionally, microbial activity could also transform P_i to organic phosphate which is not accessible by plants (Crombez et al., 2019).

Plants adopt various mechanisms to cope with phosphate scarcity. Plants tend to allocate more carbon from the shoot to the root under phosphate derivation, thus altering the root-to-shoot ratio which is a common developmental strategy to deal with phosphate deprivation (Crombez et al., 2019). Phosphate deficiency has been extensively studied in the model plant *Arabidopsis* (Crombez et al., 2019). Under low phosphate concentration, shorter primary root and more lateral roots have been observed in *Arabidopsis*. These developmental changes allow the plant to explore larger soil patches and thus acquire phosphate. Most of these developmental changes are regulated by the phosphate starvation response factor (PHR1) (Crombez et al., 2019).

1.4.1 Effects of phosphate deprivation on PR development

Phosphate deprivation results in the inhibition of primary root growth. Primary root inhibition occurs due to the reduction in the size of the root meristem. The meristematic region is situated just above the stem cell niche. Several transcription factors like SCARECROW (SCR), SHORTROOT (SHR), and PLT regulate the WOX5 which positively regulates the stem cell fate (Crombez et al., 2019). It has been proposed that PR growth under low phosphate concentrations is not entirely regulated by P_i-deprivation signaling

pathways. These responses could be regulated by multiple hormone signaling pathways and thus could be PHR1 independent (Crombez et al., 2019).

Iron (Fe) is proposed to be a key regulator of PR inhibition under low phosphate conditions. Iron (Fe) is redistributed towards the stem cell niche because of Fe^{2+} converting to Fe^{3+}. In the apoplast, Fe^{2+} serves as a source of Reactive Oxygen Species (ROS) (Crombez et al., 2019). The SHR protein cannot move the way it should when ROS produce callose to obstruct the plasmodesmata that connects the plant cells. This obstruction can result in decreased amounts of the WOX5 protein, which is critical for maintaining the health and proliferation of the root stem cells (Crombez et al., 2019). Although Fe is a key regulator of P_i-starvation induced root growth inhibition, P_i-starvation signaling also helps to regulate the response. There should be a balance between low P_i and high Fe suggesting that P_i-Fe ratio is a vital regulator of PR growth inhibition. PHR1 is an important factor for PR growth inhibition although sometimes this response could be independent of PHR1 (Crombez et al., 2019). The gene FERRITIN (FER) is required for Fe-homeostasis, induced by PHR1. Apart from this it also has been suggested that PHR1 interacts with multiple hormone signaling pathways that are required for the maintenance of stem cell niche (Crombez et al., 2019).

Previous studies propose that the inhibition of primary root under low phosphate conditions are regulated by multiple hormone signaling pathways. For example, cytokinin activates the cytokinin response factors (CRF) ARR1 and ARR12 that in turn

inhibit the activity of WOX5 and SCR. These findings demonstrate that P_i-dependent root growth inhibition includes cytokinin-dependent factors which could be potential PHR1 targets including ARR1 and ARR12 (Figure 1.6). PLT transcription factors are regulated by auxin in a dose-dependent way. Cell differentiation is inhibited in the QC due to the high levels of auxin maxima (Crombez et al., 2019). On the contrary, higher up in the root, the auxin levels decrease and result in more cell differentiation. In addition, root meristem development requires the activity of auxin biosynthesis via YUCCA (YUC) and auxin transport regulated by PIN transporters and phospholipase (PLD2) (Crombez et al., 2019) (Figure 1.6). Accumulation of auxin in the QC via the polar transport of auxin is necessary to maintain the root meristem size (Figure 1.6). This polar transport is mediated by different auxin transporters. Activity of these PIN transporters is positively regulated by CRFs and downregulated by SHY2/IAA3 (Figure 1.6). Gibberellin-dependent factors which are activated by cytokinin response regulators ARR1 and ARR12 cause the degradation of SHY2/IAA3 (Figure 1.6). Therefore, all these findings suggest that multiple hormone signaling pathways are involved in primary root growth inhibition under phosphate deprivation (Crombez et al., 2019).

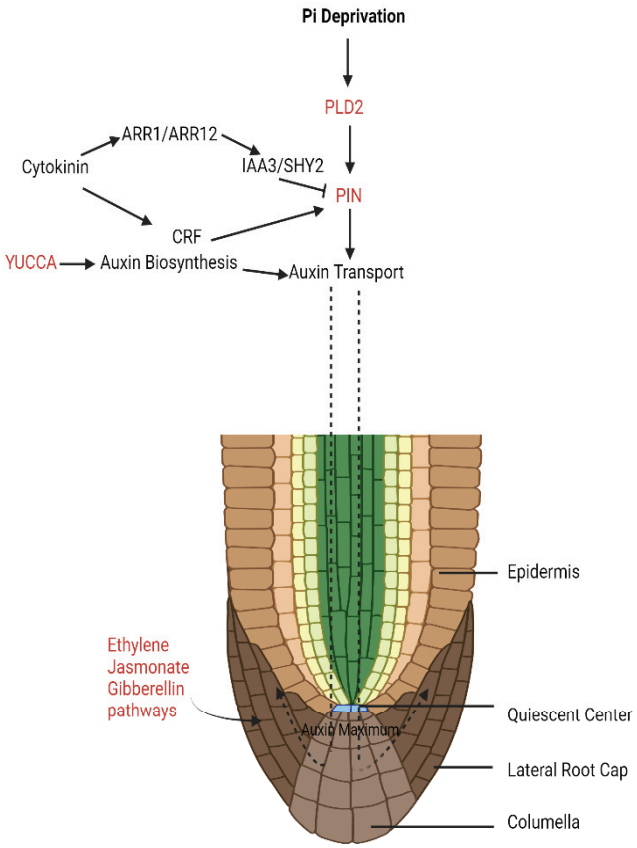

Figure 1.6: Diagram of a root tip showing pathways involved in reduced primary root growth under inorganic phosphate deprivation. The different root zones are shown in different colours. Arrows indicate a pathway of influence, with pointed heads indicating positive influence and vertical lines indicating inhibition. The dashed lines indicate the accumulation of auxin in the quiescent center. At low phosphate, the cell division is reduced in the root apical meristem resulting in shorter primary root possibly via auxin, ethylene, jasmonate, and gibberellin regulated pathways. Potential phosphate starvation response factor (PHR1) targets are indicated in red. *Figure redrawn from- Tackling Plant Phosphate Starvation by the Roots, Developmental Cell, Crombez et al., 2019. Image illustrated with Biorender.*

1.4.2 The Complex Interaction between Phosphate Deprivation and Lateral Root Development

Considering lateral roots are crucial for P_i uptake, higher fitness has been observed in species or genotypes that exhibit lateral root induction under P_i deficient conditions. Root tips are considered hotspots for P_i because the root cap acts as a protective structure covering the root tip and an important site of Pi uptake (Crombez et al., 2019). In *Arabidopsis*, members of the PHOSPHATE TRANSPORTER 1 (PHT1) family are most important for P_i uptake and are primarily expressed in the root cap and as a result a significant portion of phosphate uptake occurs in this region . The increased number of lateral roots not only increases the foraged soil volume but also creates substantial uptake potential caused by expanded number of root tips. As a result, formation of lateral root is a common developmental strategy adopted by *Arabidopsis* under phosphate deficiency (Crombez et al., 2019).

In *Arabidopsis*, P_i deprivation causes enhanced auxin signaling, especially in the root tip and lateral root primordia. Both enhanced auxin levels and enhanced expression of auxin receptor TIR1 were observed in these tissues under low phosphate availability (Figure 1.7). As described earlier, lateral root initiation relies on auxin and TIR1 dependent auxin signaling, but the mechanism by which they relate to Pi-deprivation signaling is still unknown (Crombez et al., 2019). TIR1 was found to act as a co-receptor with PHR1 (Phosphate Starvation Response Factor), suggesting a reasonably direct correlation among Pi-deprivation, auxin signaling and lateral root development (Figure

1.7). Polyphosphorylated inositol hexaphosphate (IP6, InsP6) is a versatile signaling carbohydrate that drops under low phosphate concentration functions and acts as a co-factor of TIR1 for binding as well as an essential Pi-deprivation signaling molecule (Crombez et al., 2019). The crystal structure of TIR1 positions IP6 just below the auxin binding site in the center of the TIR1 LRR domain, suggesting that IP6 facilitates the receptor's ability to bind auxin. These observations indicate that IP6 potentially acts as further connection between auxin receptor and P_i availability (Crombez et al., 2019).

P_i deprivation signaling in both *Arabidopsis* and rice requires IAAs and ARFs which are important for lateral root initiation. ARF17 and ARF19 both positively regulate PHR1 (Figure 1.7) and expression of PHR1 partially rescues the lateral rootless phenotype of the *arf7*/*arf19* mutant supporting a PHR1-ARF feedback mechanism. PHR1 targets PIN1 and various other proteins which are crucial for vesicle trafficking and PIN localization suggesting that P_i availability could interact with auxin transport and influence various aspects of LR development (Crombez et al., 2019).

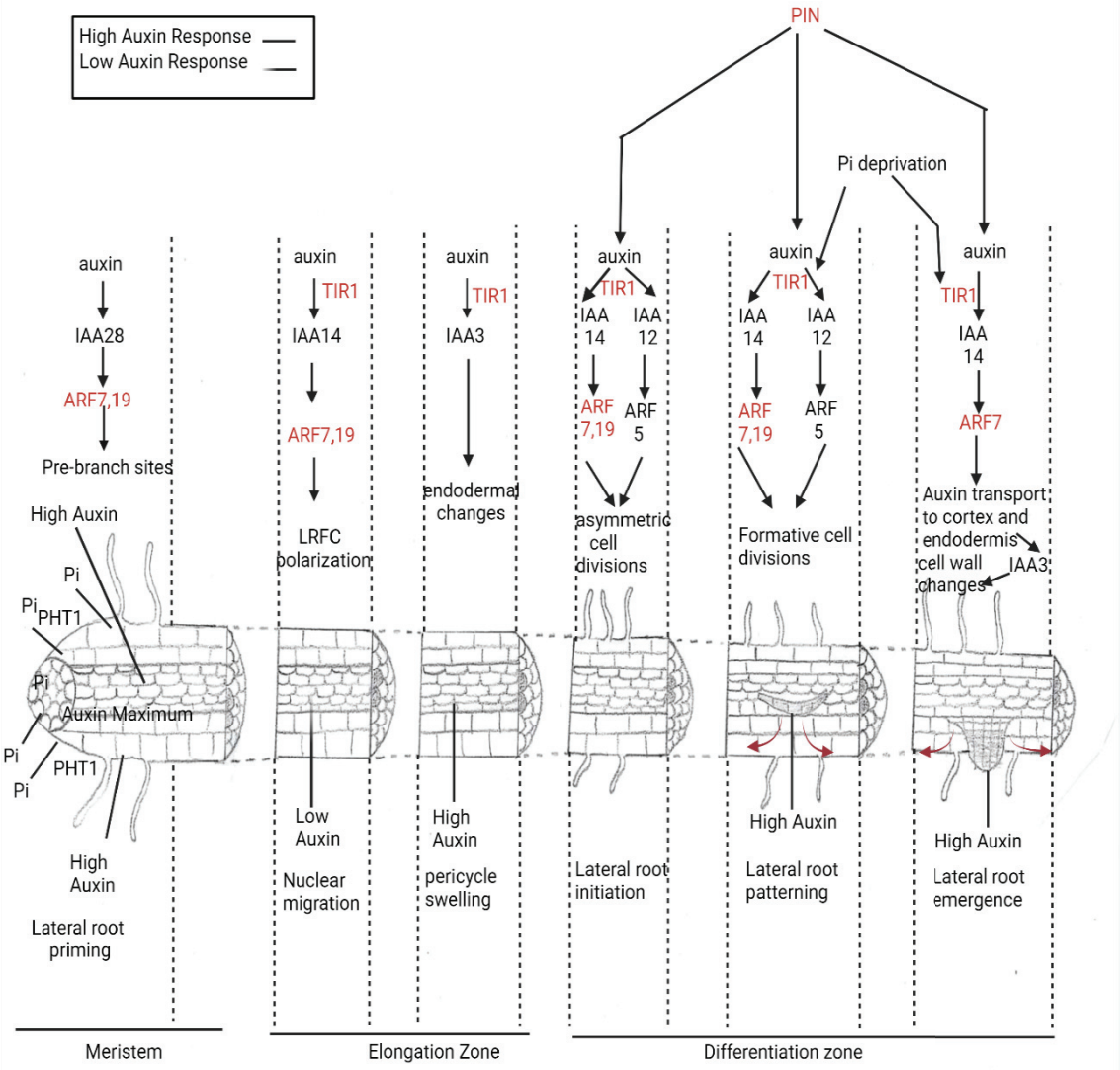

Figure 1.7: Various stages of lateral root development and interaction between phosphate deprivation and phosphate deprivation signaling and lateral root induction (PHR1 targets indicated in red). Arrows indicate pathways of influence, with pointed heads indicating a positive influence. *Figure redrawn from- Tackling Plant Phosphate Starvation by the Roots, Developmental Cell, Crombez et al., 2019. Image illustrated with Biorender.*

1.4.3 Effects of P_i on Root Hair Development

P_i deficiency may cause increased number of root hairs and/or longer root hairs. Firstly, because an effect of P_i deficiency is an increase in the number of cortical cell files, the

number of trichoblasts competent to form root hairs is increased (Crombez et al., 2019). PHR1 plays an important role in increasing cortical cell files via transcriptional regulation of genes with a PHR1-binding site (P1BS) in the promoter (Li et al., 2015). P_i-deprivation induces PLDΣ1, a phospholipase that is assumed to be a PHR1 target (Figure 1.8). PLDΣ1 increases the cortical cell files via translocation of the membrane proteins involved in signal transduction, including those for phytohormones (Crombez et al., 2019) (Figure 1.8). Root hair formation and elongation also involve other potential PHR1 targets such as *ROOT HAIR DEFECTIVE2* (*RHD2*), *RHD2LIKE(RSL4)* and *ROOT HAIR SPECIFIC19 (RSL19)* which play crucial roles in root hair associated ROS production (Crombez et al., 2019) (Figure 1.8), while others such as *SYNTAXIN OF PLANT123* (*SYP123*) help with membrane trafficking in the root hair. Moreover, Pi-deprivation dependent root hair signaling requires *PIP5K3* and *PIP5K4*, which can synthesize vesicle trafficking ptdlns(4,5)P2 (Crombez et al., 2019) (Figure 1.8). PHR1 and its paralog(s) transcriptionally activate *PIP5K3* and *PIP5K4* genes through upstream P1BSs hence promoting the root hair elongation response to P_i shortage. The proteins mentioned above may also be responsible for localizing PIN auxin transporters, which are necessary for the development of root hair (Crombez et al., 2019).

Apart from auxin, ethylene and jasmonate pathways also help regulate root hair growth under Pi deprivation. In addition to inducing *RSL4*, ethylene also activates *RSL2*, *RSL4*'s closest homolog. Moreover, to cooperatively promote root hair responses, RSL4 and *ETHYLENE INSENSITIVE* (*EIN3*), a transcription factor necessary for ethylene response,

share multiple direct targets implicated in root hair formation. Jasmonate acts to induce *EIN3* by removing repressive JAZ proteins (Crombez et al., 2019) (Figure 1.8). PHR1 partially regulates the kinetics of the Pi deficiency-induced activation of the jasmonate signaling pathway. Thibaud et al., (2010) demonstrated that systemic signaling controls the transcription of phosphate starvation induced (*PSI*) genes involved in Pi transport, signaling, and recycling. The *PSI* genes that fall within these functional categories are also those whose expression is controlled by ethylene (Lei et al., 2011; Wang et al., 2012; Yu et al., 2012) (Figure 1.8). Ethylene may therefore be a component of a regulatory loop that controls *PSI* gene expression systemically. However, it is unknown how ethylene signaling contributes to the systemic regulation of *PSI* gene expression after it is initiated. Thus, PHR1 may contribute to the P_i-starvation-induced growth of root hair similarly to the other P_i-starvation responses, by potentially regulating auxin, ethylene, or jasmonate-related pathways (Crombez et al., 2019) (Figure 1.8).

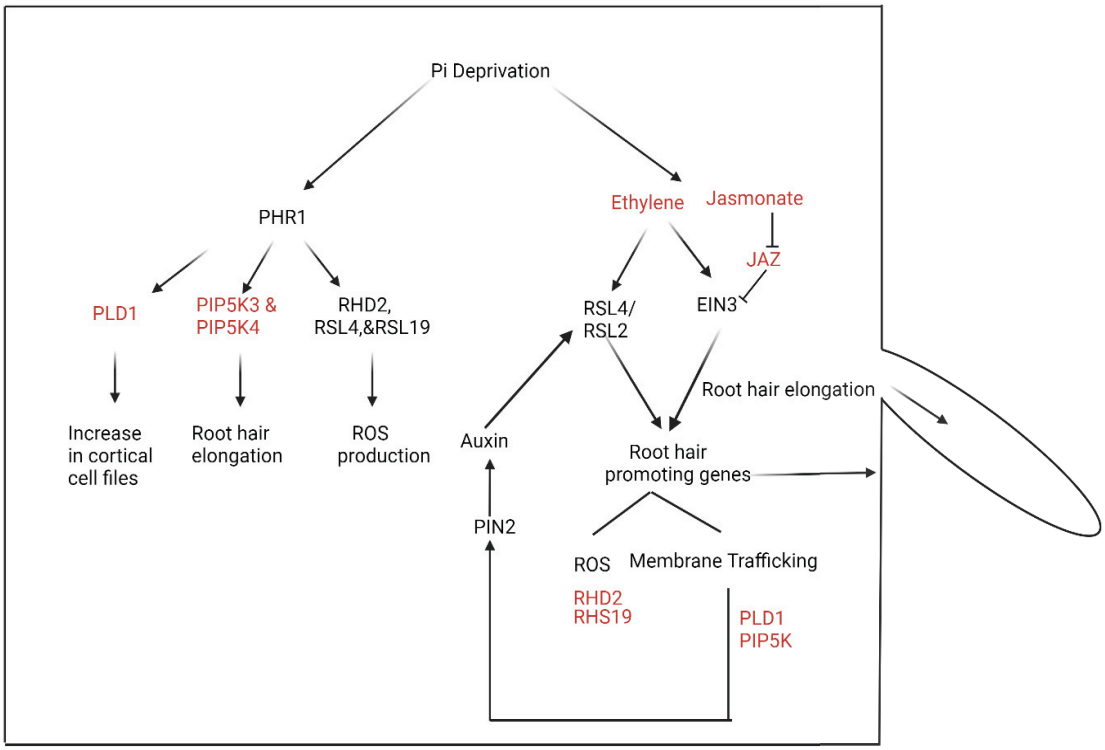

Figure 1.8: Root hair development and possible interaction with P_i-deprivation signaling (PHR1 targets indicated in red). Arrows indicate pathways of influence, with pointed heads indicating a positive influence. *Figure redrawn from- Tackling Plant phosphate starvation by the roots, Developmental Cell, Crombez et al., 2019. Image illustrated with Biorender.*

1.5 PIN transporters influencing root system architecture:

The directional transport of auxin through the tissues via the PIN-FORMED (PIN) auxin efflux transporters helps to regulate the amount of auxin in the cells (Adamowski and Friml, 2015). The plant endomembrane system and post-translational modification are required for the polar localization of PIN proteins (Mariyamma et al., 2018) and are therefore critical for plant developmental processes including root system architecture.

Like RSA, leaf vein formation is dependent on auxin transport and PIN-mediated auxin transport is crucial for vein pattern development. Several genes necessary for PIN localization during the development of *Arabidopsis* leaf veins have been discovered because their mutation results in anomalies in vein connection (Pahari et al., 2014). When mutated, several genes including *FORKED1* (*FKD1*), *SCARFACE*/*VASCULAR NETWORK DEFECTIVE* (*SFC*/*VAN3*), *COTYLEDON VASCULAR PATTERN* (*CVP2*), and *CVP2-LIKE* (*CVL1*), result in discontinuous leaf venation. These genes are proposed to function in the localization of PIN to the PM via the secretory pathway (Mariyamma et al., 2018; Carland and Nelson, 2009; Naramoto et al., 2010).

SFC/VAN3 regulates vesicle trafficking and is an ADP RIBOSYLATION FACTOR-GUANOSINE TRYPHOSPHATE HYDROLASE (GTPase) ACTIVATING PROTEIN (ARF-GAP). Leaf vein discontinuities are observed in the *sfc*/*van*3 mutants (Koizumi et al., 2005; Sieburth et al., 2006). The pleckstrin homology (PH) domain found in SFC/VAN3 is frequently linked to phosphoinositide binding, and SFC/VAN3 binds to phosphatidylinositol-4 phosphate [Ptdlns(4)p] with a high affinity (Koizumi et al., 2005). Docking of SFC to PI4P controls localization to the TGN (trans-Golgi Network) and requires the wild-type PH domain (Naramoto et al., 2009). Mutations in the (*CVP2*) or *CVP2 LIKE* (*CVL1*) genes, which encode type 1 Inositol Polyphosphate 5- Phosphatases 6 (At5Ptase6) and produce Ptdlns(4) from Ptlns(4,5)P2, phenocopy the *sfc*/*van*3 phenotype, highlighting the significance of phosphoinositides to vein formation (Carland and Nelson, 2009). SFC/VAN3 localization becomes more cytosolic in *cvp*2*cvl*1 mutants,

supporting the notion that contact with Ptdlns(4P) is required for recruitment SFC/VAN3 to the TGN, most likely via the PH domain (Carland and Nelson, 2009; Naramoto et al., 2009).

The number of vein connections is decreased in plants with mutations to *FKD1* (Hou et al., 2010), also known as *VAN3 BINDING PROTEIN*, *VAB* (Naramoto et al., 2009) which encodes a protein with Pleckstrin-Like (PL) and DUF828 domains. This is because PIN1 fails to establish consistent localization in developing vein cells (Hou et al., 2010). *FKD1* and *sfc*/*van*3 double mutants are more severe than single mutants, indicating that these genes may cooperate (Steynen and Schultz, 2003). It has been suggested that VAN3/SFC and FKD1 create a complex localized to TGN through their individual PH or PL domains. Either the SFC/VAN3 PH domain or the pleckstrin-like (PL) domain of FKD1 is sufficient to localize both SFC and FKD1 proteins to the TGN (Naramoto et al., 2009). PIN1 localization is defective in *sfc*/*van*3 and *fkd*1 mutants, suggesting that FKD1 and SFC complex plays a role in controlling vascular differentiation by ensuring that PIN1 is localized effectively in provascular cell files (Mariyamma et al., 2017).

Like *FKD1*, eight other genes in the *Arabidopsis* genome encode proteins with the PL domain the plant-specific DUF828 domain; this gene family is known as the *FORKED1-LIKE* (*FL*) gene family. It has been suggested that several FL proteins (FL1, FL2, and FL3) are localized to the TGN and secretory pathway, where they work in tandem with FKD1 to localize PIN1 (Mariyamma et al., 2018). The *fkd*1/*fl*1-2/*fl*2/*fl*3 quadruple mutants and

*fkd*1/*fl*1-2 double mutants exhibit decreased gravitropic responses and root elongation (Mariyamma et al., 2018), suggesting that *FKD1* and the other genes function within the root.

From the discussion above, it is evident that both leaf vein pattern and RSA rely on localization of PIN proteins. The effects of mutations that alter auxin transport mostly have been observed on leaf vein pattern, but I predict that the *Arabidopsis* auxin transport mutants *fkd1/fl1-2/fl2/fl3*, *cvp2cvl1*, and *sfc40*, which show defective vein pattern formation, would also demonstrate altered RSA due to their inability to maintain the asymmetric localization of PIN transporters. My research aims at investigating the effects of *Arabidopsis* auxin transport mutants on RSA and on the response of RSA to phosphate deprivation.

1.6 Hypothesis and Objectives:

I hypothesize that the mutants' inability to maintain the asymmetric localization of PIN transporters could cause them to exhibit significantly different RSA and RSA response to phosphate deprivation compared to the Wt.

Hypothesis 1: Auxin transport mutants would affect the RSA including primary root length, tip to the first lateral root distance, and root hair length.

Hypothesis 2: The mutants would exhibit significantly different RSA response to P_i deprivation than the Wt.

Objectives:

Objective 1: To assess if the disruption in the localization of PIN transporters could alter the RSA of the mutants.

Objective 2: To determine if the defective PIN localization could also affect the mutants; ability to modulate the RSA under phosphate deprivation.

Chapter Two: Materials and Methods

2.1 Seed Lines

The Columbia (Col-0) ecotype of *Arabidopsis* was used as a wild-type (Wt) in all experiments. The *fkd*1/*fl*1-2/*fl*2/*fl*3 quadruple mutant was generated as described in Mariyamma et al., 2018. Both *sfc-40* and *cvp2cvl1* seed were donated by Francine Carland (Department of Genetics, Harvard Medical School, MA); mutant *sfc-40* was generated from a population that had been diepoxybutane-mutagenized (Carland and Nelson, 2005) and the homozygous double mutant strain *cvp2cvl1* was described in Carland and Nelson, 1999.

2.2 Media Preparation

To assess the RSA response to changes in phosphate concentration, *Arabidopsis* growth media (ATS) was prepared according to Ruegger et al., 1998, adding 0.8% sucrose to ensure uniform growth of the seedlings, with 4 different phosphate concentrations that had been used in previous analyses of RSA response to P_i-deprivation : 0.01mM, 0.1mM (Williamson et al., 2001), 1mM (Lopez-Bucio et al., 2002), and 2.5mM (Williamson et al., 2001). The different concentration of phosphate was from KH_2PO_4, therefore as the phosphate (P) concentration was altered, the potassium (K) concentration was also altered. To balance potassium (K) concentration in low phosphate media to be the same as that in high phosphate, appropriate amounts of KCl (Williamson et al., 2001) or K_2SO_4

were added. Following an initial test to determine if K_2SO_4 or KCl had different effects on RSA, K2SO4 was used in subsequent experiments (see results for details).

The agar most suitable for developing an appropriate phosphate deficient environment was tested. Four different agars (Bioshop, EMD, Fisher, and Phytotech) with 4 different phosphate concentrations (2.5 mM, 1 mM, 0.1 mM, 0.01 mM) were tested, and Phytotech agar was used for all the remaining experiments (see results for details).

2.3 Growth Conditions

Seeds of the 4 genotypes (Wt*, fkd1/fl1-2/fl2/fl3, cvp2cvl1*, and *sfc40*) were sterilized using 20% bleach, followed by 70% ethanol for 10-15 seconds, and rinsed in distilled water (Ruegger et al., 1998). For each of phosphate concentration, two plates with 15 seedlings were prepared for each of the 4 genotypes (2 plates per genotype x P concentration). The seeds were planted in a line on ATS media in vertically oriented petri dishes (Ruegger et al., 1998). Plates were transferred to the cold room for stratification at 4°C. After 24 hours, the plates were transferred to the growth chamber at 21°C under continuous LED lights with an intensity of approximately 120 uE m^{-2} s^{-2}. The day of transfer was considered 0 DAG. Plates remained in the growth chamber 8 days for lateral root analysis and 5 days for root hair growth.

2.4 Staining and Microscopy

Seedlings of 8 DAG (lateral roots) and 5 DAG (root hairs) were stained with 0.05% toluidine blue for 15 seconds to improve root visualization. The roots were cut at the

hypocotyl region. For lateral roots, the roots were mounted on slides and the images were captured using a NIKON camera, using a ring light as the light source.

For root hair measurements, the roots were mounted on slides using deionized water (dH_2O) and observed with a NIKON ECLIPSE E600 microscope and images were captured using QCapture software. Root hairs were imaged in the region where the root hairs exhibited uniform length and had stopped elongation. A standard root hair area was chosen that included the beginning of the differentiation zone and multiple captures were taken of each area to facilitate the visualization of all cells producing root hairs.

2.5 Measurements

Lateral root length and the distance from the tip to the first lateral root (to determine a shift in the differentiation zone) were measured using ImageJ (Figure 2.1). The density of lateral roots was measured by dividing the total number of lateral roots by the length of the differentiation zone (the region where lateral roots start to emerge). Ten root hairs were measured from each root. Root hair length was calculated starting from the base of bulging site to the end of the root tip using ImageJ.

2.6 Statistical Analysis

All statistical analysis was done using R studio software version 4.1.3. The normality of data distribution was determined with Shapiro-Wilk's normality test. I used a one-way ANOVA test to determine the significant differences in primary root length, tip to the first lateral root distance, total lateral root length, and lateral root density in response to

four different concentrations of phosphate. I used a two-way ANOVA to test the effects of different phosphate treatments, four genotypes, and their interaction affecting the phenotypes mentioned above as well as root hair length. The one-way and two-way ANOVA tests were followed by a Tukey's HSD test to determine the pairwise differences (significance $p < 0.05$).

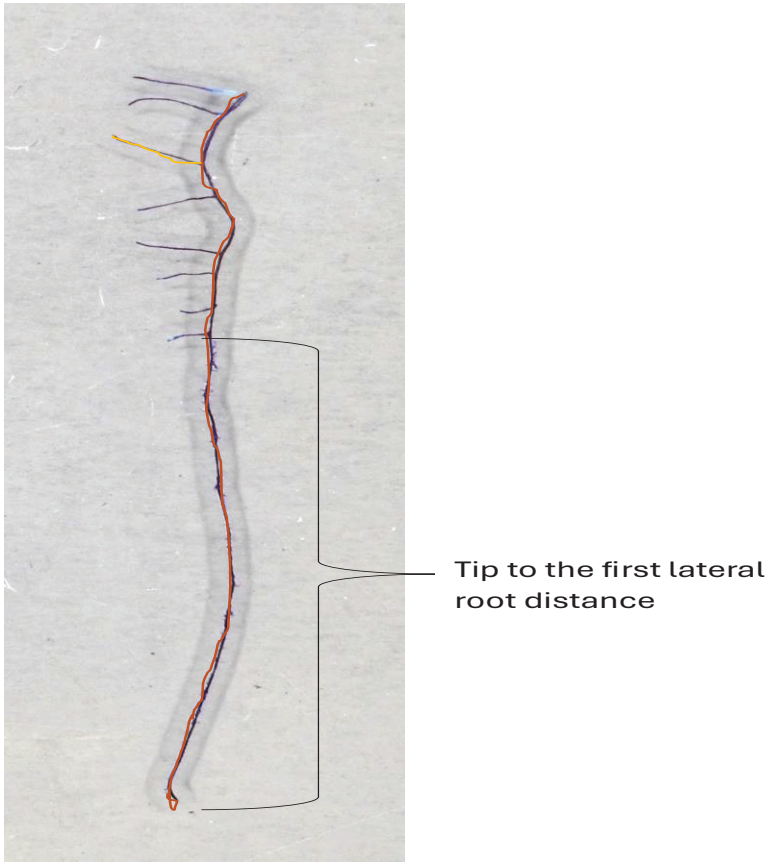

Figure 2.1: Primary root length, lateral root length and tip to the first lateral root distance measurement of Wt *Arabidopsis* at 8 DAG. The red line depicts primary root length, and the orange line indicates lateral root length.

Chapter Three: Results

Auxin transport is proposed to play a significant role in modulating *Arabidopsis thaliana'*s response to phosphorus deprivation through the modification of RSA. I tested the *Arabidopsis* auxin transport mutants to see if, compared to Wt, defects in auxin transport could affect their ability to respond to phosphorus deprivation.

3.1 Testing the response of agars to different sources of Potassium:

I ran a preliminary experiment with Wt grown on AT media solidified with the Bioshop agar and with three phosphate concentrations 0.01 mM, 0.1 mM, and 1 mM P. I observed that primary root length was longer under low phosphate concentrations (data not shown) which contradicts the findings of previous literature. I first tested if the unexpected result might be explained by the type of agar or source of Potassium. At a phosphate concentration of 0.01 mM, I tested two agars, Bioshop and EMD, and two reagents that can be used to compensate the loss of potassium in the media, K_2SO_4 and KCl (Williamson et al., 2001) and compared primary root length and distance from the tip to the first lateral root of the Wt (30 seedlings per treatment combination).

3.1.1 Primary Root Length:

There was a significant effect of the type of agar used in the media on the primary root length but there was no significant effect of the source of potassium. I also did not observe any interaction between the type of agars and the source of potassium

according to a two-way ANOVA ($P < 0.05$) (Table 3.1). Roots were significantly longer when plants were grown on Bioshop agar compared to those grown on EMD agar. For both agar types, the primary root length was not significantly different whether I used K_2SO_4 or KCl in the media, under 0.01 mM phosphate treatment suggesting that the source of potassium was not interacting with the agars (Figure 3.1).

3.1.2 Tip to the first lateral root length:

The response to phosphate treatment of tip to the first lateral root length was significantly affected by the type of agar but not by the source of potassium according to a two-way ANOVA test ($P < 0.05$) (Table 3.1). I observed a significant interaction between the type of agars and the source of potassium on the response ($P < 0.05$). The tip to the first lateral root length was not significantly different for both the agars (Bioshop and EMD) under 0.01 mM phosphate treatment (Figure 3.1).

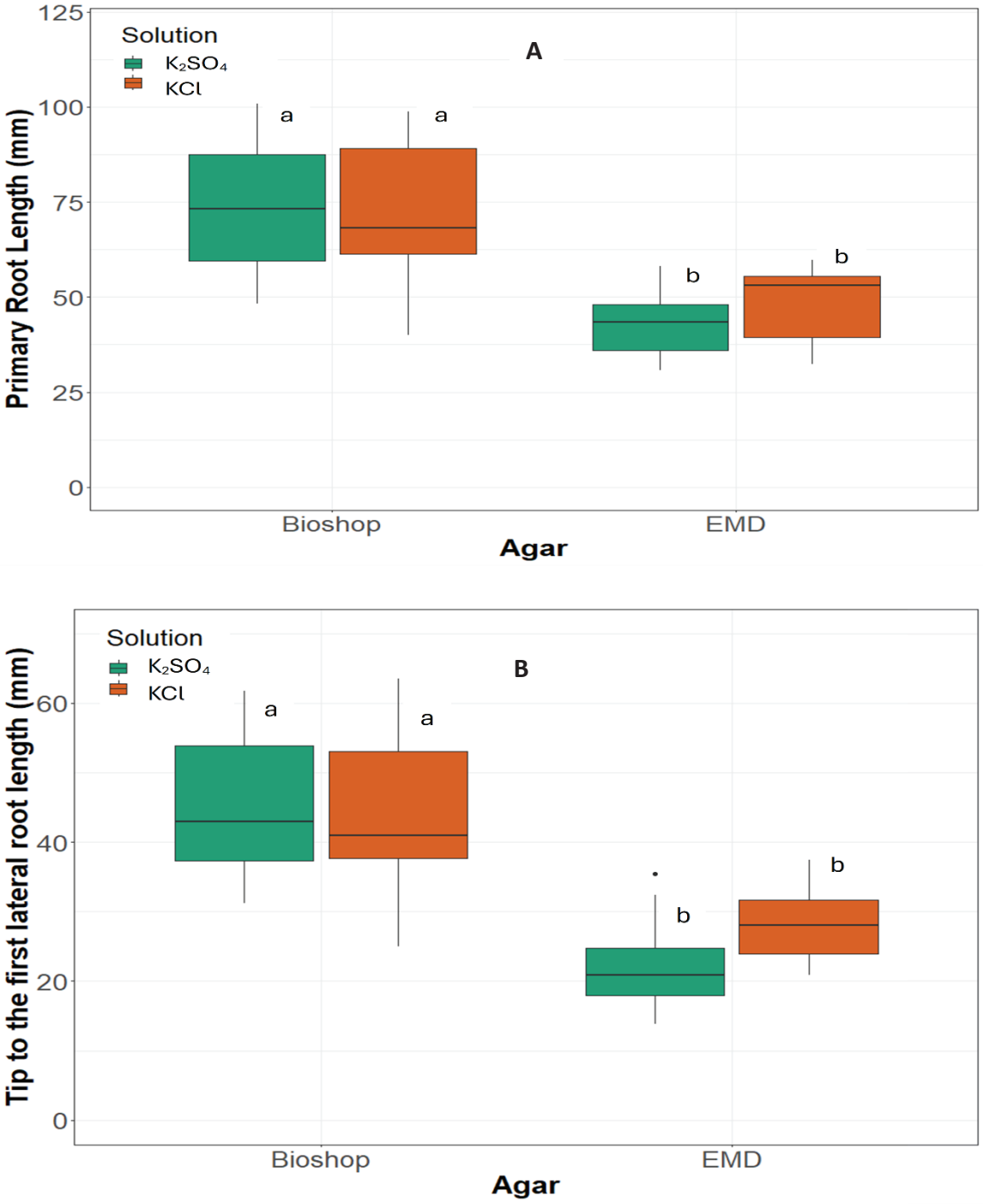

Figure 3.1: Boxplots presenting A) mean primary root length, B) tip to the first lateral root length of 8 DAG Wt seedlings assessed after growth on two different types of agars (Bioshop and EMD) with one phosphate concentration (0.01 mM)and two sources of Potassium (K_2SO_4 and KCl). Sample size was 30 plants per treatment combination (n = 30). The black line inside the boxes represents the median, error bars indicate plus/minus one standard error of the mean, and the letters represent significant differences ($p < 0.05$) based on a Tukey HSD test.

Table 3.1: Two-Way Analysis of Variance (ANOVA) results testing the effect of two different agars- (Bioshop and EMD) and sources of Potassium- (K_2SO_4 and KCl) on Wt *Arabidopsis* on root parameters.

Root Parameters	Source of Variation	Degree of Freedom (Df)	Sum of Squares (SS)	Mean Sum of Squares (MSS)	F-value	P-value
Primary Root Length (mm)	Agar	1	18229	18229	113.433	<2e-16
	Source of Potassium	1	139	139	0.863	0.355
	Agar: Source of Potassium	1	190	190	1.180	0.280
	Residuals	87	13981	161		
Tip to the first lateral root length (mm)	Agar	1	8980	8980	145.363	<2e-16
	Source of Potassium	1	116	116	1.885	0.1733
	Agar: Source of Potassium	1	319	319	5.164	0.0255
	Residuals	87	5375	62		

3.2 Effects of agar on response to phosphate

To test which agar resulted in the most typical response to phosphate levels, I assessed primary root length, tip to the first lateral root density, and lateral root density of Wt *Arabidopsis* when grown on media solidified by four different agars (Bioshop, EMD, Fisher, and Phytotech) with two different phosphate concentrations (0.01 mM, 2.5 mM P)

3.2.1 Primary Root:

Primary root length was measured in 8 DAG Wt plants (30 seedlings per agar x phosphate concentrations). A two-way ANOVA indicated that type of agar had a significant effect on primary root length (Table 3.2). Seedlings grown on Bioshop agar had significantly longer primary roots than those grown on EMD, Fisher, and Phytotech at 0.01 mM phosphate. At 2.5 mM phosphate, the primary root length on Bioshop agar was significantly shorter than the Phytotech agar but not different from EMD and Fisher agar.

The two-way ANOVA also indicated that phosphate had a significant effect on primary root length and there was a significant interaction of agar type with phosphate level (Table 3.2). Under low phosphate (0.01 mM) seedlings grown on, EMD, Fisher, and Phytotech agar exhibited shorter primary root length than under high phosphate concentration (2.5 mM phosphate). Seedlings grown on the Bioshop agar demonstrated a response to the phosphate levels, but in an opposite manner. Primary roots were longer under 0.01 mM phosphate with Bioshop agar and shorter under 2.5 mM phosphate (Figure 3.2).

3.2.2 Distance from the Tip to the Appearance of the First Lateral Root:

A two-way ANOVA revealed that the type of agar also had significant effect on the distance from the tip to the first lateral root. At 0.01 mM phosphate, seedlings grown on the Bioshop agar had significantly longer distance (38.5±2.5 mm) than those grown on

EMD, Fisher, and Phytotech agar and the seedlings grown on these agars exhibited similar length (22±3.5; 21±2.5; 24±3.5 mm) respectively. At 2.5 mM phosphate, no difference in distance was observed among the seedlings grown on different agars- Bioshop, EMD, Fisher, and Phytotech (38±1.5; 39±2.5; 38.5±2; 40±2.0 mm respectively).

A significant agar: treatment effect was observed ($p < 0.05$) on the distance from the tip to the appearance of the first lateral root for all four agars after a two-way ANOVA test (Table 3.2) and it also revealed a significant phosphate effect on the distance from the tip to the first lateral root (Table 3.2). Seedlings grown on EMD, Phytotech, and Fisher agars all exhibited increased distance from the tip to the first lateral root under high phosphate concentration and decreased distance under low phosphate concentration, which was consistent with previous findings (Figure 3.2). In contrast, seedlings grown on the Bioshop agar demonstrated an opposite effect with increased distance from tip to the first lateral root under low phosphate and decreased distance under high phosphate concentrations (Figure 3.2).

3.2.3 Lateral Root Density:

A significant agar effect was observed ($p <0.05$) on lateral root density after a conducting a two-way ANOVA test (Table 3.2). Seedlings grown on Bioshop, EMD, Fisher, and Phytotech did not show any significant difference in density at 0.01 mM phosphate (Figure 3.2). At 2.5 mM phosphate, seedlings grown on Bioshop and EMD

exhibited significantly higher density compared to those grown on Phyto and Fisher agar (Figure 3.2) Only seedlings grown on EMD agar had a response to phosphate deprivation. The seedlings grown on EMD at 2.5 mM phosphate showed less lateral root density compared to 0.01 mM phosphate, although the difference was barely significant ($p = 0.045$).

Overall, seedlings grown on Fisher, EMD, and Phytotech had similar RSA responses to phosphate, which was consistent with previous studies. In contrast, seedlings grown on Bioshop agar had a different RSA response to phosphate, perhaps because of some unknown compound within the Bioshop agar. Because it has widely been used in plant-based studies, we decided to use Phytotech agar for our remaining experiments.

Table 3.2: Two-way Analysis of Variance (ANOVA) results testing the interaction between four different types of agars (Bioshop, EMD, Phytotech, and Fisher) and two different phosphate concentrations (0.01mM and 2.5mM phosphate) and their individual effects on root parameters in Wt *Arabidopsis*.

Root Parameter	Source of Variation	Degree of Freedom (Df)	Sum of squares (SS)	Mean sum of squares (MSS)	F value	P-value
Primary Root Length (mm)	Agar	3	3608	1202.7	53.74	<2e-16
	Treatment	1	1508	1508.3	67.39	2.81e-14
	Agar*Treatment	3	6373	2124.3	94.92	<2e-16
	Residuals	198	4431	22.4		
Tip to the first lateral root length (mm)	Agar	3	2257	752.3	42.55	<2e-16
	Treatment	1	1914	1913.6	108.23	<2e-16
	Agar*Treatment	3	3803	1267.8	71.70	<2e-16
	Residuals	198	3147	17.7		
Lateral root density (no of lateral roots/mm)	Agar	3	1.495	0.4983	17.13	8.14e-10
	Treatment	1	0.348	0.3484	11.97	0.000676
	Agar*Treatment	3	0.453	0.1580	5.19	0.001845
	Residuals	198	5.180	0.0291		

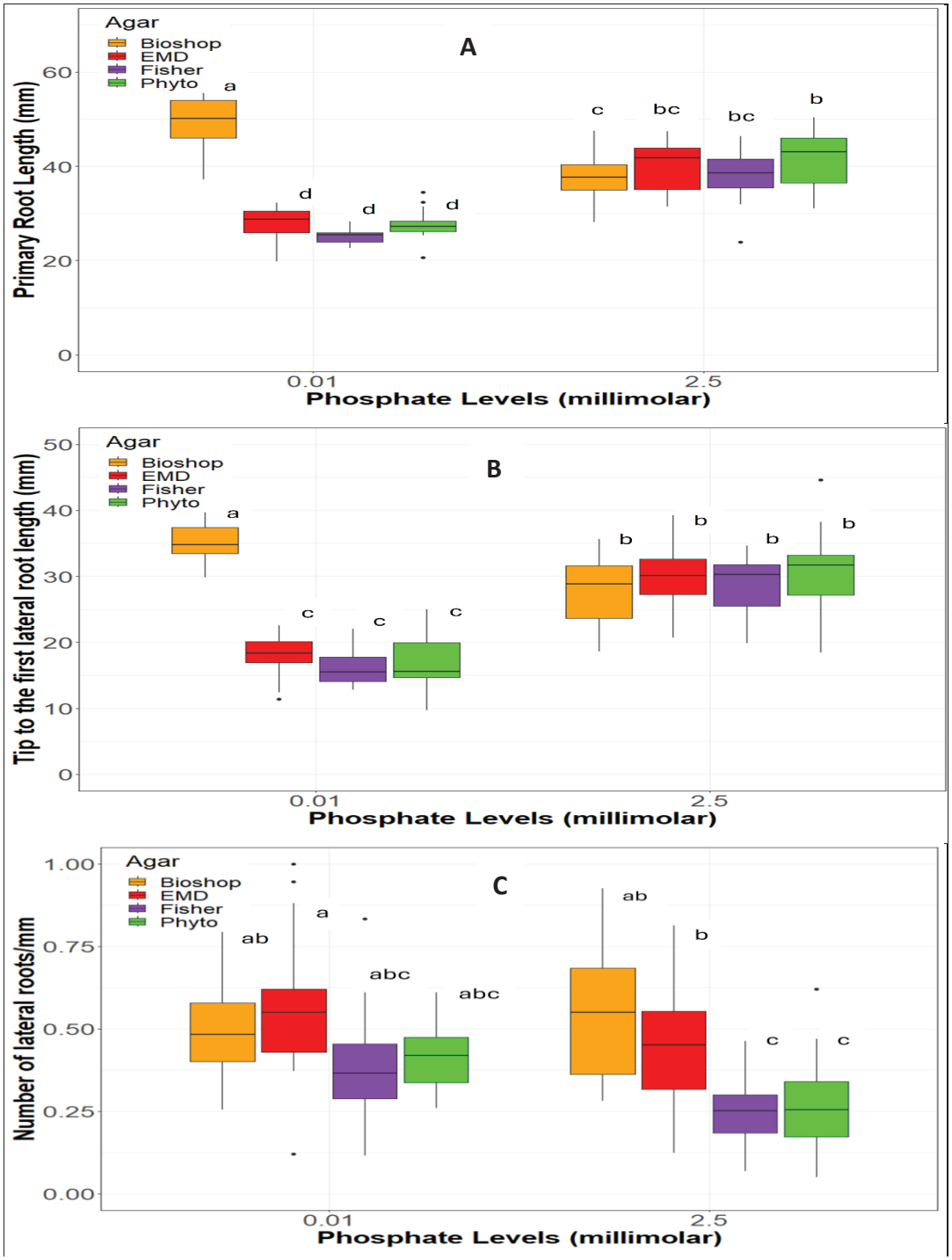

Figure 3.2: Boxplots presenting A) mean primary root length, B) tip to the first lateral root length, and C) lateral root density of 8 DAG Wt seedlings assessed after growth on four different types of agars (Bioshop, EMD, Fisher, and Phytotech) with two different phosphate concentrations (0.01 mM and 2.5 mM phosphate). Sample size was 30 plants per treatment combination (n = 30). The black line inside the boxes represents the median, error bars indicate plus/minus one standard error of the mean, and the letters represent significant differences ($p < 0.05$) based on a Tukey HSD test.

3.3 RSA in response to four different phosphate concentrations:

I next determined the concentrations of phosphate that would cause differences in RSA when Phytotech agar was used as a solidifying agent. Because 2.5 mM and 0.1 mM phosphate were used by Williamson et al., 2001, and 1 mM phosphate by Lopez-Bucio et al., 2002, I tested these three concentrations. Because I predicted that the mutants might show reduced sensitivity to phosphate depletion, I added a tenfold lower phosphate treatment (0.01 mM). I conducted this experiment on the Wt with 30 seedlings for each treatment.

3.3.1 Primary Root Length:

A significant treatment effect was observed on primary root length after a one-way ANOVA test ($p < 0.05$) (Table 3.3). Primary root length was significantly shorter at 0.01 mM than at 0.1 mM, and both were shorter than 1 mM and 2.5 mM phosphate (Figure 3.3). There was no difference in primary root length between 1 mM and 2.5 mM phosphate concentrations.

3.3.2 Distance from the tip to the Appearance of the First Lateral Root:

A significant treatment effect was observed in the distance from the root tip to the first lateral root after conducting a one-way ANOVA test ($p < 0.05$) (Table 3.3). A shorter tip to the first lateral root distance was observed (Figure 3.3) under 0.01 mM and 0.1 mM phosphate than at high phosphate concentrations (1 mM and 2.5 mM). Again, there was

no significant difference between 1 mM and 2.5 mM phosphate concentrations and no difference between 0.01 mM and 0.1 mM (Figure 3.3).

3.3.3 Lateral Root Density:

There was no significant treatment effect observed on lateral root density (Table 3.3) and density was similar under all four phosphate treatments (Figure 3.3).

As there was no significant different response between the treatments 1 mM and 2.5 mM phosphate for any character measured, I decided to use 1 mM phosphate as the highest concentration along with 0.1 mM and 0.01 mM phosphate.

Table 3.3: One-way Analysis of Variance (ANOVA) testing the effects of four different phosphate concentrations (0.01 mM, 0.1 mM, 1 mM, and 2.5 mM) on primary root length, tip to the first lateral root length, and lateral root density in Wt *Arabidopsis.*

Root Parameter	Source of Variation	Degree of Freedom (Df)	Sum of Squares (SS)	Mean Sum of Squares (MSS)	F-value	P-value
Primary root length (mm)	Treatment	3	10117	3372	141.2	<2e-16
	Residuals	115	2746	24		
Tip to the first lateral root length (mm)	Treatment	3	5391	1796.9	136.6	<2e-16
	Residuals	115	1500	13.2		
Lateral root density (number of lateral roots/mm)	Treatment	3	0.079	0.02635	1.108	0.349
	Residuals	115	2.710	0.02377		

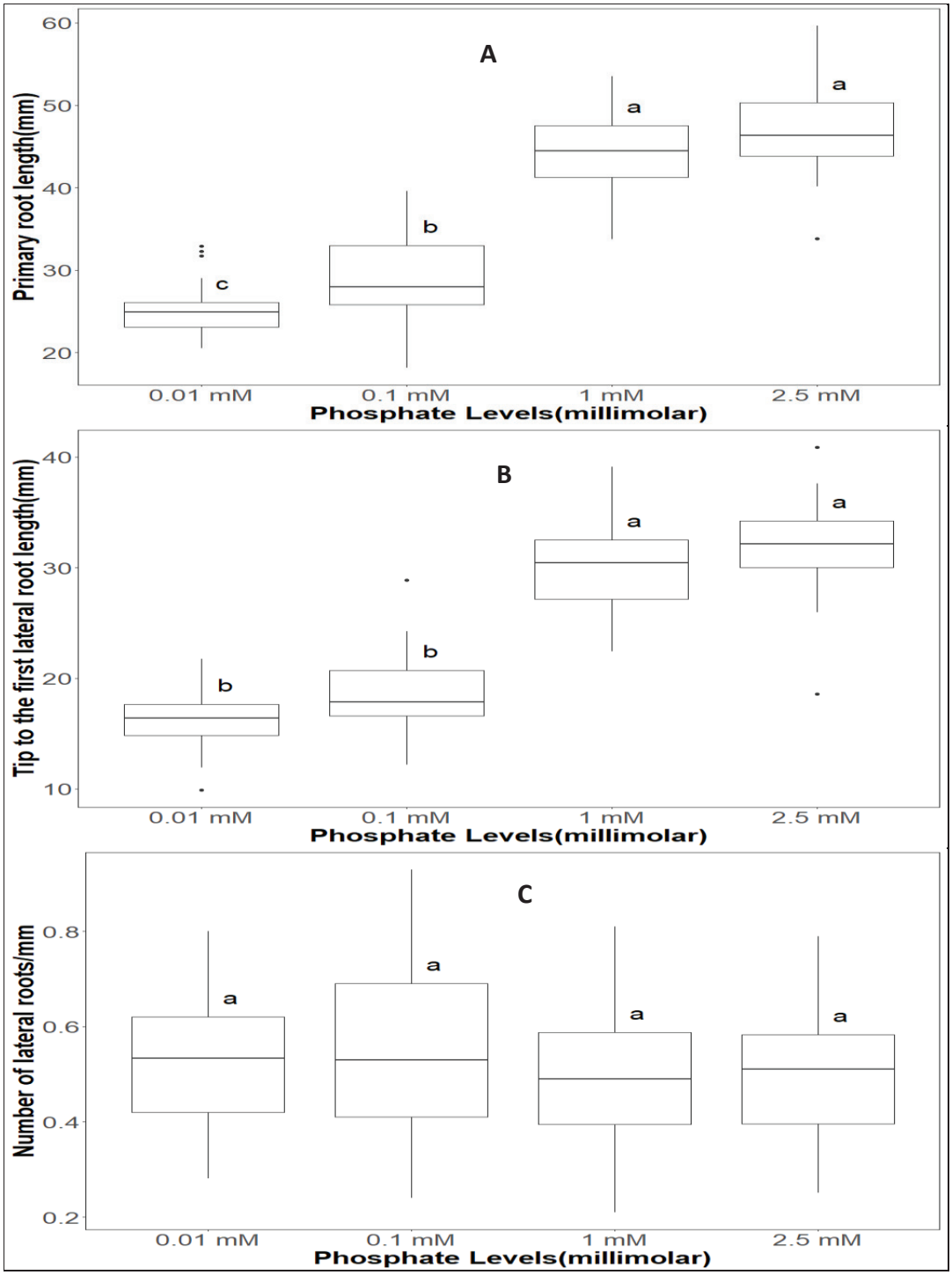

Figure 3.3: Boxplots presenting A) mean primary root length, B) tip to the first lateral root length, and C) lateral root density of 8 DAG Wt seedlings assessed after growth on four different phosphate concentrations (0.01 mM, 0.1 mM, 1 mM, and 2.5 mM). Sample size was 30 plants per treatment (n = 30). The black line inside the boxes represents the median, error bars indicate plus/minus one standard error of the mean, and the letters represent significant differences ($p < 0.05$) based on a Tukey HSD test.

3.4 Comparison of RSA among Wt and *Arabidopsis* auxin transport mutants:

3.4.1 Comparison of primary root length between Arabidopsis *auxin transport mutants and Wt:*

In my final experiment I compared the response of the *Arabidopsis* auxin-transport mutants RSA to phosphate deprivation to that of the Wt. A significant genotype effect was observed on the primary root length after conducting a two-way ANOVA test ($P < 0.05$) (Table 3.4). At 1 mM phosphate treatment, Wt exhibited significantly longer primary root length compared to the mutants *fkd1/fl1-2/fl2/fl3*, *cvp*2*cvl*1, and *sfc*40. At 1 mM phosphate concentration, the primary root length was the same for all mutants *fkd1/fl1-2/fl2/fl3, sfc*40 and *cvp*2*cvl*1 (Figure-3.5)

A significant effect of phosphate, and interaction between phosphate-genotype was observed (Table 3.4). At 0.01 and 0.1 mM phosphate concentrations, Wt showed significantly shorter root compared to 1 mM phosphate treatment. The mutants *sfc*40 and *fkd1/fl1-2/fl2/fl3* did not exhibit any significant response to phosphate deprivation with similar primary root length under all three phosphate concentrations (Figure 3.6). The mutant *cvp*2*cvl*1 showed response to phosphate deficiency with the primary root length significantly decreased under 0.01 and 0.1 mM phosphate compared to 1 mM phosphate (Figure 3.6).

3.4.2 Comparison of distance from tip to the first lateral root length between Arabidopsis *auxin transport mutants and Wt:*

A significant genotype effect was observed on the distance from the tip to the first lateral root length after conducting a two-way ANOVA (Table 3.4). Significantly longer tip to the first lateral root distance was observed in Wt under 1mM phosphate concentration compared to all the mutants (Figure 3.5). At 1 mM phosphate, the distance was similar for *sfc40* and *cvp2cvl1* which were both longer than *fkd1/fl1-2/fl2/fl3* (Figure 3.5).

A two-way ANOVA (Table 3.4) revealed significant treatment and genotype effects and an interaction between treatment and genotype on the distance from the tip to the first lateral root. All mutants demonstrated shorter tip to the first lateral root distance compared to the Wt (Figure 3.7). The Wt exhibited significantly shorter tip to the first lateral root distance under 0.1 and 0.01 mM phosphate compared to the 1mM phosphate and thus responded to phosphate deprivation (Figure 3.7). The mutant *cvp2cvl1* also showed a significant response by demonstrating shorter distance under 0.1 and 0.01 mM phosphate compared to 1 mM phosphate (23±2.5 mm) (Figure 3.7). The mutant *sfc*40 exhibited shorter distance under 0.01 mM phosphate compared to 1 mM but there was no difference between 0.1 mM and 1 mM phosphate treatments and thus showed less sensitivity than the Wt and *cvp2cvl1* to phosphate deficiency (Figure 3.7). The mutant *fkd1/fl1-2/fl2/fl3* did not show any response to phosphate deprivation (Figure 3.7).

3.4.3 Comparison of total lateral root length between Arabidopsis *auxin transport mutants and Wt:*

A significant genotype effect was observed on total lateral root length following a two-way ANOVA test ($p < 0.05$) (Table 3.4). At 1 mM phosphate concentration, Wt and *fkd1/fl1-2/fl2/fl3* exhibited significantly longer total lateral root length compared to the mutants *cvp2cvl1* and *sfc40* and under 1 mM phosphate the mutant *fkd1/fl1-2/fl2/fl3* was longer than Wt (Figure 3.5). There was no significant difference between the mutants *cvp*2*cvl*1 and *sfc*40 under 1 mM phosphate treatment (Figure 3.5).

A significant treatment effect was observed on the total lateral root length and there was a significant interaction between the treatment and genotype (Table 3.4). At 0.01 mM phosphate, Wt exhibited shorter total lateral root length than at 0.1 mM phosphate (30±3 mm) but not significantly different from 1 mM phosphate (Figure 3.8). The mutant *fkd1/fl1-2/fl2/fl3* showed shorter length at 0.01 mM phosphate compared to 0.1 mM and 1 mM phosphate, showing a significant response (Figure 3.8). The mutants *cvp*2*cvl*1 and *sfc*40 did not show any significant response to phosphate deficiency and had similar lateral root length at all three phosphate concentrations (Figure 3.8).

3.4.4 Comparison of lateral root density between Arabidopsis *auxin transport mutants and Wt:*

A significant genotype effect was observed on the lateral root density after a two-way ANOVA (Table 3.4). At 1 mM phosphate concentrations, *fkd1/fl1-2/fl2/fl3* demonstrated significantly higher lateral root density compared to Wt, *cvp*2*cvl*1, and *sfc*40 (Figure 3.5).

A two-way ANOVA revealed that treatment had a significant effect on lateral root density, but there was no interaction between genotype and treatment (Table 3.4). Wt lateral root density demonstrated no response to phosphate deficiency along with the mutant *cvp2cvl1* and *sfc40* (Figure 3.9).

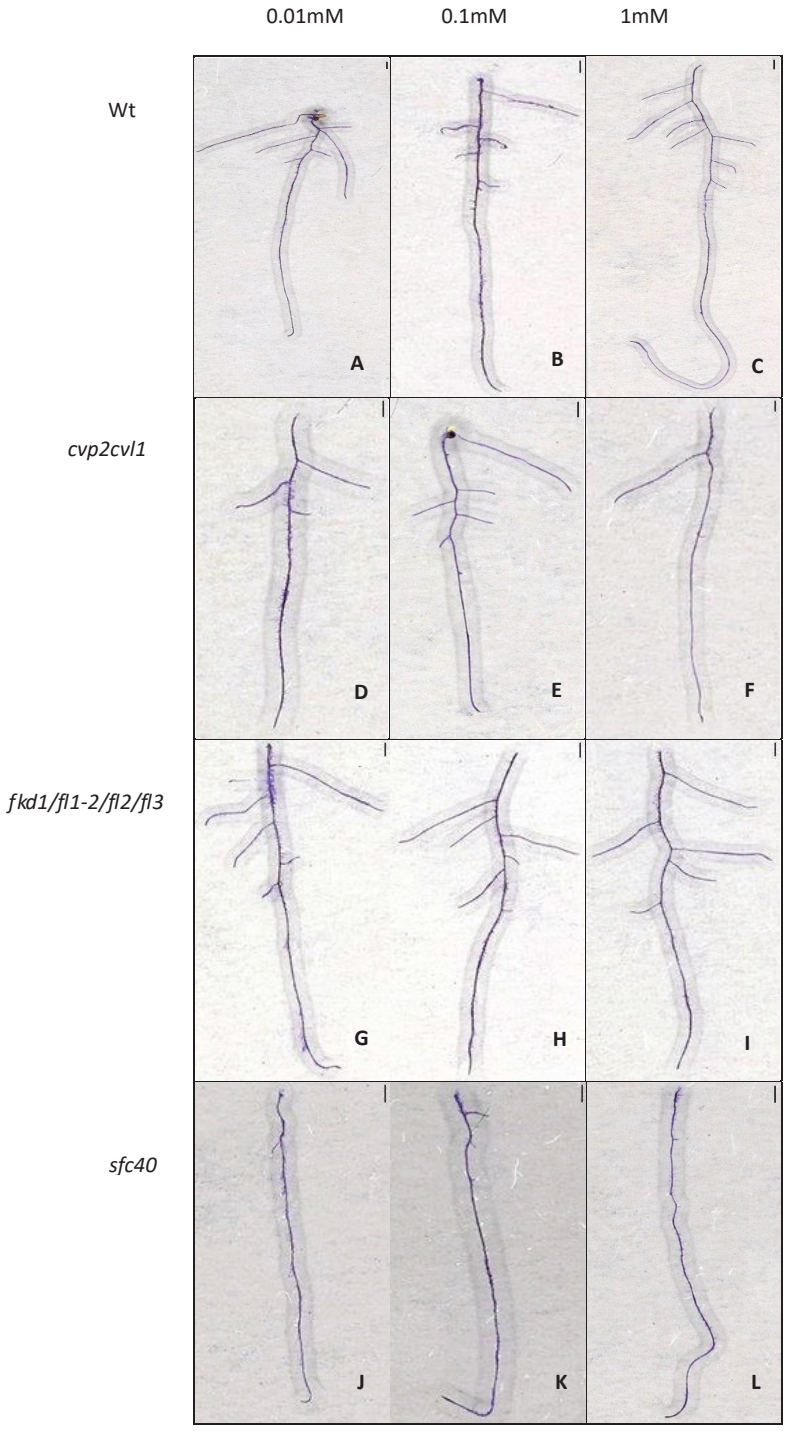

Figure 3.4: Representative images of the 8 DAG roots of Wt and the mutants- *cvp*2*cvl*1, *fkd1/fl1-2/fl2/fl3* and *sfc*40 grown on 0.01 mM, 0.1 mM, and 1 mM phosphate. Scale bar= 1 mm.

3.4.5 Comparison of root hair length between Arabidopsis *auxin transport mutants and Wt:*

A significant genotype effect was observed on root hair length upon conducting a two-way ANOVA test (Table 3.4). At 1 mM phosphate concentration, *fkd1/fl1-2/fl2/fl3* exhibited significantly longer root hairs than Wt, but mutants *cvp*2*cvl*1 and *sfc*40 root hairs were not different from the Wt (Figure 3.11).

A two-way ANOVA revealed significant treatment effect on root hair length and significant treatment by genotype interaction (Table 3.4). The Wt demonstrated significantly longer root hairs at 0.1- and 0.01-mM phosphate compared to 1 mM phosphate, showing a response to phosphate deprivation (Figure 3.12). The mutants *cvp*2*cvl*1, *sfc*40 and *fkd1/fl1-2/fl2/fl3* showed the same root hair length under all three phosphate treatments and thus did not show any significant response (Figure 3.12).

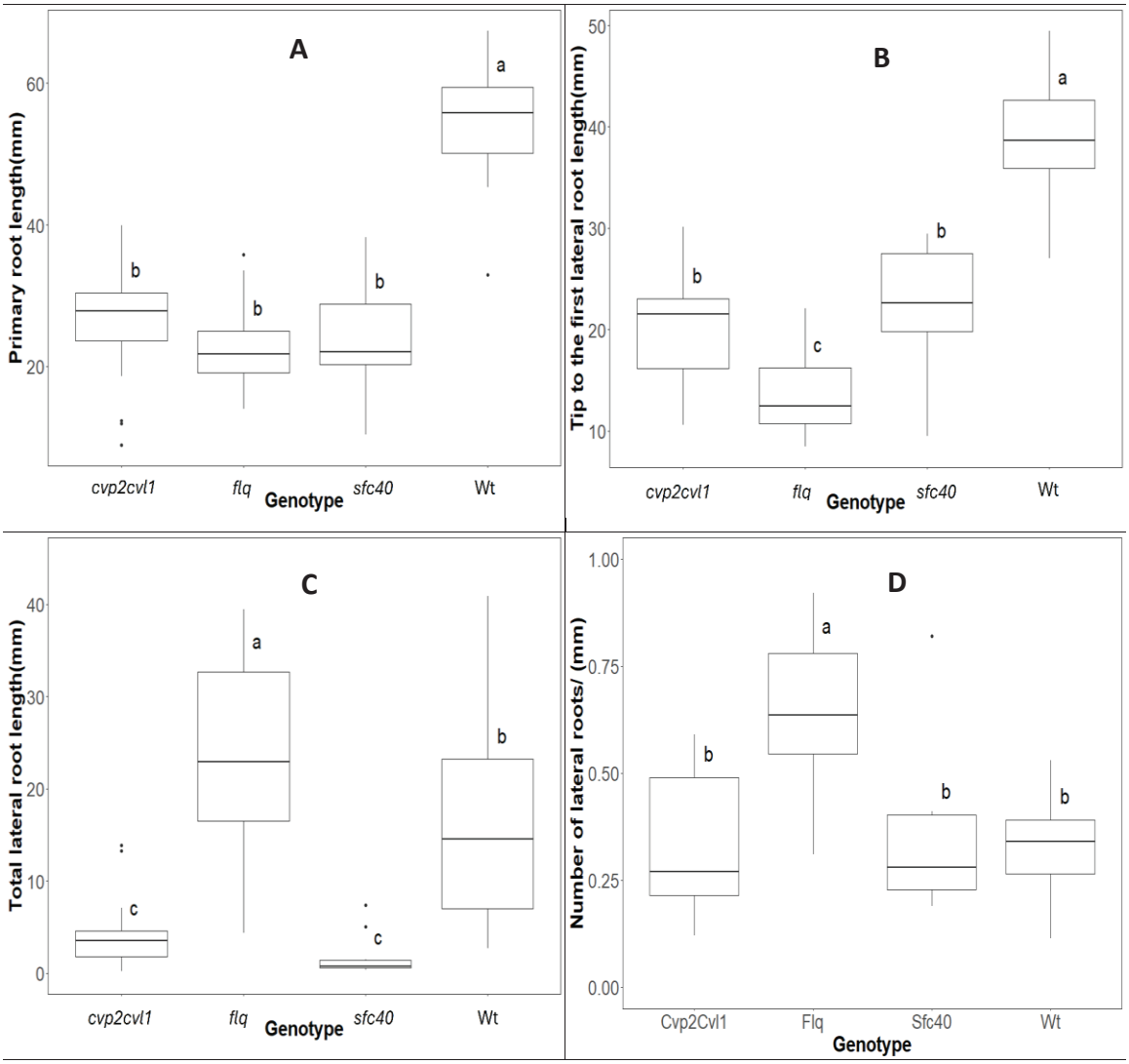

Figure 3.5: Boxplot presenting A) mean primary root length, B) tip to the first lateral root length, C) Total lateral root length, and D) lateral root density of Wt, *flq* (*fkd1/fl1-2/fl2/fl3*), *cvp2cvl1*, and *sfc40* at 8 DAG, assessed on 1 mM phosphate concentration. Sample size was 30 plants per treatment combination (n = 30). The black line inside the boxes represents the median, error bars indicate plus/minus one standard error of the mean, and the letters represent significant differences ($p < 0.05$) based on a Tukey HSD test.

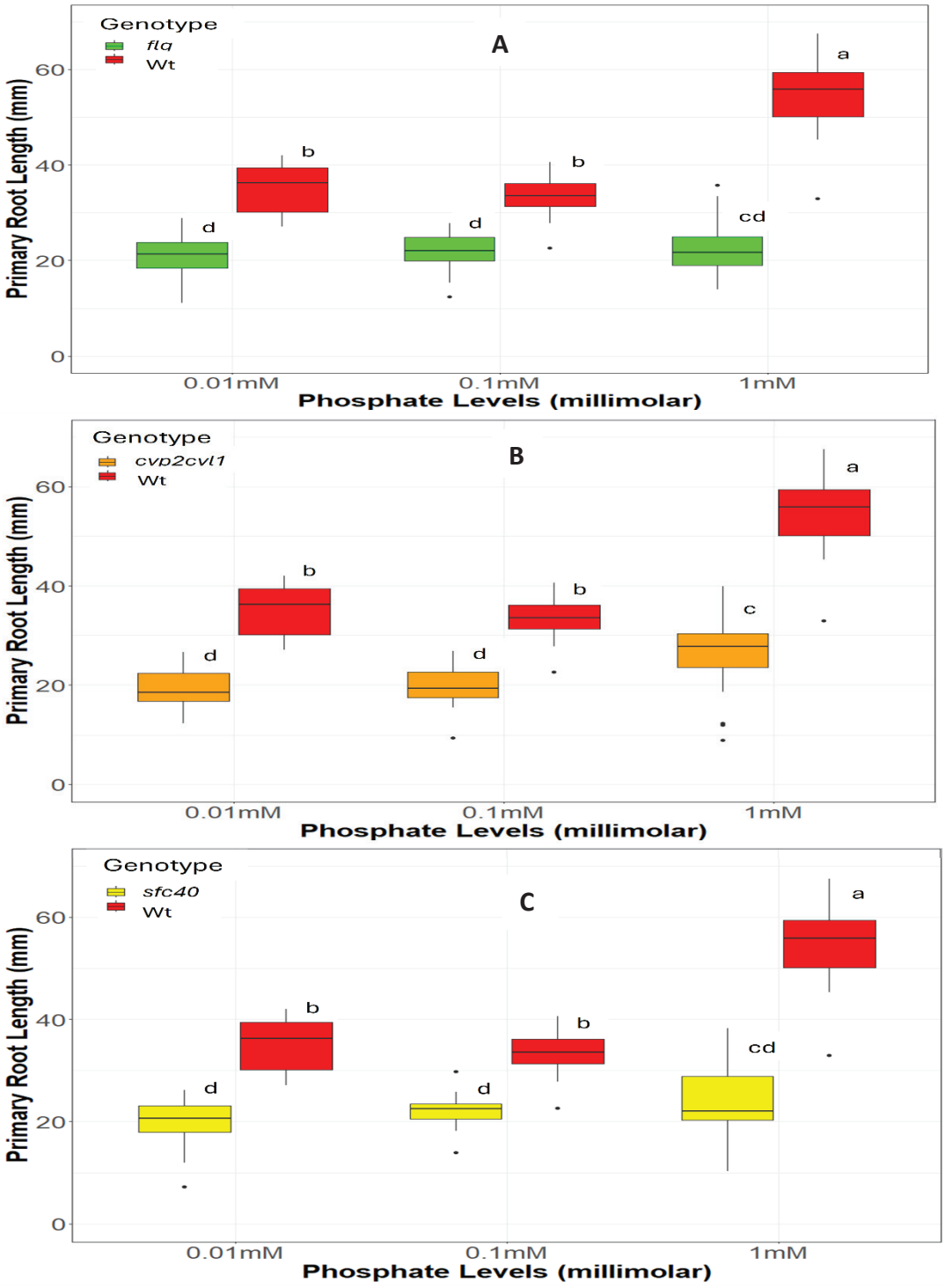

Figure 3.6: Boxplot presenting mean primary root length of A) Wt and *flq (fkd1/fl1-2/fl2/fl3)*, B) Wt and *cvp2cvl1*, and C) Wt and *sfc40* at 8 DAG, assessed on 0.01 mM, 0.1 mM, and 1 mM phosphate concentrations. Sample size was 30 plants per treatment combination (n = 30). The black line inside the boxes represents the median, error bars indicate plus/minus one standard error of the mean, and the letters represent significant differences ($p < 0.05$) based on a Tukey HSD test.

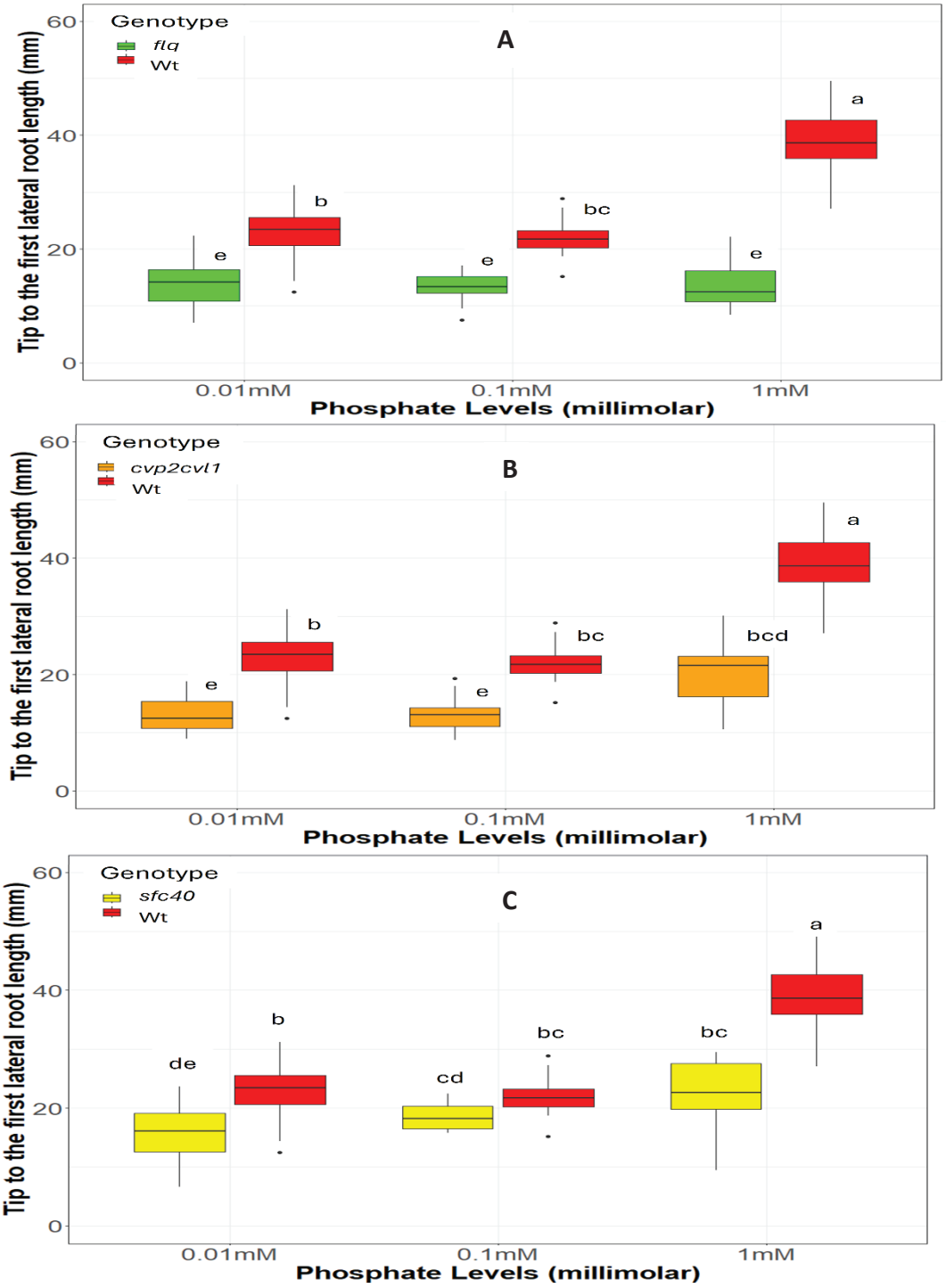

Figure 3.7: Boxplot presenting mean tip to the first lateral root length of A) Wt and *flq (fkd1/fl1-2/fl2/fl3)*, B) Wt and *cvp2cvl1*, and C) Wt and *sfc40* at 8 DAG, assessed on 0.01 mM, 0.1 mM, and 1 mM phosphate concentrations. Sample size was 30 plants per treatment combination (n = 30). The black line inside the boxes represents the median, error bars indicate plus/minus one standard error of the mean, and the letters represent significant differences ($p < 0.05$) based on a Tukey HSD test.

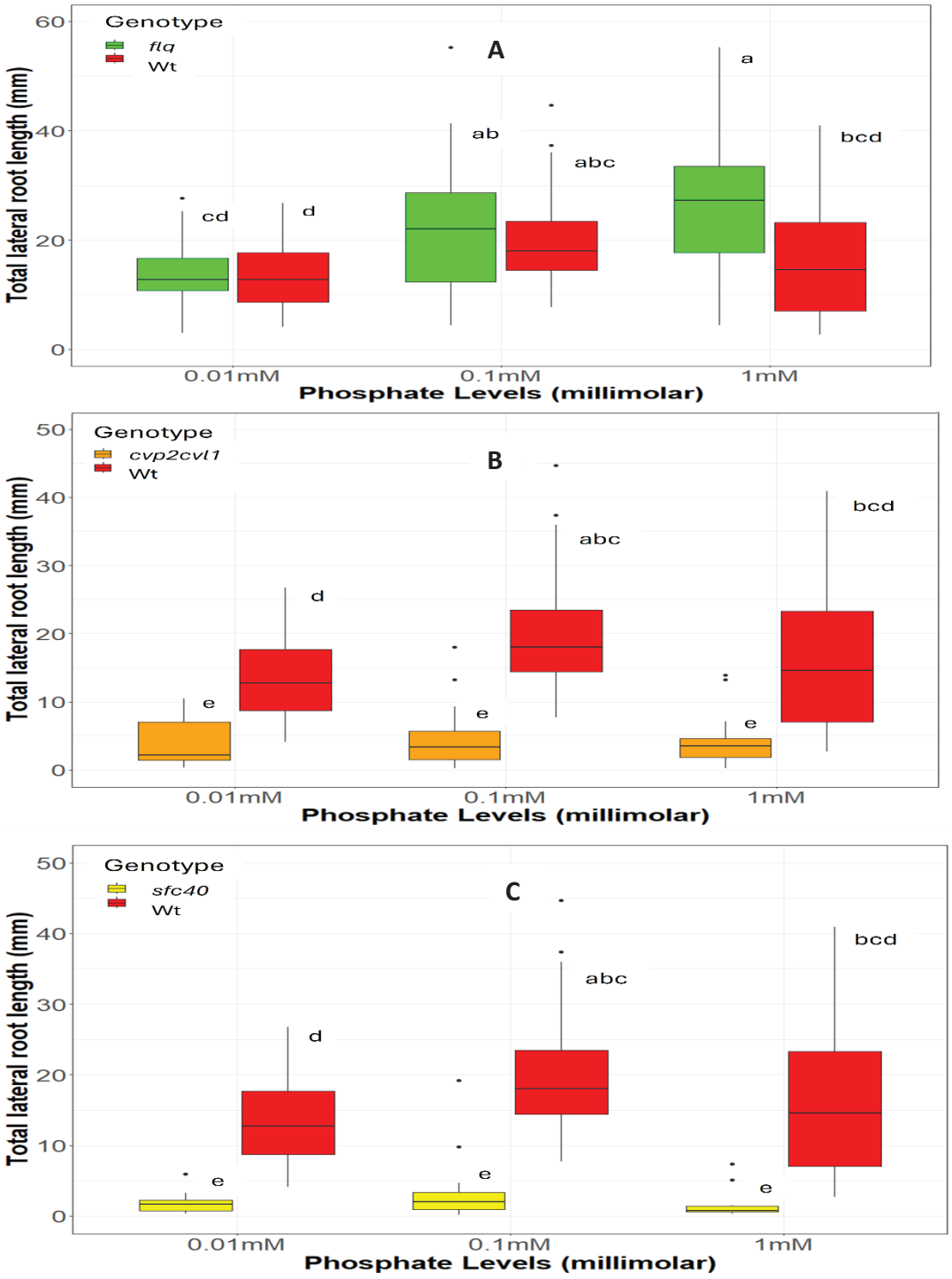

Figure 3.8: Boxplot presenting mean total lateral root length of A) Wt and *flq (fkd1/fl1-2/fl2/fl3)*, B) Wt and *cvp2cvl1*, and C) Wt and *sfc40* at 8 DAG, assessed on 0.01 mM, 0.1 mM, and 1 mM phosphate concentrations. Sample size was 30 plants per treatment combination (n = 30). The black line inside the boxes represents the median, error bars indicate plus/minus one standard error of the mean, and the letters represent significant differences ($p < 0.05$) based on a Tukey HSD test.

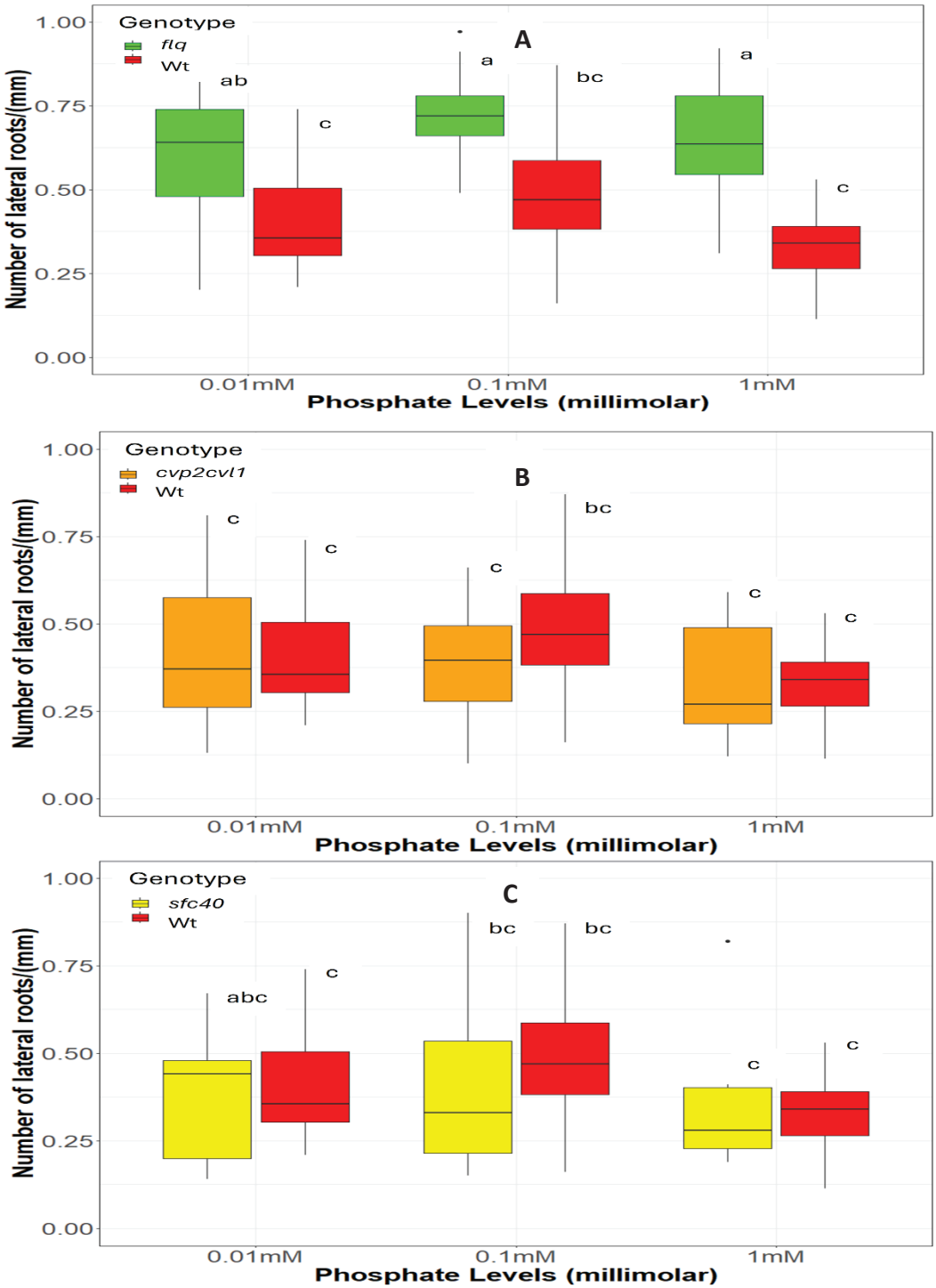

Figure 3.9: Boxplot presenting mean lateral root density of A) Wt and *flq (fkd1/fl1-2/fl2/fl3)*, B) Wt and *cvp2cvl1*, and C) Wt and *sfc40* at 8 DAG, assessed on 0.01 mM, 0.1 mM, and 1 mM phosphate concentrations. Sample size was 30 plants per treatment combination (n = 30). The black line inside the boxes represents the median, error bars indicate plus/minus one standard error of the mean, and the letters represent significant differences ($p < 0.05$) based on a Tukey HSD test.

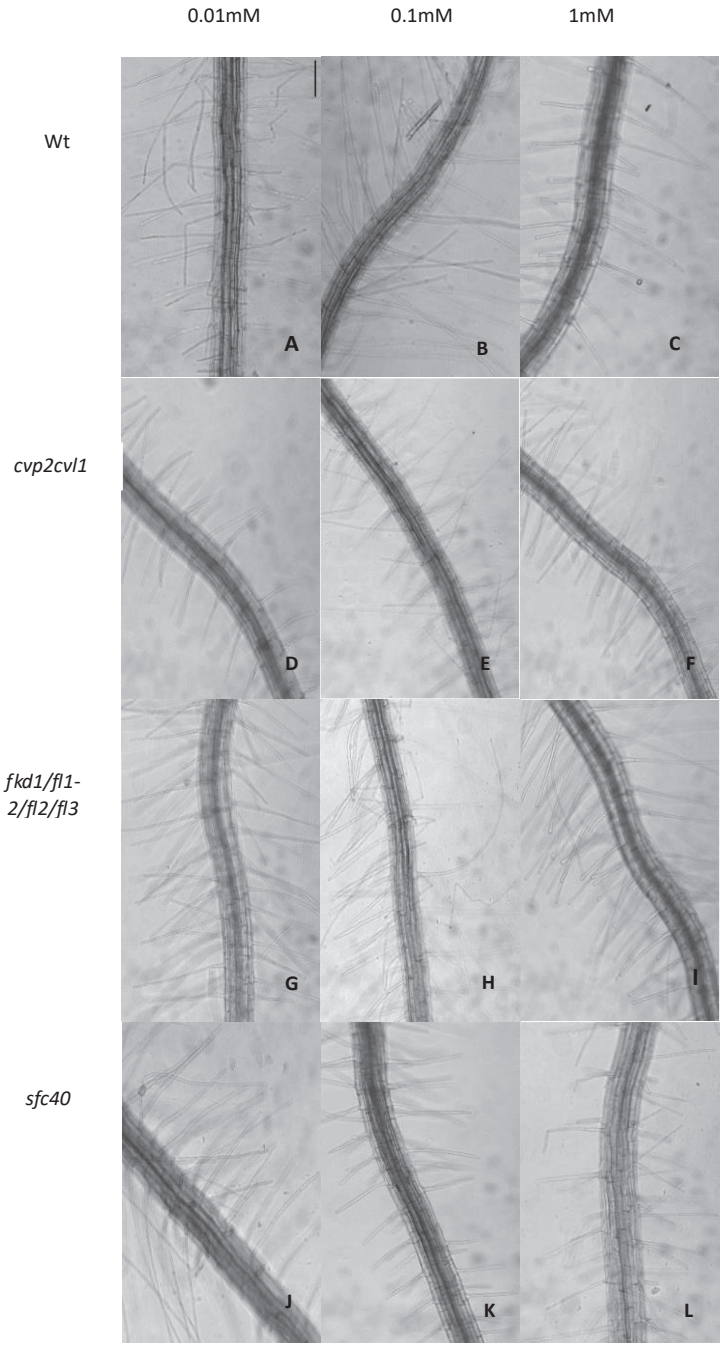

Figure 3.10: Microscopic pictures of root hairs of Wt, *cvp2cvl1*, *fkd1/fl1-2/fl2/fl3*, and *sfc40* grown on 0.01 mM, 0.1 mM, and 1 mM phosphate (10x magnification). Scale bar=0.1mm.

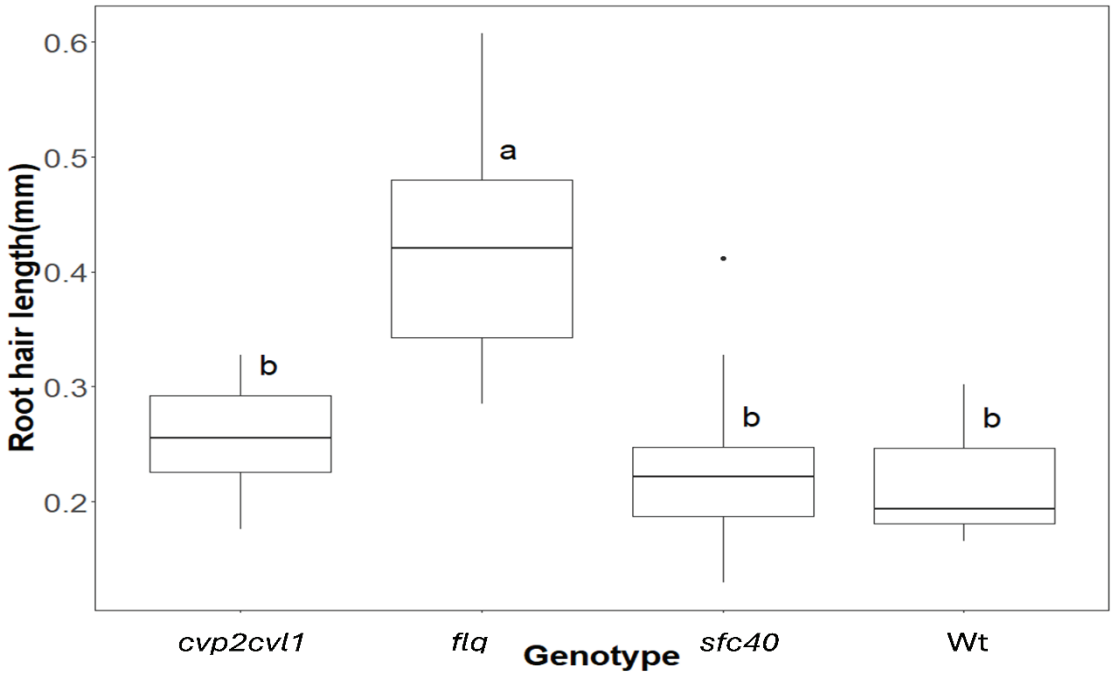

Figure 3.11: Boxplot presenting mean root hair length of Wt, *flq* (*fkd1/fl1-2/fl2/fl3*), *cvp2cvl1*, and *sfc40* at 8 DAG, assessed on 1 mM phosphate concentration. Sample size was 30 plants per treatment combination (n = 30). The black line inside the boxes represents the median, error bars indicate plus/minus one standard error of the mean, and the letters represent significant differences ($p < 0.05$) based on a Tukey HSD test.

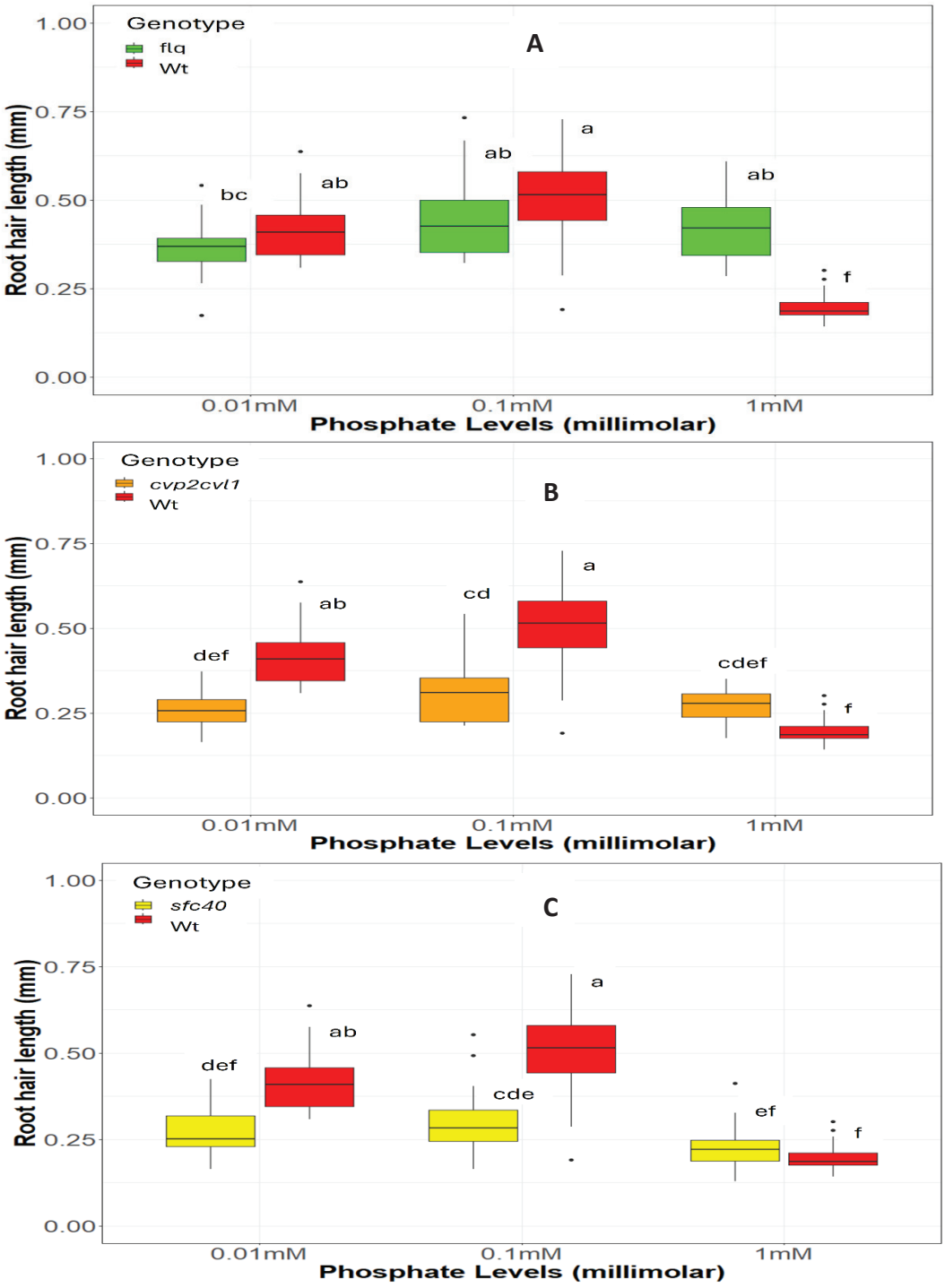

Figure 3.12: Boxplot presenting mean root hair length of A) Wt and *flq (fkd1/fl1-2/fl2/fl3)*, B) Wt and *cvp2cvl1*, and C) Wt and *sfc40* at 8 DAG, assessed on 0.01 mM, 0.1 mM, and 1 mM phosphate concentrations. Sample size was 30 plants per treatment combination (n = 30). The black line inside the boxes represents the median, error bars indicate plus/minus one standard error of the mean, and the letters represent significant differences ($p < 0.05$) based on a Tukey HSD test.

Table 3.4: Two-Way Analysis of Variance (ANOVA) results testing the effects of three different phosphate concentrations (0.01mM, 0.1mM, and 1mM) and four different genotypes (Wt, *cvp*2*cvl*1, *flq*, and *cvp*2*cvl*1) on the root parameters of *Arabidopsis*.

Root Parameter	Source of Variation	Degree of Freedom (Df)	Sum of squares (SS)	Mean sum of squares (MSS)	F-value	P-value
Primary Root Length (mm)	Genotype	3	23752	7917	315.22	<2e-16
	Treatment	2	4612	2306	91.81	<2e-16
	Genotype*Treatment	6	4698	783	31.17	<2e-16
	Residuals	328	8238	25		
Tip to the first lateral root length (mm)	Genotype	3	9953	3318	218.87	<2e-16
	Treatment	2	3187	3187	105.12	<2e-16
	Genotype*Treatment	6	2715	2715	29.85	<2e-16
	Residuals	328	4032	4032		
Total lateral root length (mm)	Genotype	3	14919	4973	76.454	<2e-16
	Treatment	2	1543	771	11.858	1.19e-05
	Genotype*Treatment	6	1295	216	3.318	0.00365
	Residuals	328	16717	65		
Lateral root density (number of lateral roots/ mm)	Genotype	3	4.735	1.5782	33.045	<2e-16
	Treatment	2	0.430	0.2148	4.498	0.012
	Genotype*Treatment	6	0.351	0.0585	1.224	0.294
	Residuals	328	12.418	0.0478		
Root hair length (mm)	Genotype	3	0.8835	0.29449	40.31	<2e-16
	Treatment	2	0.5112	0.25610	35.06	5.68e-14
	Genotype*Treatment	6	0.6233	0.10388	14.22	1.03e-13
	Residuals	328	1.6364	0.00731		

Chapter Four: Discussion

4.1 RSA of different genotypes:

Auxin transport, biosynthesis, and signaling have a crucial impact on regulating the RSA. I hypothesized that the mutants that alter auxin transport and affect leaf vein pattern could also affect the RSA, and my results suggest that the different mutants have different effects on RSA and therefore control different aspects of auxin transport within roots.

The gene products encoded by *FKD1*, *FL1-3*, *SFC/VAN3*, *CVP2*, and *CVL1* are proposed to act within the secretory pathway and to facilitate the localization of PIN proteins (Mariyamma et al., 2018; Carland and Nelson, 2009; Naramoto et al., 2010). Mutation in these genes also results in abnormal vein pattern formation and altered PIN localization to the PM has been observed in provascular cells of *fkd1/fl1-2/fl2/fl3* leaves (Mariyamma et al., 2018) whereas the *sfc/van3* mutant is unable to maintain the PIN1 polarity in the leaf procambial cells (Scarpella et al, 2006). Decreased gravitropic response and root elongation have been previously observed in *fkd1/fl1-2/fl2/fl3* quadruple mutants and *fkd1/fl1-2* double mutants (Mariyamma et al., 2018), suggesting a role for these gene products within roots. The mutants *fkd1/fl1-2/fl2/fl3*, *cvp2/cvl1* and *sfc40* all exhibit shorter primary root length at 1 mM phosphate than the Wt. Reduced cell division in the meristem could result from reduced auxin levels in the root apical meristem (Figure 4.1). By the action of PIN1, auxin is transported to the root

apical meristem through the stele. The reduced root growth of the mutants could be explained by reduced PIN1 localization to the basal membrane of stele (Figure 4.1).

The tip to the first lateral root length was also reduced in the mutants *fkd1/fl1-2/fl2/fl3*, *cvp2cvl1*, and *sfc40* which also implies a shift in the differentiation zone causing the lateral root formation closer to the tip in these mutants (Figure 4.1). Like the reduced root growth, this shift in differentiation is consistent with reduced concentration of auxin in the meristem. I propose that the mutants reduce PIN1 localization in the stele, causing reduced auxin flow to the meristem. Lower auxin in the root meristem, resulting in reduced cell division, would also shift the differentiation zone causing lateral root formation closer to the root tip (Figure 4.1).

The total lateral root length was reduced in the mutants cvp2cvl1 and sfc40. At the final stage of LR outgrowth, the newly formed LRs exhibit a fully formed meristem similar to the PR (Scheres et al., 2007; Bennett and Scheres, 2010). The formation of a functional meristem requires the proper establishment of an auxin maximum in the primordium. This process is regulated by the relocalization of PIN1 (Benková et al., 2003; Péret et al., 2009; Márhavy et al., 2011, 2014). If, as in the primary roots, the mutants *cvp2cvl1* and *sfc40* fail to maintain the asymmetric PIN1 localization to the PM in the lateral roots, this would result in reduced auxin flow from the epidermis to the apical meristem and decrease the auxin maximum in this region. This reduction in the auxin concentration

could result in reduced cell division and subsequent reduction in the size of the lateral root meristems, resulting in reduced lateral root length in these mutants.

I observed a significant genotypic effect on the root hairs. The auxin transporter PIN2 is localized to the upper PM of epidermal cells where it directs the shootward flow of auxin through the epidermis. Auxin in the trichoblasts is required for the activation of ARF19, its downstream targets RSL4 and RSL2 and ultimately, root hair elongation (Crombez et al., 2019, Velasquez et al., 2016). The longer root hairs in the mutant *fkd1/fl1-2/fl2/fl3* might suggest excess accumulation of auxin in the epidermis (Figure 4.1), which would induce more ARF19 activity in the trichoblast and higher expression of its downstream targets RSL4 and RSL2. One explanation is that the localization of PIN2 to the upper side of epidermis is disrupted in *fkd1/fl1-2/fl2/fl3* mutants, disrupting the transport of auxin through the epidermis and causing auxin to accumulate in trichoblast cells (Figure 4.1). At 1 mM phosphate, root hair length in the mutants *cvp2cvl1* and *sfc40* were not significantly different from the Wt, suggesting that these genes do not affect epidermal localization of the PIN2 transporter (Figure 4.1).

4.2 Response to different phosphate treatments:

During my experiment, the Wt exhibited a significant response to phosphate deprivation by exhibiting shorter primary root length, shorter tip to the first lateral root, and longer root hair length under low phosphate concentrations, as observed in previous studies (Crombez et al., 2019). I observed significant differences among Wt and the auxin

transport mutants. P_i-starvation induced PR inhibition relies on various signaling pathways. Auxin biosynthesis, signaling, and transport play crucial roles in mediating the response (Crombez et al., 2019). The polar transport of auxin to the QC via PIN1 is required to maintain the meristem size (Crombez et al., 2019). PIN1 is a possible target of PHR1, which could interfere with auxin transport (Castrillo et al., 2017). I proposed that the shorter root of mutants at 1 mM phosphate may result because *fkd1/fl1-2/fl2/fl3*, *cvp2cvl1* and *sfc40* are unable to maintain the asymmetric localization of PIN1 in the root stele, resulting in reduced flow of auxin to the apical meristem (Figure 4.1).

For the mutants *fkd1/fl1-2/fl2/fl3* and *sfc40*, primary root length was the same under all three phosphate treatments (0.01, 0.1, and 1 mM). Since response to phosphate deprivation occurs via PHR1 influencing PIN1, the altered localization of PIN1 in these mutants may also reduce the ability of roots' to respond to phosphate deprivation. On the other hand, despite the proposed inability to maintain the localization of PIN1, the mutant *cvp2/cvl1* produced a significant response to phosphate deprivation through exhibiting shorter primary root length under 0.01 and 0.1 mM phosphate. One possibility is that *cvp2/cvl1* alters the asymmetric localization of PIN1, but, in contrast to *fkd1/fl1-2/fl2/fl3* and *sfc40*, retains sufficient auxin transport that a PHR induced response to phosphate deprivation can occur. Alternatively, P_i-starvation induced PR inhibition is influenced by multiple hormone signaling pathways, auxin, cytokinin, and gibberellin (Crombez et al., 2019) and by the availability of Fe and Fe-P_i ratio, implying that the response could be PHR1 and auxin independent.

The amount of auxin in the meristem establishes the auxin gradient that regulates the transition to the differentiation zone (Figure 4.1). Therefore, I expected to observe the same trend in the tip to the first lateral root distance as in the primary root length. The mutant *cvp2cvl1* exhibited a shorter tip to the first lateral root length under both 0.1 and 0.01 mM phosphate treatments compared to high phosphate treatment, thus the transition to differentiation shows a response to phosphate deprivation. In contrast, the *fkd1/fl1-2/fl2/fl3* mutant exhibited similar tip to the first lateral root distance under all three phosphate treatments, and *sfc40* showed a different response only when the lowest (0.01 mM) and highest (1 mM) were compared. In *Arabidopsis* lateral root primordium, P_i deprivation causes enhanced auxin signaling and expression of auxin receptor TIR1 (Crombez et al., 2019, Du and Scheres, 2018), which leads to increased expression of ARF7 and ARF19. Both ARFs positively regulate the PHR1, which is proposed to target PIN1 and vesicle trafficking genes establishing an ARF-PHR1 feedback loop (Crombez et al., 2019). I proposed that the disrupted PIN1 localization in the *fkd1/fl1-2/fl2/fl3* and *sfc40* mutants would cause a drop in the auxin levels in the meristem (Figure 4.1). Reduced auxin could affect the PHR1-ARF feedback mechanism resulting in the lack of response phosphate deprivation. Further, I propose that the *cvp2/cvl1* mutant has sufficient auxin flow to cause the upregulation of ARF7 and ARF19 and enhanced activity of PHR1.

The *sfc40* and *cvp2cvl1* mutants exhibited shorter root hair length than the Wt at low phosphate concentrations (0.01 mM and 0.1 mM). In the *fkd1/fl1-2/fl2/fl3* mutant, root hairs are longer than wild type at 1mM phosphate, but do not elongate further at low phosphate. I proposed that the longer root hairs at 1mM phosphate are because the *fkd1/fl1-2/fl2/fl3* mutant disrupts the localization of both PIN1 in the stele and PIN2 in the epidermis, and that the disrupted localization of PIN2 to the upper side of the epidermis affects the transport of auxin and results in excess accumulation of auxin in this region (Figure 4.1). Increased auxin can cause enhanced activity of ARF19 and its downstream targets RSL4 and RSL2 causing the elongation of root hairs. This phenomenon observed at 1 mM phosphate treatment suggesting that the backlog of auxin has already occurred at the epidermis due to disrupted localization of PIN2 at 1 mM phosphate. As a result, the quadruple mutant *fkd1/fl1-2/fl2/fl3* does not exhibit further elongation of the root hairs at 0.01 mM and 0.1 mM phosphate treatments.

In contrast to *fkd1/fl1-2/fl2/fl3*, *cvp2cvl1* and *sfc40* root hairs are no different than Wt at 1 mM phosphate, but, unlike Wt, do not elongate in response to phosphate deprivation. One explanation is, the mutants *cvp2cvl1* and *sfc40* could have less epidermal levels of auxin compared to the Wt due to the reduced flow of auxin to the apical meristem. This reduced availability of auxin in the epidermis could also affect the ability of these mutants to produce longer root hairs under low phosphate conditions. Apart from this, PHR1 targets root hair elongation by increasing ROS production by activating PLD1, RHD2, RSL4, and RSL19 (Crombez et al., 2019) and vesicle trafficking by activating *PIP5K3*

and *PIP5K4* to synthesize PtdIns(4,5)P2 (Wada et al., 2015). The genes *CVP2* and *CVL1* produce an enzyme, inositolpoluphosphate5-phosphatase6 (At5PTase6), which encodes phosphoinositide PtdIns(4,5)P2 leading to the formation of PtdIns(4)P (Carland and Nelson, 2009), therefore, the mutant *cvp2/cvl1* is unable to synthesize PtdIns(4)P. It is possible that *cvp2/cvl1* could directly affect phosphoinositide homeostasis which controls proper docking of exocytic vesicles and is crucial for P_i-deprivation dependent root hair elongation.

4.3 Composition of the gel media influencing the response:

P_i limitation is not the only reason for the arrest of the primary root in gel media; another factor contributing to this arrest is an excess of accessible iron (Fe) in the low P_i media (Ward et al., 2008; Bournier et al., 2013). Numerous investigations revealed that phosphate deprivation increased the amount of iron present in the media (Hirsch et al., 2006; Ward et al., 2008; Misson et al., 2005). PHR1 has been demonstrated to directly or indirectly regulate genes encoding proteins involved in iron homeostasis, in addition to the light reactions of photosynthesis, photorespiration, sulfate transport, and the enzymes involved in ROS scavenging and detoxication (Bustos et al., 2010; Rouached et al., 2011). Bournier et al., 2013 demonstrated how plants integrate signals from various mineral elements to adjust their growth and metabolism, and that study also provided the first molecular link between iron and phosphate homeostasis. The asymmetric localization of the potential PHR1 target, PIN1, could alter its function in the mutants,

potentially affecting iron homeostasis in the media and thus modifying the response of these mutants to phosphate starvation. To comprehend the molecular underpinnings of Pi stress responses and adaptations, *Arabidopsis* has been demonstrated to be a useful model. Most of the research conducted has used gel-based medium that has an unnaturally high availability of nutrients (Hanlon et al., 2018). Gel systems allow for the direct observation of rapid and homogeneous growth, but they differ significantly from real soil settings (Hanlon et al., 2018). These phenotypes might also have developed because of the gel growth system, which has a low buffering capacity and could alter the natural soil chemistry.

4.4 Types of Agars used in the media is crucial to response:

During my study I tested four different agars (Bioshop, EMD, Phytotech, and Fisher) and observed their effect on the RSA in phosphate deficient environment. I observed that the Bioshop agar exhibited significantly different root phenotypes compared to the rest of the three agars suggesting that these phenotypes could significantly be influenced by the gelling agent used in the growth media.

Previous studies have demonstrated that different agars could be significantly different from one another in respect to their nutrient contents. Gelling agents like agar are often high in nutrient concentrations and, as a result, it is quite difficult to impose the deficiency of a specific nutrient. Therefore, chelating agents are added frequently to the media to remove the remnants of nutrient contamination which is a major disadvantage

of agar-based media (Gruber et al., 2013). My findings, provide further evidence that choosing the proper agar for the target nutrient is crucial to establish consistent nutrient deficiency.

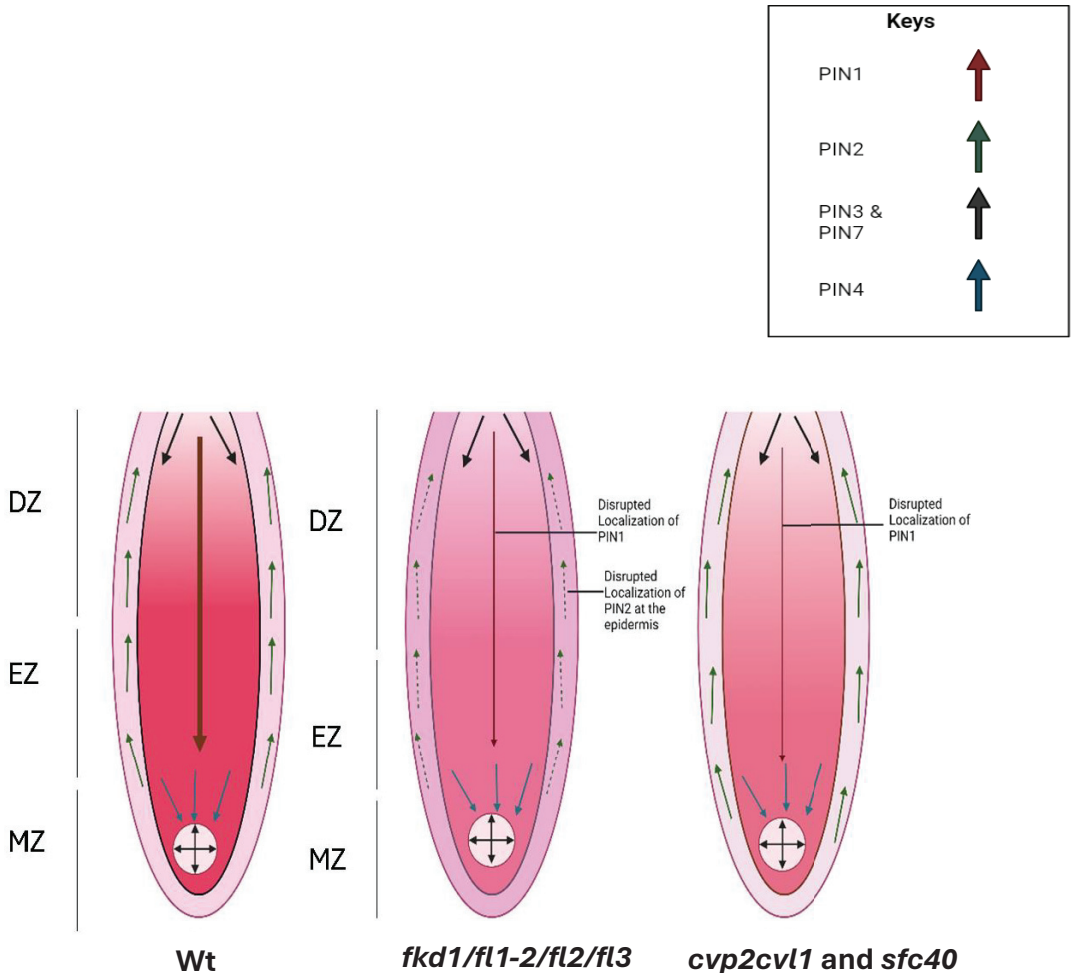

Figure 4.1: Schematic representation of the flow of auxin via different PIN transporters in the *Arabidopsis* root (MZ = Meristematic Zone, EZ = Elongation Zone, DZ = Differentiation Zone). The differently coloured arrows indicate direction of auxin transport associated with different PIN proteins, as listed in the legend. The aerially produced auxin is transported through the vascular tissue towards the apical meristem via PIN3 and PIN7. The transporters PIN1 and PIN4 accumulate in the columella. Auxin is redistributed through the root cap by PIN3 and PIN7. The shootward flow of auxin is regulated by PIN2 through the epidermis (Mischniewicz et al., 2007). In the mutant *fkd1/fl1-2/fl2/fl3*, the disrupted localization of PIN1 reduces the flow of auxin towards the apical meristem and causes the subsequent reduction of the auxin gradient. The disruption of PIN2 localization in the mutant results in excess auxin accumulation in the epidermal region. The mutants *cvp2cvl1* and *sfc40* are also unable to maintain the asymmetric PIN1 localization and reduces the auxin gradient. They also have lower epidermal auxin levels compared to the Wt and *fkd1/fl1-2/fl2/fl3* mutant due to the reduced flow of auxin in the apical meristem. *Image illustrated with Biorender*.

Chapter Five: Conclusion

The modification of Root System Architecture is a crucial response adopted by plants to deal with various environmental changes such as nutrient deficiency. In this study I worked with *Arabidopsis* auxin transport mutants in hopes to understand how the mutation in the genes *FKD1*, *FL1-3*, *CVP2*, *CVL1*, and *SFC40* that are required for asymmetric localization of PIN1 during leaf development and help regulate the auxin transport, could also alter the plant's response to phosphate deficiency via changes in root architecture. Previous studies have suggested the involvement of these genes in vein pattern formation. In my research, I have observed that these genes could also alter root phenotypes like- primary root length, the distance from the tip to the first lateral root, and root hair length.

The mutants were significantly different from the Wt in respect to these phenotypic characters. The mutants *cvp2cvl1*, *sfc40,* and *fkd1/fl1-2/fl2/fl3* exhibited significantly shorter primary root length, and tip to the first lateral root distance compared to the Wt, suggesting that these mutants could also affect the RSA along with the defective vein pattern formation. The mutant *fkd1/fl1-2/fl2/fl3* demonstrated significantly longer root hair length compared to the Wt and the mutants *cvp2cvl1* and *sfc40*. This finding suggests that this mutant could also alter the localization of PIN2 leading to the excess auxin accumulation at the epidermis and subsequent longer root hairs. Further research involving the mutant *pin2* would help us to understand its influence on root hair length.

The Wt was able to produce a response to phosphate deprivation under low phosphate concentrations. The mutants *fkd1/fl1-2/fl2/fl3* and *sfc40* failed to produce any response to phosphate deprivation suggesting that the defective localization of PIN1 could alter their responses. The mutant *cvp2cvl1* exhibited shorter primary root and tip to the first lateral root distance under low phosphate treatments, and thus showed a response. This finding suggests that the RSA's response to phosphate deficiency could also be regulated by auxin independent factors.

This research helps to understand the function of the *FL* gene family, *CVP2*, *CVL1*, and *SFC* in regulating the RSA of plants and in controlling the plant's response to phosphate deficiency. A better understanding of the involvement of these genes in phosphate starvation signaling pathways could help improve the nutrient uptake efficiency of plants. A better understanding of these genes' role in phosphate starvation signaling pathways could lead to improved strategies to breed or develop plants with better phosphate uptake efficiency from the soil. This could be beneficial for the agricultural sector and could reduce the dependency on phosphate fertilizers that are harmful for the environment. In the regions with low phosphate, improved nutrient uptake efficiency would allow the crops to require less fertilizer leading to better crop production and enhanced food security.

References

Adamowski M., Friml J. (2015). PIN-dependent Auxin Transport: Action, Regulation, and Evolution. Plant Cell, 27, 20–32.

Aida, M., Beis, D., Heidstra, R., Willemsen, V., Blilou, I., Galinha, C., Nussaume, L., Noh, Y.-S., Amasino, R., & Scheres, B. (2004). The PLETHORA Genes Mediate Patterning of the *Arabidopsis* Root Stem Cell Niche. Cell, 119(1), 109–120.

Balcerowicz, D., Schoenaers, S., & Vissenberg, K. (2015). Cell Fate Determination and the Switch from Diffuse Growth to Planar Polarity in *Arabidopsis* Root Epidermal Cells. Frontiers in Plant Science, 6, 102-107.

Baluška, F., Salaj, J., Mathur, J., Braun, M., Jasper, F., Šamaj, J., Chua, N.-H., Barlow, P. W., & Volkmann, D. (2000). Root Hair Formation: F-Actin-Dependent Tip Growth Is Initiated by Local Assembly of Profilin-Supported F-Actin Meshworks Accumulated within Expansin-Enriched Bulges. Developmental Biology, 227(2), 618–632.

Barbez, E., Kubeš, M., Rolčík, J., Béziat, C., Pěnčík, A., Wang, B., Rosquete, M. R., Zhu, J., Dobrev, P. I., Lee, Y., Zažímalovà, E., Petrášek, J., Geisler, M., Friml, J., & Kleine-Vehn, J. (2012). A Novel Putative Auxin Carrier Family Regulates Intracellular Auxin Homeostasis in Plants. Nature, 485(7396), 119–122.

Beeckman T, Burssens S, Inzé D. 2001. The Peri-Cell-Cycle in *Arabidopsis*. Journal of Experimental Botany, 52, 403–411.

Benitez-Alfonso Y, Faulkner C, Pendle A, Miyashima S, Helariutta Y, Maule A. 2013. Symplastic Intercellular Connectivity Regulates Lateral Root Patterning. Developmental Cell, 26, 136–147.

Benková, E., Michniewicz, M., Sauer, M., Teichmann, T., Seifertová, D., Jürgens, G., & Friml, J. (2003). Local, Efflux-Dependent Auxin Gradients as a Common Module for Plant Organ Formation. Cell, 115(5), 591–602.

Bennett T, Scheres B. 2010. Root Development—Two Meristems for the Price of One? Current Topics in Developmental Biology, 91, 67–102.

Berckmans, B., Vassileva, V., Schmid, S. P. C., Maes, S., Parizot, B., Naramoto, S., Magyar, Z., Kamei, C. L. A., Koncz, C., Bögre, L., Persiau, G., De Jaeger, G., Friml, J., Simon, R., Beeckman, T., & De Veylder, L. (2011). Auxin-Dependent Cell Cycle Reactivation through Transcriptional Regulation of *Arabidopsis* E2Fa by Lateral Organ Boundary Proteins. The Plant Cell, 23(10), 3671–3683.

Blilou I, Xu J, Wildwater M, Willemsen V, Paponov I, Friml J, Heidstra R, Aida M, Palme K, Scheres B. 2005. The PIN Auxin Efflux Facilitator Network Controls Growth and Patterning in *Arabidopsis* Roots. Nature, 433, 39–44.

Bournier, M., Tissot, N., Mari, S., Boucherez, J., Lacombe, E., Briat, J.-F., & Gaymard, F. (2013). *Arabidopsis* Ferritin 1 (AtFer1) Gene Regulation by the Phosphate Starvation Response 1 (AtPHR1) Transcription Factor Reveals a Direct Molecular Link between Iron and Phosphate Homeostasis. Journal of Biological Chemistry, 288(31), 22670–22680.

Bubb, M. R., Baines, I. C., & Korn, E. D. (1998). Localization of Actobindin, profilin I, profilin II, and phosphatidylinositol-4,5-bisphosphate (PIP2) in *Acanthamoeba castellanii*. Cell Motility and the Cytoskeleton, 39(2), 134–146.

Bustos R, Castrillo G, Linhares F, Puga MI, Rubio V, Pérez-Pérez J, Solano R, Leyva A, Paz-Ares J. A central Regulatory System Largely Controls Transcriptional Activation and Repression Responses to Phosphate Starvation in *Arabidopsis*. PLOS Genetics. 2010, 6(9), e1001102.

Carland, F., & Nelson, T. (2009). CVP2- and CVL1-Mediated Phosphoinositide Signaling as a Regulator of the ARF GAP SFC/VAN3 in Establishment of Foliar Vein Patterns. The Plant Journal, 59(6), 895–907.

Casimiro, I., Marchant, A., Bhalerao, R. P., Beeckman, T., Dhooge, S., Swarup, R., Graham, N., Inze, D., Sandberg, G., Casero, P. J., & Bennett, M. (2001). Auxin Transport Promotes *Arabidopsis* Lateral Root Initiation. The Plant Cell, 13(4), 843.

Castrillo, G., Teixeira, P.J.P.L., Paredes, S.H., Law, T.F., de Lorenzo, L., Feltcher, M.E., Finkel, O.M., Breakfield, N.W., Mieczkowski, P., Jones, C.D., et al. (2017). Root Microbiota Drive Direct Integration of Phosphate Stress and Immunity. Nature, 543, 513–518.

Chapman E.J., Estelle M. (2009) Mechanism of Auxin-Regulated gene expression in Plants. Annual review of genetics, 43, 265–285.

Chapman, J. M., Muhlemann, J. K., Gayomba, S. R., & Muday, G. K. (2019). RBOH-Dependent ROS Synthesis and ROS Scavenging by Plant Specialized Metabolites to Modulate Plant Development and Stress Responses. Chemical Research in Toxicology, 32(3), 370–396.

Crombez, H., Motte, H., & Beeckman, T. (2019). Tackling Plant Phosphate Starvation by the Roots. Developmental Cell, 48(5), 599–615.

Datta S, Kim CM, Pernas M et al (2011). Root Hairs: Development, Growth and Evolution at the Plant-Soil Interface. Plant Soil, 346, 1–14.

Datta, S., Prescott, H., & Dolan, L. (2015). Intensity of a Pulse of RSL4 Transcription Factor Synthesis Determines *Arabidopsis* Root Hair Cell Size. Nature Plants, 1(10), 210-256.

De Rybel, B., Audenaert, D., Xuan, W., Overvoorde, P., Strader, L. C., Kepinski, S., Hoye, R., Brisbois, R., Parizot, B., Vanneste, S., Liu, X., Gilday, A., Graham, I. A., Nguyen, L., Jansen, L., Njo, M. F., Inzé, D., Bartel, B., & Beeckman, T. (2012). A Role for the Root Cap in Root Branching Revealed by the Non-Auxin Probe Naxillin. Nature Chemical Biology, 8(9), 798–805.

De Rybel, B., Vassileva, V., Parizot, B., Demeulenaere, M., Grunewald, W., Audenaert, D., Van Campenhout, J., Overvoorde, P., Jansen, L., Vanneste, S., Möller, B., Wilson, M., Holman, T., Van Isterdael, G., Brunoud, G., Vuylsteke, M., Vernoux, T., De Veylder, L., Inzé, D., Beeckman, T.(2010). A Novel Aux/IAA28 Signaling Cascade

Activates GATA23-Dependent Specification of Lateral Root Founder Cell Identity. Current Biology, 20(19), 1697–1706.

De Smet I, Vassileva V, De Rybel B, et al. (2008). Receptor-like Kinase ACR4 Restricts Formative Cell Divisions in the *Arabidopsis* Root. Science, 322, 594–597.

De Smet, I., Tetsumura, T., De Rybel, B., Frey, N. F. d., Laplaze, L., Casimiro, I., Swarup, R., Naudts, M., Vanneste, S., Audenaert, D., Inze, D., Bennett, M. J., & Beeckman, T. (2007). Auxin-dependent Regulation of Lateral Root Positioning in the Basal Meristem of *Arabidopsis.* Development, 134(4), 681–690.

De Smet, I., Vanneste, S., Inzé, D., & Beeckman, T. (2006). Lateral Root Initiation or the Birth of a New Meristem. Plant Molecular Biology, 60(6), 871–887.

Delker, C., Raschke, A., & Quint, M. (2008). Auxin Dynamics: The Dazzling Complexity of a Small Molecule's Message. Planta, 227(5), 929–941.

Denninger, P., Reichelt, A., Schmidt, V. A. F., Mehlhorn, D. G., Asseck, L. Y., Stanley, C. E., Keinath, N. F., Evers, J.-F., Grefen, C., & Grossmann, G. (2019). Distinct RopGEFs Successively Drive Polarization and Outgrowth of Root Hairs. Current Biology, 29(11), 1854–1865.

Di Mambro, R., De Ruvo, M., Pacifici, E., Salvi, E., Sozzani, R., Benfey, P. N., Busch, W., Novak, O., Ljung, K., Di Paola, L., Marée, A. F. M., Costantino, P., Grieneisen, V. A., & Sabatini, S. (2017). Auxin Minimum Triggers the Developmental Switch from Cell Division to Cell Differentiation in the *Arabidopsis* Root. Proceedings of the National Academy of Sciences, 114(36), E7641—E7649.

Ding, Z., & Friml, J. (2010). Auxin Regulates Distal Stem Cell Differentiation in *Arabidopsis* Roots. Proceedings of the National Academy of Sciences, 107(26), 12046–12051.

Dolan L, Janmaat K, Willemsen V, Linstead P, Poethig S, Roberts K, Scheres B. (1993). Cellular Organization of the *Arabidopsis thaliana* Root. Development, 119, 71–84.

Dolan, L., and Davies, J. (2004). Cell Expansion in Roots. Current Opinions in Plant Biology. Volume 7, 33–39.

Dong, Q., Zhang, Z., Liu, Y., Tao, L., & Liu, H. (2018). FERONIA Regulates Auxin-mediated Lateral Root Development and Primary Root Gravitropism. FEBS Letters, 593(1), 97–106.

Drdova EJ, Synek L, Pecenkova T, Hala M, Kulich I, Fowler JE, Murphy AS, Zarsky V. (2013). The Exocyst Complex Contributes to PIN Auxin Efflux Carrier Recycling and Polar Auxin Transport in *Arabidopsis*. Plant Journal 73, 709–719.

Drisch RC, Stahl Y. (2015). Function and Regulation of Transcription Factors Involved in Root Apical Meristem and Stem Cell Maintenance. Frontiers in Plant Science, Volume 6, 505.

Du, Y., & Scheres, B. (2017). Lateral Root Formation and the Multiple Roles of Auxin. Journal of Experimental Botany, 69(2), 155–167.

Duan, Q., Kita, D., Li, C., Cheung, A. Y., & Wu, H.-M. (2010). FERONIA Receptor-like Kinase Regulates RHO GTPase Signaling of Root Hair Development. Proceedings of the National Academy of Sciences, 107(41), 17821–17826.

Dubrovsky JG, Gambetta GA, Hernández-Barrera A, Shishkova S, González I. (2006). Lateral Root Initiation in *Arabidopsis*: Developmental Window, Spatial Patterning, Density and Predictability. Annals of Botany, 97, 903–915.

Dubrovsky JG, Sauer M, Napsucialy-Mendivil S, Ivanchenko MG, Friml J, Shishkova S, Celenza J,Benková E. (2008). Auxin Acts as a Local Morphogenetic Trigger to Specify Lateral Root Founder Cells. Proceedings of the National Academy of Sciences, 105(3), 8790–8794.

Dubrovsky, J. G., & Laskowski, M. (2017). Lateral Root Initiation. Encyclopedia of Applied Plant Sciences, 80(2), 256–264.

Dubrovsky, J. G., Doerner, P. W., Colón-Carmona, A., & Rost, T. L. (2000). Pericycle Cell Proliferation and Lateral Root Initiation in *Arabidopsis*. Plant Physiology, 124(4), 1648–1657.

Dubrovsky, J. G., Rost, T. L., Colón-Carmona, A., & Doerner, P. (2001). Early primordium morphogenesis during lateral root initiation in *Arabidopsis thaliana*. Planta, 214(1), 30–36.

Durgaprasad K, Roy MV, Venugopal A, Kareem A, Raj K, Willemsen V, Mähönen AP, Scheres B, Prasad K. (2019). Gradient Expression of Transcription Factor Imposes

a Boundary on Organ Regeneration Potential in Plants. Cell Reports, Volume 29, 453–463.

Enders T.A., Strader L.C. (2015) Auxin activity: Past, Present, and Future. American Journal of Botany, 102(2), 180–196.

Fernandez, A., Drozdzecki, A., Hoogewijs, K., Vassileva, V., Madder, A., Beeckman, T., & Hilson, P. (2015). The GLV6/RGF8/CLEL2 Peptide Regulates Early Pericycle Divisions During Lateral Root Initiation. Journal of Experimental Botany, 66(17), 5245–5256.

Fischer, U., Ikeda, Y., & Grebe, M. (2007). Planar Polarity of Root Hair Positioning in *Arabidopsis*. Biochemical Society Transactions, 35(1), 149–151.

Foreman, J., Demidchik, V., Bothwell, J. H. F., Mylona, P., Miedema, H., Torres, M. A., Linstead, P., Costa, S., Brownlee, C., Jones, J. D. G., Davies, J. M., & Dolan, L. (2003). Reactive Oxygen Species Produced by NADPH Oxidase Regulate Plant Cell Growth. Nature, 422(6930), 442–446.

Franck, C. M., Westermann, J., Bürssner, S., Lentz, R., Lituiev, D. S., & Boisson-Dernier, A. (2018). The Protein Phosphatases ATUNIS1 and ATUNIS2 Regulate Cell Wall Integrity in Tip-Growing Cells. The Plant Cell, 30(8), 1906–1923.

Fu, Y., Li, H., & Yang, Z. (2002). The ROP2 GTPase Controls the Formation of Cortical Fine F-Actin and the Early Phase of Directional Cell Expansion during *Arabidopsis* Organogenesis. The Plant Cell, 14(4), 777–794.

Fukaki, H., Nakao, Y., Okushima, Y., Theologis, A., & Tasaka, M. (2005). Tissue-specific Expression of Stabilized SOLITARY-ROOT/IAA14 Alters Lateral Root Development in *Arabidopsis*. The Plant Journal*,* 44(3), 382–395.

Fukaki, H., Tameda, S., Masuda, H., & Tasaka, M. (2002). Lateral Root Formation is Blocked by a Gain-of-Function Mutation in the SOLITARY-ROOT/IAA14 Gene of *Arabidopsis*. The Plant Journal*,* 29(2), 153–168.

Fukui, K., & Hayashi, K.i. (2018). Manipulation and Sensing of Auxin Metabolism, Transport and Signaling. Plant and Cell Physiology, 59(8), 1500–1510.

Galinha C, Hofhuis H, Luijten M, Willemsen V, Blilou I, Heidstra R, Scheres B. (2007). PLETHORA Proteins as Dose-dependent Master Regulators of *Arabidopsis* Root Development. Nature, 449(2), 1053–1057.

García-Gómez, M. L., Garay-Arroyo, A., García-Ponce, B., Sánchez, M. d. l. P., & Álvarez-Buylla, E. R. (2021). Hormonal Regulation of Stem Cell Proliferation at the *Arabidopsis thaliana* Root Stem Cell Niche. Frontiers in Plant Science, 12.

Geldner N, Richter S, Vieten A, Marquardt S, Torres-Ruiz RA, Mayer U, Jürgens G. (2004). Partial Loss-of-function Alleles Reveal a Role for GNOM in Auxin Transport-Related, Post-Embryonic Development of *Arabidopsis*. Development, 131(5), 389–400.

Gendre, D., Baral, A., Dang, X., Esnay, N., Boutté, Y., Stanislas, T., Vain, T., Claverol, S., Gustavsson, A., Lin, D., Grebe, M., & Bhalerao, R. P. (2019). Rho-of-plant

Activated Root Hair Formation Requires *Arabidopsis* YIP4a/b Gene Function. Development, 146(5), 168-559.

Goh T, Kasahara H, Mimura T, Kamiya Y, Fukaki H. (2012). Multiple AUX/IAA-ARF Modules Regulate Lateral Root Formation: The Role of *Arabidopsis* SHY2/IAA3-mediated Auxin Signaling. Biological Sciences, 367(3), 1461–1468.

Goh, T., Toyokura, K., Wells, D. M., Swarup, K., Yamamoto, M., Mimura, T., Weijers, D., Fukaki, H., Laplaze, L., Bennett, M. J., & Guyomarc'h, S. (2016). Quiescent Center Initiation in the *Arabidopsis* Lateral Root Primordia is Dependent on the SCARECROW Transcription Factor. Journal of Cell Science, 129(19), Article e1.2-e1.5.

Grieneisen VA, Xu J, Marée AF, Hogeweg P, Scheres B. (2007). Auxin Transport is Sufficient to Generate a Maximum and Gradient Guiding Root growth. Nature 449, 1008–1013.

Grierson C, Nielsen E, Ketelaarc T, Schiefelbein J (2014). Root Hairs. The *Arabidopsis* Book, 12(3), 67-84.

Gu, F., & Nielsen, E. (2013). Targeting and Regulation of Cell Wall Synthesis During Tip Growth in Plants. Journal of Integrative Plant Biology, 55(9), 835–846.

Guseman, J. M., Hellmuth, A., Lanctot, A., Feldman, T. P., Moss, B. L., Klavins, E., Calderon Villalobos, L.I.A., & Nemhauser, J. L. (2015). Auxin-induced Degradation Dynamics Set the Pace for Lateral Root Development. Journal of Cell Science, 128(6), 97-110.

Habets, M. E. J., & Offringa, R. (2014). PIN-driven polar auxin transport in plant developmental plasticity: a key target for environmental and endogenous signals. New Phytologist, 203(2), 362–377.

Hanlon MT, Ray S, Saengwilai P, Luthe D, Lynch JP, Brown KM. (2018). Buffered Delivery of Phosphate to *Arabidopsis* Alters Responses to Low Phosphate. Journal of Experimental Botany, 69, 1207–1219.

Hayashi K. (2012). The Interaction and Integration of Auxin Signaling Components. Plant Cell Physiology, 53, 965–975.

Hayashi K., Neve J., Hirose M., Kuboki A., Shimada Y., Kepinski S., et al. (2012). Rational Design of an Auxin Antagonist of the SCF(TIR1) Auxin Receptor Complex. ACS Chemical Biology Journal, 7(9), 590–598.

Hayashi, K.-i., Arai, K., Aoi, Y., Tanaka, Y., Hira, H., Guo, R., Hu, Y., Ge, C., Zhao, Y., Kasahara, H., & Fukui, K. (2021). The Main Oxidative Inactivation Pathway of the Plant Hormone Auxin. Nature Communications, 12(1), 125-140.

Himanen K, Vuylsteke M, Vanneste S, Vercruysse S, Boucheron E, Alard P, Chriqui D, Van Montagu M, Inze D, Beeckman T. (2004).Transcript Profiling of Early Lateral Root Initiation. Proceedings of the National Academy of Sciences, 101, 5146–5151.

Himanen, K., Boucheron, E., Vanneste, S., de Almeida Engler, J., Inzé, D., & Beeckman, T. (2002). Auxin-Mediated Cell Cycle Activation During Early Lateral Root Initiation. The Plant Cell, 14(10), 2339–2351.

Hirota A, Kato T, Fukaki H, Aida M, Tasaka M. (2007). The Auxin-regulated AP2/EREBP Gene PUCHI is Required for Morphogenesis in the Early Lateral Root Primordium of *Arabidopsis*. The Plant Cell, 19(5), 2156–2168.

Hirsch J, Marin E, Floriani M. (2006). Phosphate Deficiency Promotes Modification of Iron Distribution in *Arabidopsis* plants. Biochimie, 88(11), 1767–1771.

Hofhuis H, Laskowski M, Du Y, Prasad K, Grigg S, Pinon V, Scheres B. (2013). Phyllotaxis and Rhizotaxis in *Arabidopsis* are Modified by Three PLETHORA Transcription Factors. Current Biology, 23, 956–962.

Hou, H., Erickson, J., Meservy, J., & Schultz, E. A. (2010). FORKED1 Encodes a PH Domain Protein that is Required for PIN1 Localization in Developing Leaf Veins. The Plant Journal, 63(6), 960–973.

Hu, Y., Omary, M., Hu, Y., Doron, O., Hoermayer, L., Chen, Q., Megides, O., Chekli, O., Ding, Z., Friml, J., Zhao, Y., Tsarfaty, I., & Shani, E. (2021). Cell Kinetics of Auxin Transport and Activity in *Arabidopsis* Root Growth and Skewing. Nature Communications, 12(1), 1211-1274.

Ikeda, Y., Men, S., Fischer, U., Stepanova, A. N., Alonso, J. M., Ljung, K., & Grebe, M. (2009). Local Auxin Biosynthesis Modulates Gradient-directed Planar Polarity in *Arabidopsis*. Nature Cell Biology, 11(6), 731–738.

Ioio, R. D., Nakamura, K., Moubayidin, L., Perilli, S., Taniguchi, M., Morita, M. T., Aoyama, T., Costantino, P., & Sabatini, S. (2008). A Genetic Framework for the

Control of Cell Division and Differentiation in the Root Meristem. Science, 322(5906), 1380–1384.

Jain, M., Nagar, P., Goel, P., Singh, A.K., Kumari, S., Mustafiz, A. (2018). Second Messengers: Central Regulators in Plant Abiotic Stress Response: An Omics Perspective. Springer, 12(1), 183-205.

Jones, A. R., Kramer, E. M., Knox, K., Swarup, R., Bennett, M. J., Lazarus, C. M., Leyser, H. M. O., & Grierson, C. S. (2009). Auxin Transport through Non-hair Cells Sustains Root-hair Development. Nature Cell Biology, 11(1), 78–84.

Jones, M. A., Raymond, M. J., Yang, Z., and Smirnoff, N. (2007). NADPH Oxidase-dependent Reactive Oxygen Species Formation Required for Root Hair Growth Depends on ROP GTPase. Journal of Experimental Botany, 58, 1261–1270.

Jones, M. A., Shen, J.-J., Fu, Y., Li, H., Yang, Z., & Grierson, C. S. (2002). The *Arabidopsis* Rop2 GTPase is a Positive Regulator of Both Root Hair Initiation and Tip Growth. The Plant Cell, 14(4), 763–776.

Kang NY, Lee HW, Kim J. (2013). The AP2/EREBP Gene PUCHI Co-acts with LBD16/ASL18 and LBD18/ASL20 Downstream of ARF7 and ARF19 to Regulate Lateral Root Development in *Arabidopsis*. Plant & Cell Physiology, 54, 1326–1334.

Kasahara H. (2016). Current Aspects of Auxin Biosynthesis in Plants. Bioscience, Biotechnology, and Biochemistry, 80(4), 34–42.

Kim J, Lee HW. (2013). Direct Activation of EXPANSIN14 by LBD18 in the Gene Regulatory Network of Lateral Root Formation in *Arabidopsis*. Plant Signaling & Behavior, 8(1), e22979.

Kleine-Vehn, J., Wabnik, K., Martinière, A., Łangowski, Ł., Willig, K., Naramoto, S., Leitner, J., Tanaka, H., Jakobs, S., Robert, S., Luschnig, C., Govaerts, W., W Hell, S., Runions, J., & Friml, J. (2011). Recycling, Clustering, and Endocytosis Jointly Maintain PIN Auxin Carrier Polarity at the Plasma Membrane, Molecular Systems Biology, 7(1), 540.

Knox, K. (2003). AXR3 and SHY2 Interact to Regulate Root Hair Development. Development, 130(23), 5769–5777.

Koizumi, K. (2005). VAN3 ARF-GAP-mediated Vesicle Transport is Involved in Leaf vascular network formation. Development, 132(7), 1699–1711.

Korasick D.A., Enders T.A., Strader L.C. (2013). Auxin biosynthesis and storage forms. Journal of experimental Botany, 64, 2541–2555.

Kumar, N., & Iyer-Pascuzzi, A. S. (2020). Shedding the Last Layer: Mechanisms of Root Cap Cell Release. Plants, 9(3), 308.

Kumpf R. P., Shi C.-L., Larrieu A., Stø I. M., Butenko M. A., Péret B., et al., (2013). Floral Organ Abscission Peptide IDA and its HAE/HSL2 Receptors Control Cell Separation during Lateral Root Emergence. The Proceedings of the National Academy of Sciences, 110(4), 5235–5240.

Kusano, H., Testerink, C., Vermeer, J. E. M., Tsuge, T., Shimada, H., Oka, A., Munnik, T., & Aoyama, T. (2008). The *Arabidopsis* Phosphatidylinositol Phosphate 5-Kinase PIP5K3 Is a Key Regulator of Root Hair Tip Growth. The Plant Cell, 20(2), 367–380.

Langowski, L., Wabnik, K., Li, H., Vanneste, S., Naramoto, S., Tanaka, H., & Friml, J. (2016). Cellular Mechanisms for Cargo Delivery and Polarity Maintenance at Different Polar Domains in Plant Cells. Cell Discovery, 2(1), 775-890.

Lanza, M., Garcia-Ponce, B., Castrillo, G., Catarecha, P., Sauer, M., Rodriguez-Serrano, M., Páez-García, A., Sánchez-Bermejo, E., TC, M., Leo del Puerto, Y., Sandalio, L. M., Paz-Ares, J., & Leyva, A. (2012). Role of Actin Cytoskeleton in Brassinosteroid Signaling and in its Integration with the Auxin Response in Plants. Developmental Cell, 22(6), 1275–1285.

Laplaze L, Parizot B, Baker A, Ricaud L, Martinière A, Auguy F, Franche C, Nussaume L, Bogusz D, Haseloff J. (2005). GAL4-GFP Enhancer Trap Lines for Genetic Manipulation of Lateral Root Development in *Arabidopsis thaliana*. Journal of Experimental Botany, 56, 2433–2442.

Laskowski M, Biller S, Stanley K, Kajstura T, Prusty R. (2006). Expression Profiling of Auxin-treated *Arabidopsis* Roots: toward a Molecular Analysis of Lateral Root Emergence. Plant & Cell Physiology, 47, 788–792.

Laskowski, M. J., Williams, M. E., Nusbaum, H. C., & Sussex, I. M. (1995). Formation of Lateral Root Meristems is a Two-stage Process. Development, 121(10), 3303–3310.

Laskowski, M., Grieneisen, V. A., Hofhuis, H., Hove, C. A. t., Hogeweg, P., Marée, A. F. M., & Scheres, B. (2008). Root System Architecture from Coupling Cell Shape to Auxin Transport. PLOS Biology, 6(12), 145-180.

Lavenus J, Goh T, Guyomarc'h Set al. (2015). Inference of the *Arabidopsis* Lateral Root Gene Regulatory Network Suggests a Bifurcation Mechanism that Defines Primordia Flanking and Central Zones. The Plant Cell, 27, 1368–1388.

Lavenus, J., Goh, T., Roberts, I., Guyomarc'h, S., Lucas, M., De Smet, I., Fukaki, H., Beeckman, T., Bennett, M., & Laplaze, L. (2013). Lateral Root Development in *Arabidopsis*: Fifty Shades of Auxin. Trends in Plant Science, 18(8), 450–458.

Lee HW, Kim J. (2013). EXPANSINA17 Up regulated by LBD18/ASL20 Promotes Lateral Root Formation During the auxin response. Plant & Cell Physiology,54, 1600–1611.

Lee Y, Rubio MC, Alassimone J, Geldner N. (2013). A Mechanism for Localized Lignin Deposition in the Endodermis. Cell, 153, 402–412.

Lei, M., Zhu, C., Liu, Y., Karthikeyan, A. S., Bressan, R. A., Raghothama, K. G., & Liu, D. (2011). Ethylene Signaling is Involved in Regulation of Phosphate Starvation-Induced Gene Expression and Production of Acid Phosphatases and Anthocyanin in *Arabidopsis*. New Phytologist, 189(4), 1084–1095.

Leyser, O. (2018). Auxin Signaling. Plant Physiology, 176(1), 465–479.

Li, L. H., Guo, N., Wu, Z. Y., Zhao, J. M., Sun, J. T., Wang, X. T., & Xing, H. (2015). P1BS, a Conserved Motif Involved in Tolerance to Phosphate Starvation in Soybean. Genetics and Molecular Research, 14(3), 9384–9394.

Löfke, C., Dünser, K., Scheuring, D., & Kleine-Vehn, J. (2015). Auxin Regulates SNARE-Dependent Vacuolar Morphology Restricting Cell Size. eLife, 4, 105-120.

Loio, R. D., Nakamura, K., Moubayidin, L., Perilli, S., Taniguchi, M., Morita, M. T., Aoyama, T., Costantino, P., & Sabatini, S. (2008). A Genetic Framework for the Control of Cell Division and Differentiation in the Root Meristem. Science, 322(5906), 1380–1384.

Lucas, M., Kenobi, K., von Wangenheim, D., Voss, U., Swarup, K., De Smet, I., Van Damme, D., Lawrence, T., Peret, B., Moscardi, E., Barbeau, D., Godin, C., Salt, D., Guyomarc'h, S., Stelzer, E. H. K., Maizel, A., Laplaze, L., & Bennett, M. J. (2013). Lateral Root Morphogenesis is Dependent on the Mechanical Properties of the Overlaying Tissues. Proceedings of the National Academy of Sciences, 110(13), 5229–5234.

Ludwig-Muller J. (2011). Auxin conjugates: Their Role for Plant Development and in the Evolution of Land Plants. Journal of experimental Botany, 62(3), 1757–1773.

Mähönen AP, Bishopp A, Higuchi M, Nieminen KM, Kinoshita K, Törmäkangas K, Ikeda Y, Oka A, Kakimoto T, Helariutta Y. (2006). Cytokinin Signaling and its Inhibitor AHP6 Regulate Cell Fate During Vascular Development. Science, 311, 94–98.

Mähönen AP, Ten Tusscher K, Siligato R, Smetana O, Díaz-Triviño S, Salojärvi J,Wachsman G, Prasad K, Heidstra R, Scheres B. (2014). PLETHORA Gradient Formation Mechanism Separates Auxin Responses. Nature, 515, 125–129.

Majda, M., & Robert, S. (2018). The Role of Auxin in Cell Wall Expansion. International Journal of Molecular Sciences, 19(4), 951.

Malamy, J. E., & Benfey, P. N. (1997). Organization and Cell Differentiation in Lateral Roots of *Arabidopsis thaliana*. Development, 124(1), 33–44.

Marchant A, Bhalerao R, Casimiro I, Eklöf J, Casero PJ, Bennett M, Sandberg G. (2002). AUX1 Promotes Lateral Root Formation by Facilitating Indole-3-Acetic Acid Distribution Between Sink and Source Tissues in the *Arabidopsis* Seedling. The Plant Cell, 14, 589–597.

Marchant A, Bhalerao R, Casimiro I, Eklöf J, Casero PJ, Bennett M, Sandberg G. (2002). AUX1 Promotes Lateral Root Formation by Facilitating Indole-3-Acetic Acid Distribution Between Sink and Source Tissues in the *Arabidopsis* Seedling. The Plant Cell, 14, 589–597.

Marhavý P, Bielach A, Abas L et al., (2011). Cytokinin Modulates Endocytic Trafficking of PIN1 Auxin Efflux Carrier to Control Plant Organogenesis. Developmental Cell, 21, 796–804.

Marhavý P, Duclercq J, Weller B, Feraru E, Bielach A, Offringa R, Friml J, Schwechheimer C, Murphy A, Benková E. (2014). Cytokinin Controls Polarity of PIN1-dependent

Auxin Transport During Lateral Root Organogenesis. Current Biology, 24, 1031–1037.

Marhavý, P., Montesinos, J. C., Abuzeineh, A., Van Damme, D., Vermeer, J. E. M., Duclercq, J., Rakusová, H., Nováková, P., Friml, J., Geldner, N., & Benková, E. (2016). Targeted Cell Elimination Reveals an Auxin-guided Biphasic Mode of Lateral Root Initiation. Genes & Development, 30(4), 471–483.

Marhavý, P., Vanstraelen, M., De Rybel, B., Zhaojun, D., Bennett, M. J., Beeckman, T., & Benková, E. (2013). Auxin Reflux between the Endodermis and Pericycle Promotes Lateral Root Initiation. The European Molecular Biology Organization Journal, 32(1), 149–158.

Markakis MN, De Cnodder T, Lewandowski M, Simon D, Boron A, Balcerowicz D, Doubbo T, Taconnat L, Renou JP, Höfte H, et al., (2012). Identification of Genes Involved in the ACC-mediated Control of Root Cell Elongation in *Arabidopsis*. BMC Plant Biology, 12(208), 1025-1120.

Mashiguchi K., Tanaka K., Sakai T., Sugawara S., Kawaide H., Natsume M., et al. (2011) The Main Auxin Biosynthesis Pathway in *Arabidopsis*. The Proceedings of the National Academy of Sciences, 108, 18512–18517.

Michniewicz M, Zago MK, Abas L,Weijers D, Schweighofer A, Meskiene I, Heisler MG, Ohno C, Zhang J, Huang F, et al. 2007. Antagonistic Regulation of PIN Phosphorylation by PP2A and PINOID Directs Auxin Flux. Cell, 130(2), 1044–1056.

Molendijk, A. J., Bischoff, F., Rajendrakumar, C. S. V., Friml, J., Braun, M., Gilroy, S., et al. (2001). *Arabidopsis thaliana* ROP GTPases are Localized to Tips of Root Hairs and Control Polar Growth. The European Molecular Biology Organization, 20, 2779–2788.

Monshausen, G. B., Bibikova, T. N., Messerli, M. A., Shi, C., & Gilroy, S. (2007). Oscillations in Extracellular pH and Reactive Oxygen Species Modulate Tip Growth of *Arabidopsis* Root Hairs. Proceedings of the National Academy of Sciences, 104(52), 20996–21001.

Moreno-Risueno MA, Van Norman JM, Moreno A, Zhang J, Ahnert SE, Benfey PN. (2010). Oscillating Gene Expression Determines Competence for Periodic *Arabidopsis* Root Branching. Science, 329, 1306–1311.

Naramoto S. (2017). Polar Transport in Plants Mediated by Membrane Transporters: Focus on Mechanisms of Polar Auxin Transport. Current Opinion in Plant Biology, 40, 8–14.

Naramoto, S., Sawa, S., Koizumi, K., Uemura, T., Ueda, T., Friml, J., Nakano, A., & Fukuda, H. (2009). Phosphoinositide-dependent Regulation of VAN3 ARF-GAP Localization and Activity Essential for Vascular Tissue Continuity in Plants. Development, 136(9), 1529–1538.

Naseer S, Lee Y, Lapierre C, Franke R, Nawrath C, Geldner N. (2012). Casparian Strip Diffusion Barrier in *Arabidopsis* is Made of a Lignin Polymer without Suberin. Proceedings of the National Academy of Sciences, 109, 10101–10106.

Okumura K, Goh T, Toyokura K, Kasahara H, Takebayashi Y, Mimura T, Kamiya Y, Fukaki H. (2013). GNOM/FEWER ROOTS is Required for the Establishment of an Auxin Response Maximum for *Arabidopsis* Lateral root Initiation. Plant & Cell Physiology, 54, 406–417.

Okushima Y, Fukaki H, Onoda M, Theologis A, Tasaka M. (2007). ARF7 and ARF19 Regulate Lateral Root Formation via Direct Activation of LBD/ASL Genes in *Arabidopsis*. The Plant Cell, 19, 118–130.

Okushima, Y., Overvoorde, P. J., Arima, K., Alonso, J. M., Chan, A., Chang, C., Ecker, J. R., Hughes, B., Lui, A., Nguyen, D., Onodera, C., Quach, H., Smith, A., Yu, G., & Theologis, A. (2005). Functional Genomic Analysis of the AUXIN RESPONSE FACTOR Gene Family Members in *Arabidopsis thaliana*: Unique and Overlapping Functions of ARF7 and ARF19. The Plant Cell*,* 17(2), 444–463.

Ovečka, M., Lang, I., Baluška, F., Ismail, A., Illeš, P., & Lichtscheidl, I. K. (2005). Endocytosis and Vesicle Trafficking during Tip Growth of Root Hairs. Protoplasma, 226(1-2), 39–54.

Pacifici, E., Di Mambro, R., Dello Ioio, R., Costantino, P., & Sabatini, S. (2018). Acidic Cell Elongation Drives Cell Differentiation in the *Arabidopsis* Root. The European Journal of Molecular Biology, 37(16), 567-890.

Pahari S., Cormark R. D., Blackshaw M. T., Liu C., Erickson J. L., Schultz E. A. (2014). *Arabidopsis* UNHINGED Encodes a VPS51 Homolog and Reveals a Role for the

GARP Complex in Leaf Shape and Vein Patterning. Development, 141, 1894–1905.

Parizot B, Laplaze L, Ricaud L, et al., (2008). Diarch Symmetry of the Vascular Bundle in *Arabidopsis* Root Encompasses the Pericycle and is Reflected in Distich Lateral Root Initiation. Plant Physiology, 146, 140–148.

Park, E., & Nebenführ, A. (2013). Myosin XIK of *Arabidopsis thaliana* Accumulates at the Root Hair Tip and is Required for Fast Root Hair Growth. PLOS ONE, 8(10), Article e76745.

Pei W, Du F, Zhang Y, He T, Ren H (2012). Control of the Actin Cytoskeleton in Root Hair Development. Plant Science, 187, 10–18.

Péret B, Larrieu A, Bennett MJ. (2009). Lateral Root Emergence: A Difficult Birth. Journal of Experimental Botany, 60, 3637–3643.

Péret B, Li G, Zhao Jet al. (2012). Auxin Regulates Aquaporin Function to Facilitate Lateral Root Emergence. Nature Cell Biology, 14, 991–998.

Péret B, Middleton AM, French APet al. (2013). Sequential Induction of Auxin Efflux and Influx Carriers Regulates Lateral Root Emergence. Molecular Systems Biology, 9, 699.

Pitts, R. J., Cernac, A., & Estelle, M. (1998). Auxin and Ethylene Promote Root Hair Elongation in *Arabidopsis*. The Plant Journal, 16(5), 553–560.

Porco S., Pěnčík A., Rashed A., Voß U., Casanova-Sáez R., Bishopp A., et al. (2016). Dioxygenase-encoding AtDAO1 Gene Controls IAA Oxidation and Homeostasis in *Arabidopsis*. Proceedings of the National Academy of Sciences, 113, 11016–11021.

Prabhakaran Mariyamma, N., Clarke, K. J., Yu, H., Wilton, E. E., Van Dyk, J., Hou, H., & Schultz, E. A. (2018). Members of the *Arabidopsis FORKED1-LIKE* Gene Family Act to Localize PIN1 in Developing Veins. Journal of Experimental Botany, 69(20), 4773–4790.

Prabhakaran Mariyamma, N., Hou, H., Carland, F. M., Nelson, T., & Schultz, E. A. (2017). Localization of *Arabidopsis FORKED1* to a RABA-positive Compartment Suggests a Role in Secretion. Journal of Experimental Botany, 68(13), 3375–3390.

Preuss, M. L., Schmitz, A. J., Thole, J. M., Bonner, H. K. S., Otegui, M. S., & Nielsen, E. (2006). A Role for the RabA4b Effector Protein PI-4Kβ1 in Polarized Expansion of Root Hair Cells in *Arabidopsis thaliana*. Journal of Cell Biology, 172(7), 991–998.

Preuss, M. L., Serna, J., Falbel, T. G., Bednarek, S. Y., & Nielsen, E. (2004). The *Arabidopsis* Rab GTPase RabA4b Localizes to the Tips of Growing Root Hair Cells. The Plant Cell, 16(6), 1589–1603.

Retzer, K., & Weckwerth, W. (2021). The TOR–Auxin Connection Upstream of Root Hair Growth. Plants, 10(1), 150.

Rounds CM, Bezanilla M (2013). Growth mechanisms in Tip-growing Plant Cells. Annual Review in Plant Biology, 64, 243–265.

Rouached, et al., (2011). Uncoupling Phosphate Deficiency from its Major Effects on Growth and Transcriptome via PHO1 Expression in *Arabidopsis*. Plant Journal, 65, 557–570.

Roychoudhry, S., Sageman-Furnas, K., Wolverton, C., Grones, P., Tan, S., Molnár, G., De Angelis, M., Goodman, H. L., Capstaff, N., Lloyd, J. P. B., Mullen, J., Hangarter, R., Friml, J., & Kepinski, S. (2023). Antigravitropic PIN Polarization Maintains Non-Vertical Growth in Lateral Roots. Nature Plants, 15(2), 670-816.

Roychoudhry, S., & Kepinski, S. (2021). Auxin in Root Development. Cold Spring Harbor Perspectives in Biology, 45(3), 1023-1060.

Ruegger, M., Dewey, E., Gray, W.M., Hobbie, L., Turner, J., and Estelle, M. (1998). The TIR1 Protein of *Arabidopsis* Functions in Auxin Response and is Related to Human SKP2 and Yeast grr1p. Genes and Development, 12, 198–207.

Sabatini S, Beis D, Wolkenfelt H, Murfett J, Guilfoyle T, Malamy J, Benfey P, Leyser O, Bechtold N, Weisbeek P, et al. (1999). An Auxin-dependent Distal Organizer of Pattern and Polarity in the *Arabidopsis* Root. Cell, 99, 463–472.

Sabatini S, Heidstra R, Wildwater M, Scheres B. (2003). SCARECROW is Involved in Positioning the Stem Cell Niche in the *Arabidopsis* Root Meristem. Genes and Development, 17, 354–358.

Salehin M., Bagchi R., Estelle M. (2015). SCFTIR1/AFB-based Auxin Perception: Mechanism and Role in Plant Growth and Development. Plant Cell, 27, 9–19.

Salvi E, Rutten JP, Di Mambro R, Polverari L, Licursi V, Negri R, Dello Ioio R, Sabatini S, Ten Tusscher K. (2020). A Self-organized PLT/auxin/ARR-B Network Controls the Dynamics of Root Zonation Development in *Arabidopsis thaliana*. Developmental Cell, 53, 431–443.

Santner, A., Calderon-Villalobos, L. I. A., & Estelle, M. (2009). Plant Hormones are Versatile Chemical Regulators of Plant Growth. Nature Chemical Biology, 5(5), 301–307.

Scarpella E, Marcos D, Friml J, Berleth T. (2006). Control of Leaf Vascular Patterning by Polar Auxin Transport. Genes and Development, 20, 1015–1027.

Scheres B. (2005). The PIN Auxin Efflux Facilitator Network Controls Growth and Patterning in *Arabidopsis* Roots. Nature, 433, 39–44.

Scheres, B. (2007). Stem-cell Niches: Nursery Rhymes across Kingdoms. Nature Reviews Molecular Cell Biology, 8(5), 345–354.

Scheres, B., Benfey, P., & Dolan, L. (2002). Root Development. The *Arabidopsis* Book 1, Article e0101.

Schiefelbein, J., Huang, L., & Zheng, X. (2014). Regulation of Epidermal Cell Fate in *Arabidopsis* Roots: the Importance of Multiple Feedback Loops. Frontiers in Plant Science, 5(8), 167-190.

Shibata, M., & Sugimoto, K. (2019). A Gene Regulatory Network for Root Hair Development. Journal of Plant Research, 132(3), 301–309.

Sieburth, L. E., Muday, G. K., King, E. J., Benton, G., Kim, S., Metcalf, K. E., Meyers, L., Seamen, E., & Van Norman, J. M. (2006). SCARFACE Encodes an ARF-GAP that is Required for Normal Auxin Efflux and Vein Patterning in *Arabidopsis*. The Plant Cell, 18(6), 1396–1411.

Singh SM, Bandi S, Winder SJ & Mallela KM (2014). The Actin Binding Affinity of the Utrophin Tandem Calponin-homology Domain is Primarily Determined by its N-Terminal Domain. Biochemistry, 53, 1801-1809.

Staswick, P. E., Serban, B., Rowe, M., Tiryaki, I., Maldonado, M. T., Maldonado, M. C., & Suza, W. (2005). Characterization of an *Arabidopsis* Enzyme Family that Conjugates Amino Acids to Indole-3-Acetic Acid. The Plant Cell, 17(2), 616–627.

Stenzel, I., Ischebeck, T., König, S., Hołubowska, A., Sporysz, M., Hause, B., & Heilmann, I. (2008). The Type B Phosphatidylinositol-4-Phosphate 5-Kinase 3 is Essential for Root Hair Formation in *Arabidopsis thaliana*. The Plant Cell, 20(1), 124–141.

Steynen, Q. J., & Schultz, E. A. (2003). The FORKED Genes are Essential for Distal Vein Meeting in *Arabidopsis*. Development, 130(19), 4695–4708.

Sugawara S., Hishiyama S., Jikumaru Y., Hanada A., Nishimura T., Koshiba T., et al. (2009). Biochemical Analyses of Indole-3-Acetaldoxime-dependent Auxin Biosynthesis in *Arabidopsis*. The Proceedings of the National Academy of Sciences, 106, 5430–5435.

Swarup K, Benková E, Swarup Ret et al., (2008). The Auxin Influx Carrier LAX3 Promotes Lateral Root Emergence. Nature Cell Biology, 10, 946–954.

Swarup R, Kramer EM, Perry P, Knox K, Leyser HM, Haseloff J, Beemster GT, Bhalerao R, Bennett MJ. (2005). Root Gravitropism Requires Lateral Root Cap and Epidermal Cells for Transport and Response to a Mobile Auxin Signal. Nature Cell Biology, 7, 1057–1065.

Synek, L., Schlager, N., Eliáš, M., Quentin, M., Hauser, M.-T., & Žárský, V. (2006). AtEXO70A1, a Member of a Family of Putative Exocyst Subunits Specifically Expanded in Land Plants, is Important for Polar Growth and Plant Development. The Plant Journal, 48(1), 54–72.

Takatsuka H, Umeda M. (2014). Hormonal Control of Cell Division and Elongation along Differentiation Trajectories in Roots. Journal of Experimental Botany, 65, 2633–2643.

Takatsuka, H., & Ito, M. (2020). Cytoskeletal Control of Planar Polarity in Root Hair Development. Frontiers in Plant Science, 11, 221-250.

Tan X., Calderon-Villalobos L.I., Sharon M., Zheng C., Robinson C.V., Estelle M., et al. (2007). Mechanism of Auxin Perception by the TIR1 Ubiquitin Ligase. Nature, 446, 640–645.

Tang, L. P., Zhou, C., Wang, S. S., Yuan, J., Zhang, X. S., & Su, Y. H. (2017). FUSCA 3 Interacting with LEAFY COTYLEDON 2 Controls Lateral Root Formation through Regulating YUCCA 4 Gene Expression in *Arabidopsis thaliana*. New Phytologist, 213(4), 1740–1754.

Thibaud MC, Arrighi JF, Bayle V, Chiarenza S, Creff A, Bustos R, Paz-Ares J, Poirier Y, Nussaume L. (2010). Dissection of Local and Systemic Transcriptional Responses to Phosphate Starvation in *Arabidopsis*. The Plant Journal, 64, 775–789.

Thole, J. M., Vermeer, J. E. M., Zhang, Y., Gadella, T. W. J., & Nielsen, E. (2008). ROOT HAIR DEFECTIVE4 Encodes a Phosphatidylinositol-4-Phosphate Phosphatase Required for Proper Root Hair Development in *Arabidopsis thaliana*. The Plant Cell, 20(2), 381–395.

Tian, Q., & Reed, J. W. (1999). Control of Auxin-regulated Root Development by the *Arabidopsis thaliana* SHY2/IAA3 Gene. Development, 126(4), 711–721.

Ulmasov, T., Liu, Z.-B., Hagen, G., & Guilfoyle, T. J. (1995). Composite Structure of Auxin Response Elements. The Plant Cell, 7(10), 1611.

Van Norman JM, Xuan W, Beeckman T, Benfey PN. (2013). To Branch or not to Branch: The Role of Pre-patterning in Lateral Root Formation. Development, 140, 4301–4310.

Vanneste, S., & Friml, J. (2009). Auxin: A Trigger for Change in Plant Development. Cell, 136(6), 1005–1016.

Vanneste, S., De Rybel, B., Beemster, G. T. S., Ljung, K., De Smet, I., Van Isterdael, G., Naudts, M., Iida, R., Gruissem, W., Tasaka, M., Inzé, D., Fukaki, H., & Beeckman, T. (2005). Cell Cycle Progression in the Pericycle is not Sufficient for SOLITARY ROOT/IAA14-mediated Lateral Root Initiation in *Arabidopsis thaliana*. The Plant Cell, 17(11), 3035–3050.

Velasquez, S. M., Barbez, E., Kleine-Vehn, J., & Estevez, J. M. (2016). Auxin and Cellular Elongation. Plant Physiology, 170(3), 1206–1215.

Verbelen JP, De Cnodder T, Le J, Vissenberg K, Baluska F. (2006). The Root apex of *Arabidopsis thaliana* Consists of Four Distinct Zones of Growth Activities: Meristematic Zone, Transition Zone, Fast Elongation Zone and Growth Terminating Zone. Plant Signaling & Behavior, 1, 296–304.

Vermeer, J. E. M., & Geldner, N. (2015). Lateral Root Initiation in *Arabidopsis thaliana*: A Force Awakens. F1000Prime Reports, 7, 1021-1345.

Vermeer, J. E. M., von Wangenheim, D., Barberon, M., Lee, Y., Stelzer, E. H. K., Maizel, A., & Geldner, N. (2014). A Spatial Accommodation by Neighboring Cells Is Required for Organ Initiation in *Arabidopsis*. Science, 343(6167), 178–183.

Vernoud, V., Horton, A. C., Yang, Z., & Nielsen, E. (2003). Analysis of the Small GTPase Gene Superfamily of *Arabidopsis*. Plant Physiology, 131(3), 1191–1208.

Vijayakumar, P., Datta, S., & Dolan, L. (2016). ROOT HAIR DEFECTIVE SIX-LIKE4 (RSL4) Promotes Root Hair Elongation by Transcriptionally Regulating the Expression of Genes Required for Cell Growth. New Phytologist, 212(4), 944–953.

Vilches-Barro A, Maizel A. (2015). Talking through Walls: Mechanisms of Lateral Root Emergence in *Arabidopsis thaliana*. Current Opinion in Plant Biology, 23, 31–38.

von Wangenheim, D., Fangerau, J., Schmitz, A., Smith, R. S., Leitte, H., Stelzer, E. H. K., & Maizel, A. (2016). Rules and Self-Organizing Properties of Post-embryonic Plant Organ Cell Division Patterns. Current Biology, 26(4), 439–449.

Wada, Y., Kusano, H., Tsuge, T. and Aoyama, T. (2015). Phosphatidylinositol Phosphate 5-Kinase Genes Respond to Phosphate Deficiency for Root Hair Elongation in *Arabidopsis thaliana*. Plant Journal, 81, 426-437.

Wang L., Dong J., Gao Z., Liu D. (2012). The *Arabidopsis* gene HYPERSENSITIVE TO PHOSPHATE STARVATION3 Encodes ETHYLENE OVERPRODUCTION1. Plant Cell Physiology, 53, 1093–1105.

Ward JT, Lahner B, Yakubova E, Salt DE, Raghothama KG (2008). The Effect of Iron on the Primary Root Elongation of *Arabidopsis* during Phosphate Deficiency. Plant Physiology, 147, 1181–1191.

Westermann, J., Streubel, S., Franck, C. M., Lentz, R., Dolan, L., & Boisson-Dernier, A. (2019). An Evolutionarily Conserved Receptor-like Kinases Signaling Module Controls Cell Wall Integrity During Tip Growth. Current Biology, 29(22), 3899–3908.

Wilmoth, J. C., Wang, S., Tiwari, S. B., Joshi, A. D., Hagen, G., Guilfoyle, T. J., Alonso, J. M., Ecker, J. R., & Reed, J. W. (2005). NPH4/ARF7 and ARF19 Promote Leaf Expansion and Auxin-induced Lateral Root Formation. The Plant Journal, 43(1), 118–130.

Won, C., Shen, X., Mashiguchi, K., Zheng, Z., Dai, X., Cheng, Y., Kasahara, H., Kamiya, Y., Chory, J., & Zhao, Y. (2011). Conversion of Tryptophan to Indole-3-Acetic Acid by TRYPTOPHAN AMINOTRANSFERASES OF *ARABIDOPSIS* and YUCCAs in

Arabidopsis. Proceedings of the National Academy of Sciences, 108(45), 18518–18523.

Woodward A.W., Bartel B. (2005). Auxin: Regulation, Action, and Interaction. Annals of Botany, 95, 707–735.

Xu, T., Wen, M., Nagawa, S., Fu, Y., Chen, J.-G., Wu, M.-J., Perrot-Rechenmann, C., Friml, J., Jones, A. M., & Yang, Z. (2010). Cell Surface- and Rho GTPase-Based Auxin Signaling Controls Cellular Interdigitation in *Arabidopsis*. Cell*,* 143(1), 99–110.

Xuan, W., Audenaert, D., Parizot, B., Möller, B. K., Njo, M. F., De Rybel, B., De Rop, G., Van Isterdael, G., Mähönen, A. P., Vanneste, S., & Beeckman, T. (2015). Root Cap-Derived Auxin Pre-patterns the Longitudinal Axis of the *Arabidopsis* Root. Current Biology, 25(10), 1381–1388.

Xuan, W., Band, L. R., Kumpf, R. P., Van Damme, D., Parizot, B., De Rop, G., Opdenacker, D., Moller, B. K., Skorzinski, N., Njo, M. F., De Rybel, B., Audenaert, D., Nowack, M. K., Vanneste, S., & Beeckman, T. (2016). Cyclic Programmed Cell Death Stimulates Hormone Signaling and Root Development in *Arabidopsis*. Science*,* 351(6271), 384–387.

Yalovsky, S., Bloch, D., Sorek, N., & Kost, B. (2008). Regulation of Membrane Trafficking, Cytoskeleton Dynamics, and Cell Polarity by ROP/RAC GTPases. Plant Physiology, 147(4), 1527–1543.

Yang, G., Gao, P., Zhang, H., Huang, S., & Zheng, Z.-L. (2007). A Mutation in MRH2 Kinesin Enhances the Root Hair Tip Growth Defect Caused by Constitutively Activated ROP2 Small GTPase in *Arabidopsis*. PLOS ONE, 2(10), 231-320.

Yi, K., Menand, B., Bell, E., & Dolan, L. (2010). A Basic Helix-Loop-Helix Transcription Factor Controls Cell Growth and Size in Root Hairs. Nature Genetics, 42(3), 264–267.

Yoo, C.-M., & Blancaflor, E. B. (2012). Overlapping and Divergent Signaling Pathways for ARK1 and AGD1 in the Control of Root Hair Polarity in *Arabidopsis thaliana*. Frontiers in Plant Science, 4, 1011-1045.

Yu H, Luo N, Sun L, Liu D. (2012). HPS4/SABRE Regulates Plant Responses to Phosphate Starvation through Antagonistic Interaction with Ethylene Signaling. Journal of Experimental Botany, 63, 4527–4538.

Žárský, V., Cvrčková, F., Potocký, M., & Hála, M. (2009). Exocytosis and Cell Polarity in Plants - Exocyst and Recycling Domains. New Phytologist, 183(2), 255–272.

Zazimalova E., Murphy A.S., Yang H., Hoyerova K., Hosek P. (2010). Auxin Transporters—Why So Many? Cold Spring Harbor Perspectives, 2(4), 334-456.

Zazimalova´E, Krecek P, Skupa P, Hoyerova´K, Petrasek J. (2007). Polar Transport of the Plant Hormone Auxin – The Role of PIN-FORMED (PIN) Proteins. Cellular and Molecular Life Sciences, 64, 1621–1637.

Zhang J., Peer W.A. (2017). Auxin Homeostasis: The DAO of Catabolism. Journal of Experimental Botany, 68, 3145–3154.

Zhou, X., Xiang, Y., Li, C., & Yu, G. (2020). Modulatory Role of Reactive Oxygen Species in Root Development in Model Plant of *Arabidopsis thaliana*. Frontiers in Plant Science, 11, 558-745.

Zhu, S., Martínez Pacheco, J., Estevez, J. M., & Yu, F. (2020). Autocrine Regulation of Root Hair Size by the RALF-FERONIA-RSL4 Signaling Pathway. New Phytologist, 227(1), 45–49.

Zourelidou M, Absmanner B,Weller B, Barbosa IC,Willige BC, Fastner A, StreitV, Port SA, Colcombet J, de la Fuente van Bentem S, et al., (2014). Auxin Efflux by PIN-FORMED Proteins is Activated by Two Different Protein Kinases, D6 PROTEIN KINASE and PINOID. eLife, 8(5), 1022-1134.